UNIVERSITÄT DES SAARLANDES

Analysis of intracellular trafficking and localization of the human kidney anion exchanger 1 (kAE1) in yeast

Dissertation

zur Erlangung des Grades des Doktors der Naturwissenschaften
der Naturwissenschaftlich-Technischen Fakultät
der Universität des Saarlandes

von

Xiaobing Li

Saarbrücken

2021

Tag des Kolloquiums: 12th October, 2021

Dekan:
Prüfungsausschuss:
1. Berichterstatter: Prof. Dr. Manfred J. Schmitt
2. Berichterstatter: Prof. Dr. Bruce Morgan
Vorsitzender: Prof. Dr. Uli Müller
Akademischer Mitarbeiter: Dr.-Ing. Michael Kohlstedt

' Es ist nichts Großes ohne Leidenschaft vollbracht worden, noch kann es ohne solche vollbracht werden '

-Georg Wilhelm Friedrich Hegel

Publications from the present work:

Xiaobing Li, Emmanuelle Cordat, Manfred J. Schmitt* and Björn Becker*. 2021. Boosting ER folding capacity reduces UPR activation and intracellular accumulation of human kidney anion exchanger 1 in *S. cerevisiae*. *Yeast* 1–14. https://doi.org/10.1002/yea.3652.

Hasib A. M. Sarder, **Xiaobing Li**, Charlotta Funaya, Emmanuelle Cordat, Manfred J. Schmitt*, Björn Becker*. 2020. *Saccharomyces cerevisiae*: first steps to a suitable model system to study the function and intracellular transport of human kidney anion exchanger 1. *mSphere* 5:e00802-19. https://doi.org/10.1128/mSphere.00802-19.

Abbreviation list:

α-ICs	α-intercalated cells
4-PBA	4-phenyl butyric acid
aa	Amino acid
AE1	Anion exchanger 1
Amp	Ampicillin
APS	Ammonium persulfate
bp	Base pair
BSA	Bovine serum albumin
cER	Cortical Endoplasmic Reticulum
CA II	Carbonic anhydrase II
COP	Coat protein
C-Terminus	Carboxy terminus of a protein
dRTA	Distal renal tubular acidosis
DNA	Deoxyribonucleic acid
dNTP	Deoxynucleoside triphosphate
d/o	Drop out
ds	Double-stranded
DTT	Dithiothreitol
DMSO	Dimethyl sulfoxide
eGFP	Enhanced green fluorescent protein
E. coli	*Escherichia coli*
EDTA	Ethylenediaminetetraacetic acid
ESCRT	Endosomal sorting complex required for transport
ER	Endoplasmic reticulum
ERAD	ER-associated protein degradation
EV	Empty vector
FITC	Fluorescein isothiocyanate
GLB	Gel loading buffer
GTE	Glucose-Tris-EDTA
HRP	Horseradish peroxidase
HSR	Heat shock response
IPTG	Isopropyl-β-D-thiogalactopyranoside
kAE1	Kidney anion exchanger 1
Kan	Kanamycin
kb	Kilobase
kDa	Kilodalton
MVBs	Multivesicular bodies

NatR	Nourseothricin resistance
N-Terminus	Amino terminus of a protein
OD	Optical density
PAGE	Polyacrylamide gel electrophoresis
PBS	Phosphate-buffered saline
PCR	Polymerase chain reaction
PDI	Protein disulfide isomerase
PEG	Polyethylene glycol
Perinuclear ER	Perinuclear endoplasmic reticulum
PMSF	Phenylmethylsulfonyl fluoride
PVDF	Polyvinylidene difluoride
RER	Rough endoplasmic reticulum
RNA	Ribonucleic acid
RNase	Ribonuclease
rpm	Revolutions per minute
RT	Room temperature
S. cerevisiae	*Saccharomyces cerevisiae*
SC	Synthetic complete
SD	Standard deviation of the mean
SDS	Sodium dodecyl sulfate
SIM	Structured illumination microscopy
SLC4A1	Solute carrier family 4 member 1
SR	Splicing reporter
TCA	Trichloroacetic acid
TEM	Transmission electron microscopy
TEMED	Tetramethylethylenediamine
Tris	2-Amino-2-(hydroxymethyl) propane-1,3-diol
TX100	Triton X-100
Tuni	Tunicamycin
Tween 20	Polyoxyethylene (20) sorbitan monolaurate
UPR	Unfolded protein response
UV	Ultraviolet
v/v	Volume per volume
WT	Wild type
w/v	Weight per volume
X-Gal	5-bromo-4-chloro-3-indolyl-β-D-galactopyranoside
yKAE1	Yeast codon-optimized kAE1

Table of Contents

Abstract

Der Anionentransporter kAE1 (kidney anion exchanger 1) ist Teil der basolateralen Membran renaler Zellen und essenziell für das Säure-Basen-Gleichgewicht des Organismus. Mutationen des kodierenden Gens führen zu Fehlfaltung, ER/Golgi-Retention und verfrühtem Abbau von kAE1 und stehen in Verbindung mit der Ausbildung von „distaler renaler tubulärer Azidose“ (dRTA). In dieser Arbeit wurde die Hefe *Saccharomyces cerevisiae* als Modellorganismus zur Untersuchung des intrazellulären kAE1-Transports verwendet. Hochauflösende Mikroskopieverfahren zeigten eine partielle Lokalisation des Transporters an der Plasmamembran, ein Großteil des Proteins akkumulierte jedoch in Membranstrukturen des sekretorischen Weges. Heterologe Expression von kAE1 führte zu einer signifikanten Induktion der UPR, die lediglich vom Expressionslevel und nicht der eigentlichen biologischen Aktivität des Transporters abhängig war. Mittels verkürzter kAE1-Derivate wurde dem C-Terminus des Proteins eine wesentliche Rolle in der Ausbildung von ER-Stress zugewiesen. Durch Steigerung der ER-Faltungskapazität konnte eine partielle Redistribution von akkumulierten kAE1 hin zur Plasmamembran demonstriert werden. Diese Arbeit bietet durch das Aufzeigen unterschiedlicher Strategien zur Verringerung der Akkumulation von kAE1 und zur Steigerung des Transport zur Plasmamembran eine Grundlage für zukünftige Untersuchungen des Anionentransporters oder renalen Proteinen im Allgemeinen im Modellorganismus *S. cerevisiae*.

The bicarbonate transporter ‘kidney anion exchanger 1’ (kAE1) resides in the basolateral membrane of renal epithelial cells playing an important role in the acid-base homeostasis. Various autosomal mutations in the respective encoding gene resulting in misfolding, ER/Golgi retention, and premature degradation of kAE1 are linked to the medical condition “distal renal tubular acidosis” (dRTA). In this study, *Saccharomyces cerevisiae* was used as model to further analyze the intracellular trafficking of kAE1. Electron and structured illumination microscopy analyses indicated that kAE1 partially localizes at the yeast plasma membrane, however, most of the protein was accumulated in membrane-like structures of secretory pathway compartments. Further analysis revealed that heterologous expression of kAE1 derivates led to strong UPR activation, which was solely dependent on the expression level and separated from the biological activity of the transporter. Expression of different truncated kAE1 variants also showed that the C-terminal region plays an essential role in the development of ER stress. Furthermore, the total folding capacity of the ER was significantly increased, resulting in a

partial redistribution of ER-accumulated kAE1 to the plasma membrane. By providing novel strategies to decrease intracellular kAE1 accumulation, thereby improving the desired targeting to the plasma membrane, this study opened a promising basis for future kAE1-related research.

1. Introduction

1.1. Architecture and function of the human kidney

Kidneys are the central components of the urinary system. They play an essential role in maintaining the organisms' homeostasis by balancing extracellular fluids. The main function of a kidney is to filter blood plasma (Ogawa *et al.*, 2017; Zimmerman *et al.*, 2019). To achieve this, they excrete toxins and metabolic waste through the urine and return essential substances, most of the water and solutes back to the bloodstream. By maintaining the water-electrolyte and the acid-base balance, kidneys also participate in regulating the blood volume and ionic composition as well as its pH, pressure, and osmolarity (Natochin, 2019).

Each kidney is composed of about a million nephrons. Nephrons are the functional units of the kidneys where all the processes leading to urine formation occur. Each nephron is composed of a renal corpuscle associated with a renal tubule (Miao & Abraham, 2014). The renal corpuscle consists of a capillary network called the glomerulus, surrounded by the glomerular capsule (or Bowman's capsule). After blood plasma filtration in the glomerular capsule, the filtered fluid passes through the renal tubule, which is divided into three different parts: the proximal convoluted tubule, the nephron loop (or loop of Henle), and the distal convoluted tubule (Roy *et al.*, 2015; Howie, 2019). Then, a single collecting duct collects the urine of the distal convoluted tubules from several nephrons. Each segment of the renal tubule has separate functions and is therefore composed of different cell types. Intercalated cells appear in the last part of the distal convoluted tubule and in the collecting duct, where they are interspersed among principal cells (Chen *et al.*, 2019). The function of principal cells is to maintain the water/Na^+ balance of the organisms, whereas intercalated cells play an essential role in the regulation of the acid-base homeostasis (Al-Awqati & Gao, 2011). Three different types of intercalated cells exist, each expressing specific membrane transport proteins and thus contributing differently to the process of urine formation (Figure 1). These cells are classified into type A (or α), type B (or β) and non-A, non-B intercalated cells, which are characterized by the presence of the kidney anion exchanger 1 (kAE1), by the cellular localization of the H^+-ATPase, and by the expression of the anion transporter pendrin. In α-intercalated cells, kAE1 is transported to the basolateral membrane, the H^+-ATPase is localized at the apical membrane, and no pendrin is expressed (Al-Awqati, 2013).

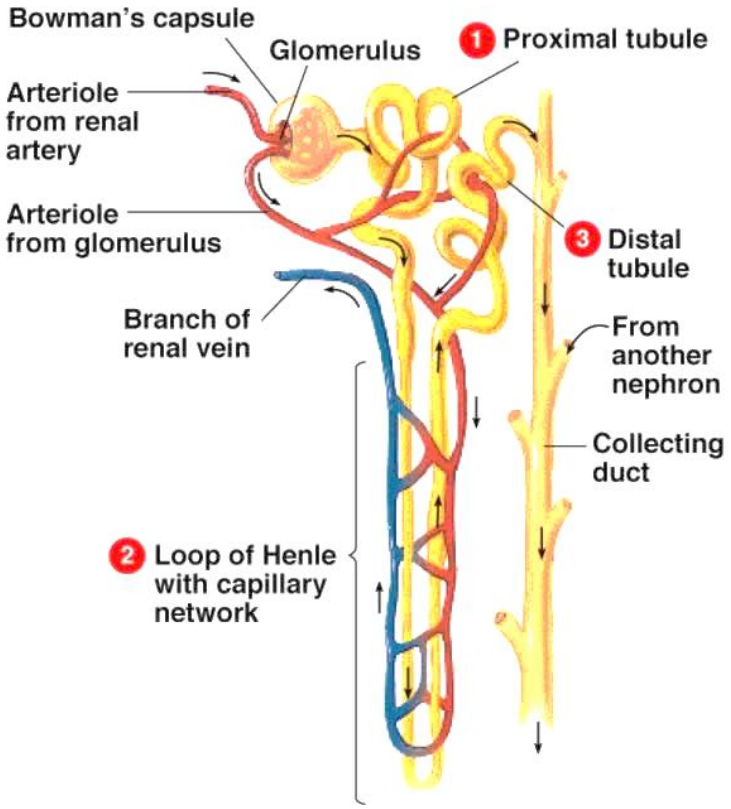

Figure 1: Schematic representation of nephron structure. Each nephron consists of a renal corpuscle associated with a renal tubule. The renal corpuscle is composed of the glomerulus, surrounded by the glomerular capsule (or Bowman's capsule). After blood plasma filtration in the glomerular capsule, the filtered fluid follows three different pathways: the proximal convoluted tubule (1), the nephron loop (2), and the distal convoluted tubule (3). The figure is adapted from Ahlstrom & Garud, 1996.

1.2. Erythroid anion exchanger 1 (AE1) and kidney anion exchanger 1 (kAE1)

SLC4A1 (solute carrier family 4, anion exchanger, member 1) is a protein-coding gene on the long arm of chromosome 17 (Yenchitsomanus *et al.*, 2005). The gene spans 19,757 bp of genomic DNA and consists of 20 exons separated by 19 introns. The start codon is located at exon 2, and the stop codon is located at exon 20 (Jain *et al.*, 2019). The gene encodes two isoforms of the anion exchanger 1 (AE1) family: eAE1 (erythroid anion exchanger 1) and kAE1 (kidney anion exchanger 1). The human integral membrane protein eAE1consisting of 911 amino acids (aa), is mainly expressed in human red blood cells at a high copy number of approximately 1×10^6 copies per cell and has a molecular weight of 95 kDa (Genetet *et al.*, 2017). It can be structurally subdivided into a cytoplasmic domain (aa 1-360, 40 kDa) and a membrane domain (aa 361-911, 55 kDa). The cytoplasmic domain works as an anchorage site for the cell skeleton based on its interactions with ankyrin, band 4.1 (EPB41), and 4.2 (EPB42), which is

critical for the maintenance of the biconcave disc shape of red blood cells (Quilty *et al.*, 2002). The membrane domain mainly plays a role in the Cl^-/HCO^-_3 exchange activity of the protein (Yenchitsomanus *et al.*, 2005). eAE1 additionally attaches to other proteins involved in trafficking, e.g., glycophorin A, to ensure its transport to the correct cellular location (Genetet *et al.*, 2017). The isoform kAE1, in contrast, is expressed in α-intercalated cells in the kidney, lacking the first 65 N-terminal aa due to the use of a second promoter in the intron 3 and alternative splicing. Therefore, mature kAE1 consists of 846 aa and has a molecular weight of ca. 87.2 kDa, while a short C-terminus is conserved in both erythroid and renal isoforms (Sun *et al.*, 2019; Abbas *et al.*, 2018). When functioning normally, the renal tubules can reabsorb substances that the body needs and excrete unneeded material into the urine (Rivera-Santiago *et al.*, 2017). The function of α-intercalated cells is to release acid into the urine, thereby removing it from the body (Chang *et al.*, 2018). The kAE1 protein is localized at the basolateral membrane of α-intercalated cells in the kidney's collecting tubule, where it mediates Cl^- exchange from the urine into cells and the exchange of HCO_3^- from the cell into the urine, thereby maintaining urine pH homeostasis (Reithmeier *et al.*, 2016). This thesis focuses on the study of kAE1, and the following part mainly reviews the knowledge of kAE1 both in mammalian and yeast cells.

1.3. Structure and function of kAE1

kAE1 is a dimeric glycoprotein with 14 transmembrane segments (TM) and cytosolic amino- (N) and carboxyl (C)-terminal ends (Takeuchi *et al.*, 2017). Each kAE1 monomer is composed of a gate domain (TM 5, 6, 7, 12, 13, and 14) and a core domain (TM1, 2, 3, 4, 8, 9, 10, and 11), whereas the later contains the anion-binding site (Figure 2). The single N-glycosylation site at Asparagine 642 (numbering relating to eAE1 isoform) is located within the fourth extracellular loop between TM7 and TM8 (Takeuchi *et al.*, 2017). In the membrane and in detergent solutions, kAE1 is present as a mixture of dimers and tetramers (Almomani *et al.*, 2011).

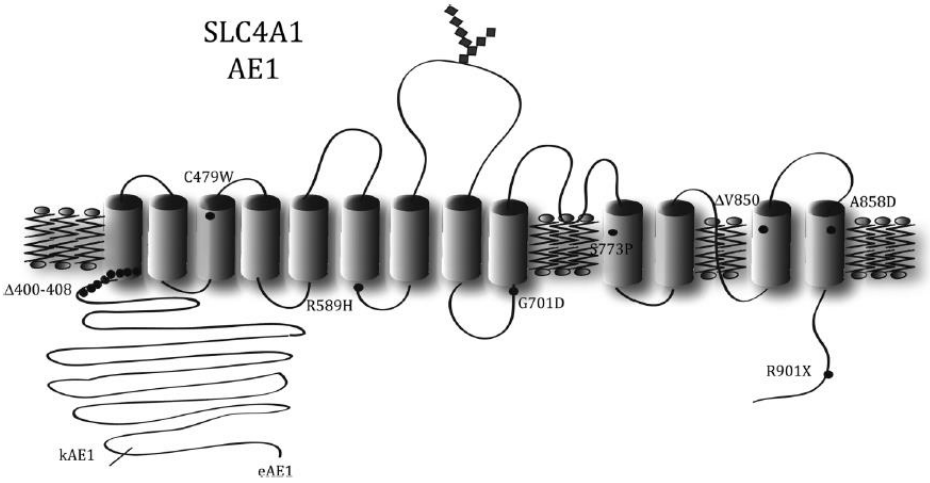

Figure 2: Topology prediction of kAE1 and eAE1. The glycosylation site at the fourth extracellular loop of the protein is indicated by black squares. Adapted from Almomani *et al.*, 2011.

kAE1 plays an essential role in the regulation of the acid-base balance by providing a major exit route for HCO_3^- in exchange for Cl^- across the basolateral membrane of α-intercalated cells. In addition to kAE1, other proteins, such as the carbonic anhydrase (CA) II, the H^+-ATPase, and H^+/K^+-ATPase, are essential for the proper bicarbonate reabsorption into the blood and acid secretion into the urine. The former catalyzes the hydration of carbon dioxide (CO_2), thus generating carbonic acid (H_2CO_3) (Almomani *et al.*, 2011). The H_2CO_3 produced can subsequently be dissociated into H^+ and $HCO3^-$ (Sorrell *et al.*, 2016). H^+ is then secreted through the apical membrane into the tubular lumen by H^+-ATPase and H^+/K^+-ATPase. HCO_3^- is reabsorbed across the basolateral membrane-mediated via kAE1 to exchange Cl^- from the urine into the cell (Kittanakom *et al*., 2004). An abnormality of kAE1 (e. g., mutations in the kAE1-encoding gene) can lead to a defect in its physiological transport activity and cause HCO_3^- to accumulate in the cells (Almomani *et al.*, 2016). To keep the intracellular acid-base homeostasis and electroneutral balance, H^+ is subsequently retained in the cell instead of being secreted into the urine (Vichot *et al.*, 2016). In the long run, the accumulation of both HCO_3^- and H^+ in the cytosol inhibits H_2CO_3 dissociation and causes its accumulation (Figure 3). Eventually, the failure of H^+ secretion into the tubular lumen and H_2CO_3 dissociation problems lead to a disease called distal renal tubular acidosis (Yenchitsomanus *et al.*, 2005; Cordat *et al*., 2006).

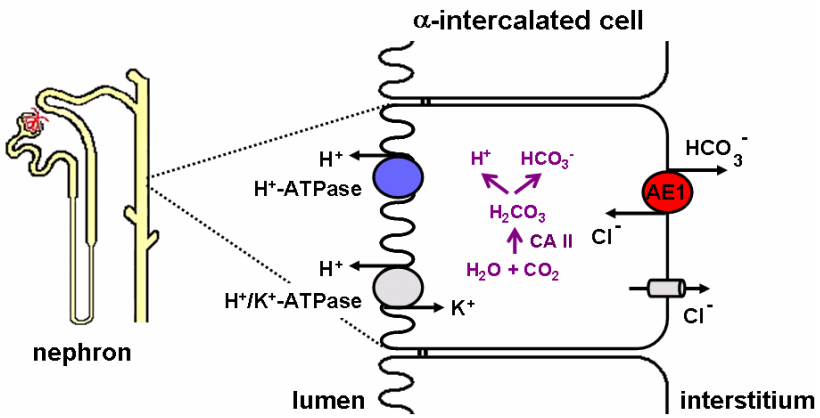

Figure 3: Schematic representation of the α-intercalated cells in the distal tubule of the nephron. Cytoplasmic carbonic anhydrase II (CA II) catalyzes the interconversion of H_2O and CO_2 into H^+ and HCO_3^-. The apical H^+-ATPase and H^+/K^+-ATPase extrude acid (H^+) into the tubular lumen while the basolateral kAE1 reabsorbs remaining HCO_3^- ions in exchange with Cl^- into the body. From Yenchitsomanus *et al.*, 2005.

1.6. Distal renal tubular acidosis (dRTA)

Distal renal tubular acidosis is generally described as a pathophysiological syndrome triggered by improper acid removal from the bloodstream into the urinary system. This leads, consequently, to excess acid being retained in the blood and subsequently causing an inability to acidify the urine to a pH < 5.5 (Jain *et al.*, 2019). Common symptoms for dRTA are renal stone formation, nephrocalcinosis, and metabolic acidosis. In addition, dRTA can also lead to muscle weakness, hypokalemia, and metabolic bone disease (Jamshidian *et al.*, 2018). Although several risk factors can lead to the development of dRTA, mutations in the kAE1-encoding gene *SLC4A1* are among the leading causes of this disease. Mutations in *SLC4A1* can alter kAE1 folding, trafficking, and functionality in α-intercalated cells (Cordat *et al.*, 2006). Some mutations can lead to two types of dRTA: autosomal dominant or autosomal recessive dRTA (Table 1). Typically, dominant dRTA mutations do not affect the anion transport activity of the protein. Instead, mutated kAE1 variants are retained intracellularly (R589H, S613F) or mistargeted to the apical membrane (R901X, G609R) instead of being correctly trafficked to the basolateral membrane (Vichot *et al.*, 2016; Seeger *et al.*, 2017). Mutations leading to recessive dRTA can cause kAE1 trafficking defects, resulting in kAE1 misfolding, retention in the Golgi apparatus (G701D) or degradation by a proteasome-dependent mechanism (S773P).

Table 1. Mutations in the gene *SLC4A1* causing autosomal dominant (AD) and autosomal recessive (AR) distal renal tubular acidosis (dRTA)

Resulting in AD	**Resulting in AR**
R589H	G701D (Bangkok I)
G609R	V488M (Coimbra)
S613F	S773P (Siriraj I)
A888L+889X	ΔV850
R901X (Walton)	R602H (Songkla I)

Adopted from Yenchitsomanus *et al.,* 2005

Both dominant and recessive kAE1 mutants can form heterodimers with wild-type kAE1 when co-expressed *in vivo* (Takeuchi *et al.*, 2016). For dominant dRTA, the formed heterodimers cause kAE1 mistargeting to the apical membrane or retention in the ER, thus showing a "dominant-negative" effect (Karet, 2004; Sun *et al.*, 2019). In the case of recessive dRTA, the formed heterodimers can promote the trafficking of wild-type kAE1 to the cell surface, presenting a "dominant-positive" effect (Yenchitsomanus *et al.,* 2005; Reithmeier *et al.*, 2016).

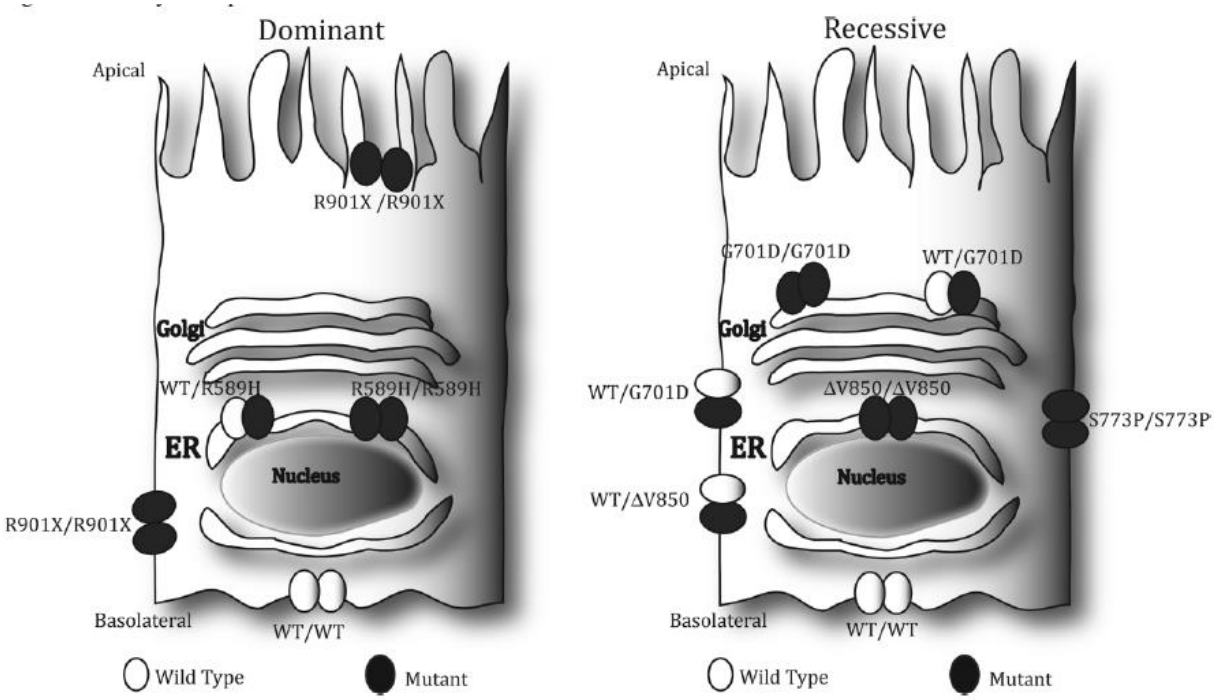

Figure 4: kAE1 mistrafficking based on recessive or dominant dRTA-causing mutations. Wild-type kAE1 (WT, white circles) is located as a homodimer at the basolateral membrane of α-intercalated renal cells under normal physiological conditions. (Left) In case of dominant dRTA-causing mutations (e.g., R901X, R589H, black circles), homodimers of R901X are either trafficked to the basolateral or the apical membrane. Homodimers of kAE1 R589H and heterodimers of this mutant with WT kAE1 are retained in the ER. (Right) kAE1 mutations resulting in recessive dRTA (e.g., G701D, S773P, ΔV850, black circles) form homodimers that are trafficked to the basolateral membrane (S773P) or are retained in ER (ΔV850) or Golgi structures (G701D), respectively. After co-expression with WT kAE1, partial localization (WT/G701D and WT/ΔV850) to the basolateral membrane can be restored. From Almomani *et al.*, 2011.

1.7. Unfolded protein response (UPR) in mammals and yeast

Protein synthesis is a core biological process that plays a vital role in the maintenance of cellular proteins through the production of new proteins. The process is divided into two important phases, transcription and translation, and many cellular organelles are involved. The ER plays a crucial role in translation-related processes because only correctly folded and assembled proteins can execute their designated function (Mori, 2015). Although many proteins with a chaperone activity are present in the ER lumen and involved in folding newly translated proteins, some may remain unfolded or misfolded. Many organisms such as yeast or mammalian cells developed specified mechanisms to prevent aggregation of inadequately folded proteins, such as the ER-associated protein degradation (ERAD), which eventually leads to the ubiquitination and degradation of such proteins (Patil & Walter 2001; Mori, 2009).

However, once the number of unfolded or misfolded proteins surpasses a certain threshold, the cell is no longer capable of counteracting the aggregation of these defective proteins in the ER (Guzel *et al.*, 2017). A continuous accumulation can subsequently trigger a cellular stress response called unfolded protein response (UPR) (Geiler-Samerotte *et al.*, 2011; Wu *et al.*, 2014). UPR is an adaptive mechanism of the ER, allowing cells to cope with ER stress conditions via different molecular mechanisms to eventually restore cellular protein homeostasis (Ogawa & Mori, 2004).

1.7.1. UPR mechanisms in mammals

To date, it is generally accepted that the UPR is controlled by three ER transmembrane proteins which act as crucial regulators: inositol-requiring enzyme 1 (IRE1), double-stranded RNA-activated protein kinase-like ER kinase (PERK), and activating transcription factor 6 (ATF6) (Oslowski & Urano, 2011). Under normal physiological conditions, the ER chaperone BiP is bound to the luminal domains of IRE1/PERK/ATF6, thereby keeping them inactive. In the case of ER stress, BiP dissociates from the regulators, which leads to their activation (Lee *et al.*, 2002). The activated sensors will trigger downstream effectors and initiate the following functions: adaptive response, feedback control, and cell fate regulation (Ogawa & Mori, 2004). Cells will first use adaptive measures to reduce or even avoid ER stress, which can be turned off via feedback-controlled mechanisms in case of a successful restoration or maintenance of the ER homeostasis. Furthermore, UPR also regulates cell survival or death depending on the severity of the ER stress conditions (Figure 5).

In the process of dealing with UPR, IRE1, PERK, and ATF6 play an essential role in deciding the subsequent ER stress pathways. IRE1, which belongs to a type I ER transmembrane kinase, senses ER stress by its N-terminal luminal domain. Upon detecting the existence of unfolded proteins, IRE1 autophosphorylates and dimerizes to become active. The continuing ER stress can trigger IRE1 to recruit TNF-receptor-associated factor 2 (TRAF2) and the activation of apoptosis-signaling-kinase 1 (ASK1). Next, the activated ASK1 can activate c-Jun N-terminal protein kinase (JNK), regulating apoptosis via controlling members of the BCL2 protein family. Furthermore, IRE1 has two isoforms: IRE1α and IRE1β. IRE1α is expressed in all cell types, and a knockout leads to embryonic lethality in mice. However, expression of IRE1β is limited in the cell, and no lethal effects can be found in knockout mice. The second type of regulator is PERK, an ER-resident transmembrane protein kinase, which self-activates via autophosphorylation and oligomerization in case of ER stress to control the cell cycle (Oslowski & Urano, 2011). The third type of key regulator, ATF6, also has two

isoforms, ATF6α and ATF6β. In an ER stress scenario, ATF6α transits to the Golgi, where it is cleaved by site 1 (S1) and site 2 (S2) proteases, thus generating an active b-ZIP transcription factor. This, in turn, leads to the expression of various UPR-related genes coding for proteins that are involved in protein folding, maturation, and degradation (Oslowski & Urano, 2011).

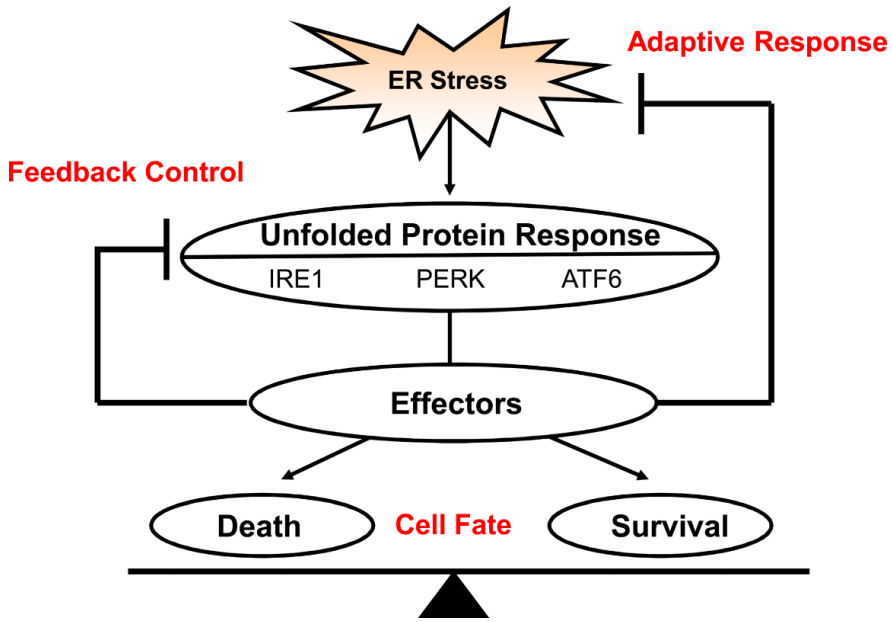

Figure 5: How mammalian cells tackle unfolded protein responses (UPR). The key UPR regulators (IRE1/PERK/ATF6) are sensing ER stress and activating downstream effectors to decide the cell fate (death or survival). From Oslowski & Urano, 2011.

1.7.2. UPR mechanisms in yeast

The unfolded protein response also exists in yeast. In yeast cells, ER stress is monitored by the ER-located transmembrane sensor protein Ire1p. When yeast cells have to cope with ER stress, Ire1p is activated by either the release of the molecular chaperone Kar2p (homolog of the mammalian protein BiP) from the lumenal domain of Ire1p or the direct binding of unfolded proteins (Yoshida *et al.*, 2013; Wu *et al.*, 2014). After oligomerization and autophosphorylation of the kinase, the cytosolic ribonuclease domain of Ire1p splices the sole intron in the *HAC1*-pre-mRNA, initiating its translation into the transcription factor Hac1p (Chakraborty *et al.*, 2016). Finally, Hac1p is translocated into the nucleus to regulate the expression of UPR target genes (Figure 6). This Ire1p-Hac1p unfolded-protein-response element (UPRE) is important and sufficient to activate transcription in response to some agents that cause ER stress in yeast cells (Ishikawa *et al.*, 2011; Shpilka & Haynes, 2018). Through the activation of the UPR, cells try to alleviate stress via up-regulation of nearly 400 target genes, including lipid biosynthesis

enzymes, ER chaperones, and proteins of the ERAD machinery. Notably, among all up-regulated genes, the yeast ER-lumenal chaperone Kar2p, which belongs to the Hsp70 family, plays a vital role in the UPR due to its interaction with Ire1p (Okamura *et al.*, 2000). Kar2p interaction with polypeptide chains during post-translational ER import via the Sec61p complex has also been shown to minimize potential inefficient backward motions of the nascent protein, eventually facilitating ER translocation (Sanders *et al.*, 1992; Matlack *et al.*, 1999). The potential aggregation of heterologously expressed proteins in yeast ER structures initiating cellular stress responses like the UPR has already been described by various studies. Sarder *et al.* (2020) studied the function and intracellular transport of kAE1 in *Saccharomyces cerevisiae* and found that most of the kAE1 accumulated in ER or ER-derived vesicles (Sarder *et al.*, 2020). Therefore, this thesis further examined and addressed the reasons for this massive accumulation and explored the yeast cell UPR process after heterologous kAE1 overexpression.

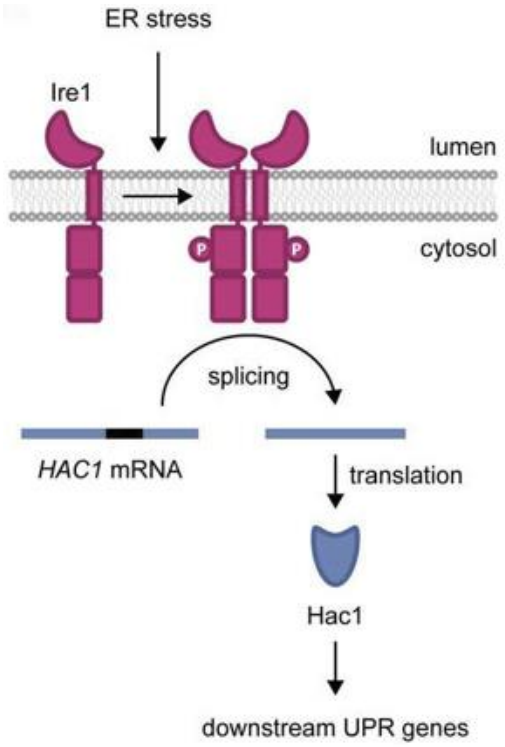

Figure 6: Ire1p-mediated unfolded protein response (UPR) in yeast. In case of ER stress, Ire1p oligomerizes and autophosphorylates through its cytosolic kinase domain. Following this activation, Ire1p is responsible for the splicing of *HAC1*-mRNA. After translation, the active transcription factor Hac1p up-regulates downstream UPR genes to mediate ER-stress in the cell. Adapted from Wu *et al.*, 2014.

1.8. *S. cerevisiae* as model system to study renal proteins

Several systems have been employed to characterize kidney diseases, such as mouse models

or tissue culture cell lines (Botstein *et al.*, 1997). Although many of these model systems have been used in various studies and helped in the understanding of different research questions, they also have several disadvantages. Especially animal systems such as mouse models are expensive and need special handling. Additionally, the generation and establishment of mutations takes a long time and is often unstable (Kolb *et al.*, 2011). While tissue cultures are more straightforward to use in different experimental set-ups, it is often very problematic to find the best cell line to answer a specific scientific question (Hsu *et al.*, 2007). Hence, the search for a more economical model system with better genetic manipulation tools and a shorter generation time to study the basics of renal proteins is always desirable (Flower *et al.*, 2005).

Both, yeast and mammalian cells are of eukaryotic origin, and many cellular mechanisms are conserved between them. Some basic cellular processes were even firstly discovered in yeast cells (Gershon & Gershon, 2000). Compared with mammalian cells, yeast has some unique advantages: First and foremost, due to the relatively fast cell cycle, yeast cells can be efficiently and ecologically used in various types of assays (Suzuki & Ohsumi, 2007). Secondly, the main protein glycosylation pathways are highly conserved between yeast and mammalian cells (Hauser *et al.*, 2001). Thirdly, various experimental approaches are available for yeast facilitating the uptake of foreign DNA, thus providing the possibility to easily express genes heterologously (Gershon & Gershon, 2000). Additionally, there are many useful tools and large numbers of databases, such as yeast knockout collections, which provide an ideal starting point for genome-wide screenings or the study of protein-protein interactions. In summary, using yeast cells as a model system is eligible to study the basics of human renal proteins in a cheap, fast, and easy way (Kolb *et al.*, 2011). However, like every model system, *S. cerevisiae* also has some limitations when studying renal proteins (Petschnigg *et al.*, 2011). Yeasts are single-cell organisms, so the cells are not polarized in contrast to kidney epithelial cells. For this reason, yeast cannot be used to investigate cell-to-cell interactions that occur in the complex human kidney (Cherry *et al.*, 2011; Verghese *et al.*, 2012).

In yeast, there is no *SLC4A1* homolog; however, Bor1p is the best-characterized example of a *SLC4A1*-like protein (Kaya *et al.*, 2009; Thurtle-Schmidt *et al.*, 2016). The protein is encoded by the gene *BOR1* (systematic name YNL275W) and functions as the boric acid/borate efflux transporter binding HCO_3^-, I^-, Br^-, NO_3^- and Cl^- (Nozawa *et al.*, 2006). In *Saccharomyces*, Bor1p is localized at the plasma membrane, where it manages the boron or borate efflux pathway to help cells survive high levels of boric acid (Takano *et al.*, 2005). Recent studies identified the phosphate transporter Pho88p as partner of Bor1p, suggesting that Bor1p is

involved in inorganic phosphate transport in *S. cerevisiae* by forming a larger integral membrane protein complex (Parker & Boron, 2013). Furthermore, Pyle *et al.* (2019) used Bor1p from *S. cerevisiae* to explore its structure and function as transporter; the results showed that Bor1p potentially forms dimers under normal physiological conditions that are stabilized through the interaction with membrane lipids, while its transport activity is mediated by the Bor1p monomer (Pyle *et al.*, 2019).

1.9. *S. cerevisiae* as model system to study kAE1

So far, different renal membrane proteins and kidney-localized ion channel proteins have been successfully expressed and studied in yeast (Figure 8) (Kolb *et al.*, 2011). Additionally, some of the disease-causing mutant proteins identified in mammalian cells could also be expressed in yeast cells (Zhao & Reithmeier, 2001). Notably, the AE1 anion transport domain B3mem has already been expressed at high levels in *S. cerevisiae* and was successfully targeted to the yeast plasma membrane, where it could mediate chloride transport. Additionally, its overexpression did not influence the survival or growth of the yeast cells (Sekler *et al.*, 1995; Groves *et al.*, 1996). The latest study expressed yeast codon-optimized full-length kAE1 (ykAE1) in *S. cerevisiae* and also showed a partial localization of biologically active protein at the yeast plasma membrane (PM), indicating the potential of *S. cerevisiae* as model system to study trafficking, activity, and/or degradation of human kAE1 (Sarder *et al.*, 2020; Li *et al.*, 2021). For these reasons, yeast represents a promising model to study intracellular trafficking of wild-type kAE1 and mistrafficking of mutant kAE1 variants responsible for dRTA (Zhao & Reithmeier, 2001).

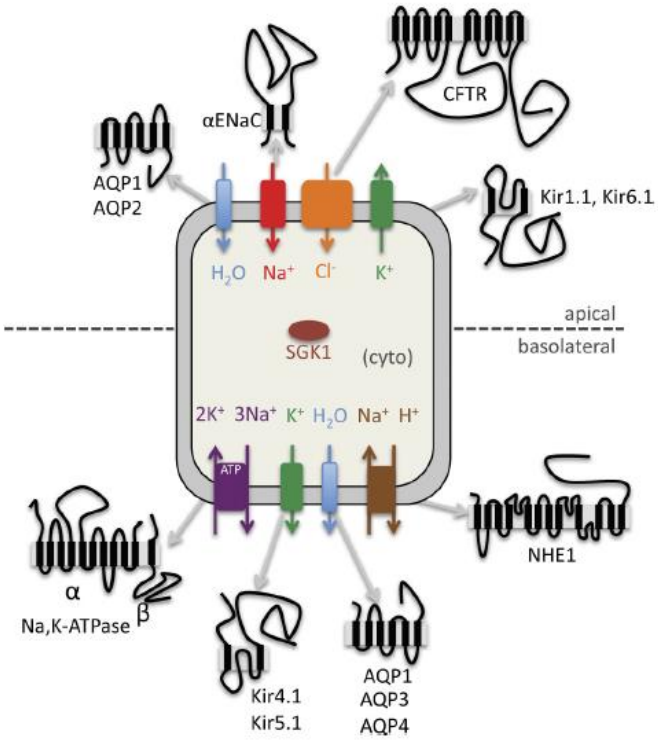

Figure 8: Summary for varieties of human renal proteins expressed in yeast. Overview of heterologously expressed renal membrane proteins in yeast. From Kolb *et al.*, 2011.

1.10. Aim of the study

The anion transporter kAE1 mediates the coupled efflux of bicarbonate ions and the absorption of chloride in α-intercalated cells. Together with the proton pump V-H^+-ATPase and the carbonic anhydrase II, and the anion transporter pendrin, the transporter plays a crucial role in the systemic acid-base equilibrium (Cordat *et al.*, 2006). In mammals, mutations in the kAE1-encoding gene *SLC4A1* are connected to the development of the pathological disorder called distal renal tubular acidosis. Some of the disease-related kAE1 mutations are associated with the retention and/or the mistrafficking of the anion transporter. However, the molecular mechanisms involved in the transport of kAE1 to the basolateral membrane are not well characterized. Additionally, the importance of kAE1 mistrafficking in the actual development of dRTA is still debated (Almomani *et al.*, 2011; Li *et al.*, 2021). This thesis aims to use yeast as a model system for the identification of proteins affecting intracellular kAE1 trafficking to its designated location in the cell.

To achieve the goal, the first step was to check the heterologous expression of various

yeast codon-optimized kAE1 variants in yeast and their localization at the yeast plasma membrane by using SIM (super-resolution microscopy) and EM (electron microscopy). Based on the results pointing to a massive accumulation of all tested kAE1 variants in different membrane structures, the cause of these aggregations was further analyzed using various techniques. Because the accumulation of kAE1 mainly occurred in yeast ER membranes and COPII vesicles, inducing a significant UPR activation and severe growth defects, several methods for boosting the folding capacity of the yeast ER were tested to potentially redistribute and/or to prevent the accumulation and improve kAE1 plasma membrane targeting directly.

2. Materials and Methods

2.1. Organisms

2.1.1. Escherichia coli strains

Bacterial strains used in this thesis are listed in Table 2.

Table 2: *Escherichia coli* strains, genotype, and reference

Strain	Genotype	Reference
NEB-5α	*fhuA2 Δ(argF-lacZ) U169 phoA glnV44 Φ80Δ (lacZ)M15 gyrA96 recA1 relA1 endA1 thi-1 hsdR17*	New England Biolabs
YSC3868	*DH5F-)80lacZM15 (lacZYA-argF) U169 deoR recA1 endA1 hsdR17 (rk-, mk+) phoA supE44 - thi-1 gyrA96 relA1*	GE Dharmacon
TOP10	F⁻ *mcr*A Δ(*mrr-hsd*RMS-*mcr*BC) φ80*lac*ZΔM15 Δ*lac*X74 *rec*A1 *ara*D139 Δ(*ara-leu*)7697 *gal*U *gal*K λ⁻ *rps*L(Str^R) *end*A1 *nup*G	Thermo Fisher Scientific

2.1.2. Yeast strains

Yeast strains, genotype, and references are listed in Table 3

Table 3. Yeast strains and deletion mutants used in this study

Strain	Genotype	Reference
BY4741	MAT*a his3Δ1 leu2Δ0 met15Δ0 ura3Δ0*	OpenBiosystems
Δ*ist2* (BY4741)	MAT*a his3Δ1 leu2Δ0 met15Δ0 ura3Δ0 ist2Δ:: loxP*	Prof. Dr. M. Schmitt Group
BY4742	MATα *his3Δ1 leu2Δ0 lys2Δ0 ura3Δ0*	OpenBiosystems
Δ*ire1* (BY4742)	MATα *ire1Δ0::KAN4 his3Δ1 leu2Δ0 lys2Δ0 ura3Δ0*	OpenBiosystems
Δ*hac1* (BY4742)	MATα *hac1Δ0::KAN4 his3Δ1 leu2Δ0 lys2Δ0 ura3Δ0*	OpenBiosystems
Δ*end3* (BY4742)	MATα *end3Δ0::KAN4 his3Δ1 leu2Δ0 lys2Δ0 ura3Δ0*	OpenBiosystems
BY4742-GEV	MATα *his3Δ1 leu2Δ0 lys2Δ0 ura3Δ0, leu2Δ0*::PACT1-GEV-NatMX	Sarder *et al*. (2020)
S288C	MATα *his3Δ1 leu2Δ0 lys2+/lys+ met15Δ0 ura3Δ0*	OpenBiosystems
S288C Sec63p-mCherry	MATα *his3Δ1 leu2Δ0 met15Δ0 ura3Δ0 lys+ can1Δ::GAL1pr-SceI::STE2pr-SpHIS5 lyp1Δ::STE3pr-LEU2 NAT::TEF2pr-mCherry-Sec63*	Maya Schuldiner
S288C Sec13p-	MATα *his3Δ1 leu2Δ0 lys2+/lys+ met15Δ0 ura3Δ0 can1Δ::STE2pr-*	Maya Schuldiner

mCherry		*sp HIS5 lyp1Δ::STE3pr-LEU2 Sec13_mCherry::Nat*	
S288C mCherry	Erg6p-	MAT*α his3Δ1 leu2Δ0 lys2+/lys+ met15Δ0 ura3Δ0 can1Δ::STE2pr-sp HIS5 lyp1Δ::STE3pr-LEU2 Erg6_mCherry::Nat*	Maya Schuldiner
S288C mCherry	Chc1p-	MAT*α his3Δ1 leu2Δ0 lys2+/lys+ met15Δ0 ura3Δ0 can1Δ::STE2pr-sp HIS5 lyp1Δ::STE3pr-LEU2 Chc1_mCherry::Nat*	Maya Schuldiner
S288C mCherry	Cop1-	MAT*α his3Δ1 leu2Δ0 lys2+/lys+ met15Δ0 ura3Δ0 can1Δ::STE2pr-sp HIS5 lyp1Δ::STE3pr-LEU2 Cop1_mCherry::Nat*	Maya Schuldiner
S288C mCherry	Anp1p-	MAT*α his3Δ1 leu2Δ0 lys2+/lys+ met15Δ0 ura3delta0 can1Δ::STE2pr-sp HIS5 lyp1Δ::STE3pr-LEU2 Anp1_mCherry::Nat*	Maya Schuldiner
S288C mCherry	Sec7p-	MAT*α his3Δ1 leu2Δ0 lys2+/lys+ met15Δ0 ura3Δ0 can1Δ::STE2pr-sp HIS5 lyp1Δ::STE3pr-LEU2 Sec7_mCherry::Nat*	Maya Schuldiner
S288C mCherry	Snf7-	MAT*α his3Δ1 leu2Δ0 lys2+/lys+ met15Δ0 ura3Δ0 can1Δ::STE2pr-sp HIS5 lyp1Δ::STE3pr-LEU2 Snf7_mCherry::Nat*	Maya Schuldiner
S288C mCherry	Vam6p-	MAT*α his3Δ1 leu2Δ0 lys2+/lys+ met15Δ0 ura3Δf0 can1Δ::STE2pr-sp HIS5 lyp1Δ::STE3pr-LEU2 Vam6_mCherry::Nat*	Maya Schuldiner

2.1.3. Plasmids

In Table 4, all plasmids and their characteristics are listed with their appropriate sources.

Table 4. Plasmids used for this thesis, their characteristics, and source

Plasmid	Characteristics	Source
pYES2.1/V5-His-TOPO	*S. cerevisiae* expression vector, Amp resistance marker, *GAL1* promoter, *URA3* gene, TOPO-Cloning site, V5-epitope (C-term), polyhistidine (6×His) -tag (C-term)	Invitrogen
pSTBlue-1 AccepTor™ Vector	Multiple cloning region, *LacZα* gene for blue-white screening, pUC origin, Amp and Kan resistance marker.	Roche
pESC-HIS Vector	*S. cerevisiae* expression vector, Amp resistance marker, GAL1 promoters, *HIS3* gene.	Obtained from Molecular- and Cell Biology, Prof. Dr. M. Schmitt Group
pESC-Leu Vector	*S. cerevisiae* expression vector, Amp resistance marker, GAL1 promoter, *LEU2* gene.	Obtained from Molecular- and Cell Biology, Prof. Dr. M. Schmitt Group
YIp128-Pma1-mRFP	Yeast integrative plasmid, linearized before yeast transformation by *BglII*, *LEU2* gene	Dr. Malinsky's lab
YIp211-Pma1-mRFP	Yeast integrative plasmid, linearized before yeast transformation by *BglII*, *URA3* gene	Dr. Malinsky's lab
pYES2.1 kAE1	pYES2.1 with kAE1 sequence	This study
pYES2.1 kAE1^{FLAG}	pYES2.1-kAE1 with FLAG-tag	This study
pYES2.1 kAE1^{HA}	pYES2.1-kAE1 with HA-tag	This study
pYES2.1 kAE1^{E681Q}	pYES2.1 kAE1 with E681Q mutation	Sarder *et al.* (2020)
pYES2.1-yeGFP-kAE1^{WT}	pYES2.1kAE1 with yeGFP-tag	This study

pYES2.1-kAE1$^{1-491}$	pYES2.1 with kAE1.1-491 amino acids(aa)	This study
pYES2.1-kAE1$^{1-666}$	pYES2.1 with kAE1.1-666 aa	This study
pYES2.1-kAE1^{B3mem}	pYES2.1 with kAE1 C-terminal membrane domain (360–911 amino acids)	Sarder *et al.* (2020)
pYES2.1-ERD2^{V5}	pYES2.1 with V5-tagged H/KDEL receptor Erd2	Obtained from Molecular- and Cell Biology, Prof. Dr. M. Schmitt Group
pESC$_{HIS}$-yeGFP-kAE1^{WT}	pESC$_{HIS}$ kAE1 with yeGFP-tag	Sarder *et al.* (2020)
pBG1805- EV	pBG1805 self-ligation	Thermo Fisher Scientific
pBG1805-*Lag1*	pBG1805 with Lag1p	Thermo Fisher Scientific
pBG1805-*Ice2*	pBG1805 with Ice2p	Thermo Fisher Scientific
pBG1805-*Ist2*	pBG1805 with Ist2p	Thermo Fisher Scientific
pBG1805-*Lip1*	pBG1805 with Lip1p	Thermo Fisher Scientific
pBG1805-*Bor1*	pBG1805 with Bor1p	Thermo Fisher Scientific
pBG1805-*Pma1*	pBG1805 with Pma1p	Thermo Fisher Scientific
pBG1805-*Pdi1*	pBG1805 with Pdi1p	Thermo Fisher Scientific
pBG1805-*Emc1*	pBG1805 with Emc1p	Thermo Fisher Scientific
pBG1805-*Emc4*	pBG1805 with Emc4p	Thermo Fisher Scientific
pBG1805-*Emc5*	pBG1805 with Emc5p	Thermo Fisher Scientific
pBG1805-*Mpd2*	pBG1805 with Mpd2p	Thermo Fisher Scientific
pBG1805-*Eug1*	pBG1805 with Eug1p	Thermo Fisher Scientific
pBG1805-*Scj1*	pBG1805 with Scj1p	Thermo Fisher Scientific
pBG1805-*Ero1*	pBG1805 with Ero1p	Thermo Fisher Scientific

2.2.2. Subcloning

2.2.2.1 TOPO cloning

2 µl of linearized DNA and 0.5 µl pYES2.1/V5-His-TOPO vector were gently mixed with 0.5 µl salt solution (Thermo Fisher Scientific, USA) and incubated for 15 minutes at room temperature, and an aliquot of the reaction mixture was used for the transformation of chemically competent *E. coli* TOP10 cells (Thermo Fisher Scientific, USA). After incubation on ice for 5-30 min, cells were heat-shocked for 30 s at 42°C without shaking and immediately transferred onto ice. 250 µl pre-warmed SOC medium was added and cell suspension was incubated for 1 h at 37 °C at 220 rpm. Afterward, 200 µl were spread on a pre-warmed agar plate containing ampicillin or kanamycin. Finally, plates were incubated at 37 °C overnight.

2.2.2.2 pSTBlue-1 AccepTor^{TM}-Cloning

2 µl of linearized DNA were mixed with 0.5 µl pSTBlue-1 AcceptTor^{TM} vector (Merck-Milllipore) and 2.5 µl 2xligation premix. After incubation at 16 ℃ for 1 h, 2 µl of the reaction mix was transferred to competent cells (NovaBlueSingle Cells). The cell suspension was gently

mixed and incubated on ice for 5 min. Next, the cells were heat-shocked for 30 s at 42 °C and immediately put on ice for 2 min. Following the addition of 250 µl pre-warmed SOC medium, the cells were incubated for 1 h at 37 °C and 220 rpm. 300 µl of each sample were spread on pre-warmed agar plates containing kanamycin, X-Gal, and IPTG.

X-Gal stock solution

X-Gal	20 mg/ml

Dissolved in dimethylsulfoxide (DMSO). Stored at -20 °C protected from light.

IPTG stock solution

IPTG	100 mM

The solution was sterile-filtered and stored at -20 °C

2.2.3. Plasmid construction

2.2.3.1 Sequences of kAE1 variants

kAE1 sequences are listed in the Appendix.

2.2.3.2 Plasmid construction procedure

kAE1^{WT} was generated by conventional PCR with primers listed in Table 5, and cloned into the vector pYES2.1. For construction of the different kAE1 expression plasmids pYES-kAE1^{HA}, pYES-kAE1^{FLAG}, pYES-kAE1^{B3mem}, pYES-kAE1$^{1-491}$, and pYES-kAE1$^{1-666}$, a synthetic cDNA of yeast codon-optimized kAE1 (GeneArts, ThermoScientific) was integrated into pYES2.1 vector and correct integration direction was subsequently checked via *Xba*I/*Bam*HI digestion. For the pYES-yeGFP-kAE1 construct, yeGFP was initially amplified by conventional PCR with the appropriate primers and later ligated with pYES2.1 to obtain pYES2.1-yeGFP. Finally, pYES2.1-yeGFP was linearized again to ligate with pYES-kAE1^{HA} vector (digested both with *Xho*I) to obtain pYES-yeGFP-kAE1 (Sarder *et al.*, 2020). pYES-kAE1^{E681Q} was generated via side-directed mutagenesis using the Q5 mutagenesis kit (NEB) and pYES-kAE1^{WT} as a template by following manufacturer's instructions (Sarder *et al.*, 2020). All DNA constructs were routinely checked for correct sequence (GATC).

Table 5. Primers used in this study (specific mutation sites are underlined)

Primer	Description	5'-3' Sequence	Sources
5' Erd2^{V5}	PCR primer for pYES-Erd2^{V5}	CTCGAGGAATTCATGAATCCGTTTAGA ATCTTAGGTGATTTATCACAT	Becker *et al.* (2016)
3' Erd2^{V5}	PCR primer for pYES-Erd2^{V5}	GGATCCGTCGACCTACGTAGAATCGAG ACCGAGGAGAGGGTTAGGGATAGGCC	Becker *et al.* (2016)

5' kAE1	Amplification of untagged, wild type kAE1 with yeast-optimized codon usage	TACCTGCCGGCAAACTCAACTTCTTCC ctcgaggaattcATGGACGAAAAGAATCAAG AATTGAGATG	
3' kAE1	Amplification of untagged wild type kAE1 with yeast-optimized codon usage	gtcgacggatccTTAAACTGGCATAGCAACT TCATCGTATTC	
5' kAE1^{E681Q}	Mutagenesis primer for kAE1^{E681Q}	GATATTCTTGCAATCCCAAATCAC	Sarder *et al.* (2020)
3' kAE1^{E681Q}	Mutagenesis primer for kAE1^{E681Q}	AAGATAAAAACCAATAAAGCTG	Sarder *et al.* (2020)
5' yeGFP	Overhang primer for *in vivo* recombination in yeast with pYES vector	CACTATAGGGAATATTAAGCTCGCctcgag ATGTCT AAAGGTGAAGAATTATTCAC	Sarder *et al.* (2020)
3' yeGFP	Overhang primer for *in vivo* recombination in yeast with ykAE1	CATCTCAATTCTTGATTCTTTTCGTCacta ccaccaccacc TTTGTACAATTCATCCATACCA	Sarder *et al.* (2020)

2.3. Plasmid isolation from *E. coli*

2.3.1. Alkaline lysis

Alkaline lysis was performed following a modified protocol from Birnboim and Doly (1979). After overnight cultivation, 1.5 ml of the *E. coli* cells were pelleted by centrifugation at 13,000 rpm for 20 s. The pellet was then resuspended in 100 µl GTE-solution. GTE-solution contains EDTA, which chelates divalent cations, therefore inducing destabilization of the bacterial cell wall. It also contains Tris and glucose to maintain the osmotic pressure and pH. Afterward, 150 µl of NaOH/SDS-solution were added, and the suspension was incubated for 5 min at RT. SDS solubilizes membrane proteins and lipids, ensuring cell lysis, whereas NaOH is supplemented to increase the pH leading to precipitation of plasmid and chromosomal DNA. 150 µl potassium acetate were added, the solution was gently mixed and incubated on ice for 3 min. This step causes pH neutralization and enables plasmid DNA to re-nature. To remove chromosomal DNA, proteins and other cellular debris, the solution was centrifuged for 10 min at 13,000 rpm. The supernatant was collected, and plasmid DNA was precipitated by the addition of 800 µl 99% ethanol. After centrifugation (13 000 rpm, 3 min, RT), the supernatant was discarded, and the pellet was air-dried before re-suspension in 20 µl dH_2O; plasmid DNA was stored at -20 °C.

GTE-solution

Glucose	50 mM
Tris-HCl pH 8.0	25 mM
Na_2EDTA	10 mM

GTE-solution was autoclaved and stored at RT.

NaOH/SDS-solution

NaOH	0.2 M
SDS	1% (w/v)

NaOH/SDS-solution was autoclaved and stored at RT.

KAc-solution

Acetic Acid	29.5%

pH was adjusted with KOH pellets to 4.8, and the solution was subsequently autoclaved.

2.3.2. Plasmid miniprep (innuPREP Plasmid Mini Kit)

The innuPREP Plasmid Mini Kit (Analytik Jena) was used to isolate bacterial plasmid DNA in a pure manner and high concentration. To achieve this, the instructions provided with the kit were followed. The method is based on alkaline lysis with subsequent binding of plasmid DNA to a spin filter membrane. After several washing steps, the plasmid DNA was eluted from the spin filter with dH_2O and stored at -20 °C.

2.4. DNA digestion and isolation

2.4.1. Determination of DNA concentration

To determine DNA concentrations, the NanoDrop 2000/2000c spectrophotometer (Thermo Scientific) was used. After establishing the blank by using the same solution which was used to elute DNA (dH_2O), 1-2 µl of test samples were placed directly onto the measurement pedestal to measure DNA concentration at an absorbance of 260 nm.

2.4.2. Restriction digest of plasmid DNA

For restriction digest of plasmid DNA, restriction enzymes from Thermo Scientific were used. Single digestions were performed as followed:

10xbuffer	2.0 µl
Restriction enzyme	0.4 µl
RNase	0.1 µl
DNA	1.0 µl
dH_2O	16.5 µl

The mixture was incubated for 2-3 hours at 37 °C.

For double digestions, the recommended mix composition was checked in the DoubleDigest Calculator (Thermo Scientific) to provide the optimal buffering range and restriction enzyme concentrations.

2.4.3. Agarose gel electrophoresis

For the electrophoretic separation of DNA fragments, 0.5%-2% agarose gels in 1xTBE buffer were used. 20 µl of the DNA samples were mixed with 5 µl of gel loading buffer (GLB) and loaded on a gel. As a molecular weight marker HyperLadder™ 1kb (Bioline) was used (Figure 10). Migration occurred at constant voltage in a BlueMarine™ (SERVA) electrophoresis unit filled with 1xTBE-buffer at 160 V. Subsequently, the gel was stained for 15-20 min in an ethidium bromide bath, and DNA fragments were visualized under UV light. Gel imaging and analysis were carried out with a ChemiDoc XRS System (BIO-RAD).

TBE Buffer (10x)

Tris	890 mM
Boric acid	890 mM
Na_2EDTA	20 mM

GLB Buffer

Glycerol	50% (v/v)
SDS	1% (w/v)
Na_2EDTA	125 mM
Bromophenol blue	0.05% (w/v)
Xylene cyanol	0.05% (w/v)

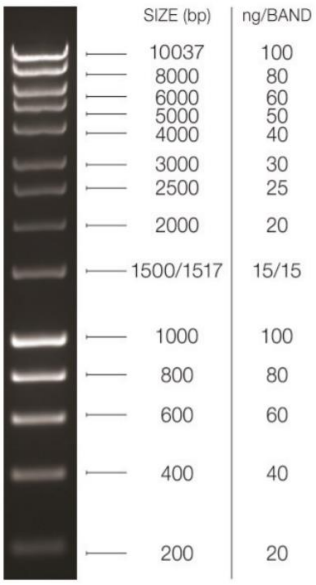

Figure 10: Band profile of the HyperLadder 1 kb (Bioline). Size range: 200 bp to 10037 bp.

2.4.4. DNA extraction from agarose gels

To isolate and purify DNA fragments after separation via agarose gel electrophoresis, the E.Z.N.A.® Gel Extraction Kit (Omega Bio-Tek) was used according to the manufacturer's instructions. This method allows DNA recovery of more than 90% and the isolation of DNA fragments with a length from 70 bp up to 20 kb.

2.4.5. DNA sequencing

Plasmid DNA was isolated by the Miniprep method and subsequently sent for sequence analysis to GATC Biotech (Konstanz). The obtained sequences were analyzed with the software SeqMan (DNASTAR, Lasergene).

2.5. Growth media

2.5.1. Growth media for bacteria

LB-Medium

Tryptone	1.0%
Yeast extract	0.5%
NaCl	0.5%
Agar (only for plates)	1.5%

S.O.C-Medium

Yeast extract	0.5%
Pepton	2.0%
NaCl	10 mM
Glucose	20 mM
KCl	10 mM
$MgCl_2$	10 mM
$MgSO_4$	2.5 mM

Chemicals were dissolved in dH_2O and autoclaved for sterilization. Liquid media were stored at RT and agar plates at 4 °C.

2.5.2. Growth media for yeast

YPD-medium

Glucose	2%
Peptone	2%
Yeast extract	1%

Glucose was autoclaved separately.

Drop-out (d/o) medium (Glucose or Galactose)

Solution A:

Glucose / Galactose	2% / 3%
Agar	1.5%

Solution B:

Ammonium sulfate	0.5%
d/o Mix	0.087%

Solution C:

Yeast Nitrogen Base (YNB)	0.17%

Solution A and B were autoclaved separately. Solution C was sterile filtered. All solutions were finally mixed to obtain the d/o medium.

d/o Mix

Adenine	0.2 g	Leucine	1.0 g	Tryptophan	0.2 g
Arginine	0.2 g	Lysine	0.3 g	Tyrosine	0.3 g
Asparagine	1.0 g	Methionine	0.2 g	Uracil	0.2 g
Isoleucine	0.3 g	Threonine	2.0 g	Valine	1.5 g
Histidine	0.2 g	Phenylalanine	0.5 g		

To prepare the d/o mix, the desired amino acid or base, determined by the selection marker of the plasmid, was excluded; d/o mix was stored at 4 °C.

2.5.3. Antibiotics and other media additives

Antibiotics used in this thesis are listed in Table 6. They were sterile-filtered and stored at -20°C.

Table 6. Stock solutions of the antibiotics and other media additives used

Substance	Concentration	Solvent
Ampicillin	50 mg/ml	50 % ethanol
Kanamycin	25 mg/ml	dH_2O

For selection in liquid medium, 40 µl ampicillin or 20 µl kanamycin stock solution were added to 5 ml LB-medium (final antibiotics concentrations: 400 µg/ ml and 200 µg/ml, respectively). For selection on agar plates, 200 µl of 1:5 diluted ampicillin or 200 µl of 1:10 diluted kanamycin stock solution was added to the plate.

2.6. Cultivation conditions

2.6.1. Bacteria

For *Escherichia coli* growth in liquid medium, a single colony was inoculated in 5 ml LB-Medium containing the appropriated antibiotic (50 mg/ml Ampicillin or 25 mg/ml Kanamycin) and incubated in a shaker at 37 °C with 220 rpm. To grow *E. coli* on solid culture medium, antibiotics were added on LB agar plates, and the cell mixture was plated out. Finally, plates were incubated overnight in an incubator at 37 °C.

2.6.2. Yeasts

To prepare a liquid culture of yeast cells, a single colony was inoculated in 5 ml medium (YPD or d/o-medium) and incubated at 30°C (220 rpm) until the desired optical density (OD) was reached. Agar plates were incubated at 30 °C for 2-3 d.

2.6.3. Cryocultures

For long-term storage of bacteria and yeast strains, 1 ml of an overnight culture was mixed with 1 ml sterile glycerol (99 %) in a 2 ml cryotube and stored in a -80°C freezer.

2.7 Yeast transformation

For transformation of *S. cerevisiae*, 1 ml of an overnight culture was centrifuged at 8 000 rpm for 5 min. The cell pellet was washed once in 500 µl LiAc/TE buffer and resuspended in 100 µl LiAc/TE buffer. 10 µl Carrier-DNA (denatured single-stranded salmon sperm DNA), 2 µl plasmid-DNA, and 3 µl 10xLiAc buffer were mixed and added to the cell suspension with

600 µl PEG-solution. After incubating the transformation mixtures at 30 °C for 30-45 min and 220 rpm, a heat shock was performed in a water bath at 42 °C for 15 min, and the cells were centrifuged for 1 min at 13 000 rpm. The pellet was then washed twice in 500 µl 1xTE buffer and finally resuspended in 500 µl 1xTE buffer before the cell suspension was plated on an appropriate d/o mix agar plate.

10xLithium acetate solution:

Lithium acetate	1 M

Solution was adjusted to pH 7.5 (Acetic acid) and subsequently autoclaved.

10xTE

Tris	100 mM
Na_2EDTA	10 mM

HCl was added until pH 7.5, and the solution was autoclaved

50% PEG-Solution

PEG 4000	50% (v/v)

PEG-Solution was autoclaved.

LiAc/TE-Solution

10x LiAc	10% (v/v)
10x TE	10% (v/v)
dH_2O	80% (v/v)

PEG-Solution

10x LiAc	10% (v/v)
10xTE	10% (v/v)
PEG 4000 (50%)	80% (v/v)

PEG-solutions were freshly prepared before usage.

2.8. Yeast growth assay

2.8.1. Growth conditions

For general experimental purposes, yeast cells were usually grown in YPD or synthetic liquid media at 30 °C and 220 rpm.

2.8.2. Determination of cell growth by optical density (OD) measurement

OD was measured with a spectrophotometer at a wavelength of 600 nm to monitor the growth of microorganisms. Plastic cuvettes with a thickness of 1 cm were used, and the appropriate growth medium was utilized as a blank.

2.8.3. Growth assay

BY4742 cells were transformed with either an empty vector (EV) control, pYES-ERD2^{V5} or different kAE1 expression plasmids (pYES-kAE1^{HA}, pYES-kAE1^{WT}, pYES-kAE1^{B3mem} or pYES-kAE1^{E681Q}). Colonies of each transformant were cultivated in uracil d/o glucose medium overnight at 30 °C (220 rpm). Induction of protein expression was initiated by diluting the cells in galactose-containing uracil d/o medium with a start OD_{600} of 0.1 in an end volume of 50 ml; cell growth was determined by OD_{600} measurement every 90 min over 30 h (n = 3). Additionally, empty vector cells were treated with 2.5 mM dithiothreitol (DTT) (solved in DMSO) and served as positive control. Untreated and DMSO-treated (reference for DTT-treated cells) empty vector cells were used as negative controls. The respective OD_{600} values of the triplicates were plotted as a function of time to calculate the yeast growth rate, and data were fitted via exponential regression. The resulting equation was further used to evaluate the mean growth rates per hour (curve slope) ± SD.

2.9. Yeast homologous recombination

2.9.1. Vector linearization

The integrative plasmids YIp128-Pma1-mRFP and YIp211-Pma1-mRFP donated from Dr. Malinsky's lab (Czech Academy of Sciences, Czech) were used for homologous recombination. Both plasmids were linearized by the restriction enzyme *Bgl*II, DNA fragments were isolated and purified after separation on agarose gels and eluted using the E.Z.N.A.® Gel Extraction Kit (Omega Bio-Tek).

2.9.2. Transformation into yeast

Lithium acetate transformation of yeast was performed as previously described (Kawai *et al.*, 2010). Yeast containing linearized vector DNA from YIp128-Pma1-mRFP was selected on leucine d/o plates, while YIp211-Pma1-mRFP was selected on uracil d/o plates.

2.9.3. Genomic integration detection

Single colonies grown on d/o plates were picked and cultivated in appropriate selective liquid media, and successful homologous recombination was verified by Western blot analysis.

2.10. Yeast cell lysis

2.10.1. Initial protocol

After approximately 24 h of cultivation, yeast cells (OD_{600} = 5) were harvested by centrifugation at 8 000 rpm for 5 min. Next, cells were washed with 1 ml dH_2O and resuspended in 160 µl SUMEB buffer and 40 µl of protease inhibitor cocktail solution (Complete EDTA-free, Roche). The mixture was then transferred into tubes containing glass beads (diameter 0.75-1 mm), and cell lysis was conducted using a tissue homogenizer (Precellys® Evolution, Bertin Corp) with the following program: 6 000 rpm, 3x20 s, pause/interval 30 s. After the run, the samples were centrifuged at 13 000 rpm for 1 min at 4 °C. The final supernatant was collected for subsequent SDS-PAGE.

SUMEB Buffer

SDS	1%
Urea	8 M
MOPS pH 6,8	10 mM
EDTA	10 mM
Bromophenol blue	0.01%

Protease inhibitor cocktail solution

One tablet of EDTA-free Protease Inhibitor Cocktail (Roche) was dissolved in 2 ml dH_2O.

2.10.2. Optimized protocol

In this optimized protocol, a different cell lysis buffer was used, and some other modifications have been implemented compared to the first protocol, leading to improved protein extraction. After harvesting yeast cells (OD_{600} = 5) by centrifugation at 8 000 rpm for 5 min, cell pellets were washed twice with dH_2O and resuspended in 140 µl of optimized cell lysis buffer (PMSF was added to the buffer before use) and 60 µl of protease inhibitor cocktail solution (Complete EDTA-free, Roche). Cell disruption was conducted using glass beads and a homogenizator (6 000 rpm, 3x20 s shaking interval, 30s break/interval). Cell lysates were incubated at 37 °C for 15 min, and cell debris was removed via centrifugation (14 000 rpm, 4 °C, 10 min). The respective supernatants were collected and supplemented with 10 µl 2×SDS sample buffer before they were used for SDS-PAGE.

Optimized cell lysis buffer

Tris	10 mM
EDTA	1 mM
β-mercaptoethanol	0.1% (v/v)
PMSF	1 mM

PMSF is rapidly degraded in aqueous solutions. Therefore, a stock solution of 100 mM in absolute ethanol was prepared ahead and added separately to the cell lysis buffer before use.

2xSDS sample buffer

Tris-Cl (pH=6.8)	100 mM
SDS	4% (w/v)
Bromophenol blue	0.2% (w/v)
Glycerol	20% (v/v)
β-mercaptoethanol	200 mM

2.10.3. TCA precipitation

Yeast cell proteins can be efficiently and directly isolated using TCA precipitation because proteins are not readily and easily degraded by proteases under the low pH of the TCA solution. Yeast cells grown to OD_{600} = 1 were centrifuged at 5 000 rpm for 5 min, the supernatant was removed, and the pellet was resuspended in 250 µl NaOH/Mercaptoethanol solution. After incubation for 10 min on ice, 160 µl 50% TCA solution was added, and cells were incubated again for 10 min on ice. The pellet obtained after centrifugation (14 000 rpm, 10 min) was washed in 1 ml of ice-cold acetone, finally air-dried and resuspended in 100-200 µl SDS sample buffer followed by SDS-PAGE.

NaOH/Mercaptoethanol solution

β-Mercaptoethanol	1 % (v/v)
NaOH	0.25 M

50% TCA

Trichloroacetic Acid (TCA)	50% (w/v)

SDS Sample Buffer

β-Mercaptoethanol	2% (w/v)
Tris	125 mM
Glycerol	20% (v/v)
Bromophenol Blue	0.001% (w/v)
SDS	4% (w/v)

2.11.SDS-Polyacrylamide gel electrophoresis (PAGE) and Western blot analysis

2.11.1. SDS-Polyacrylamide gel electrophoresis (PAGE)

10% or 15% polyacrylamide gels were used within a discontinuous Tris-Tricine buffer system. In this system, two different gel layers, the stacking gel with large pores and the separating gel with smaller pores, are used to separate proteins. Gels were prepared and run using the Mini-PROTEAN® 3 Cell (BIO-RAD) components. The separating gel was poured first and overlaid with isopropanol until polymerization. After removing the isopropanol, stacking gel was poured on top of the separating gel, and a comb (1 mm or 1.5 mm thickness) was inserted between the plates to define the desired wells. Before loading on the gel, protein samples were mixed with 2x SDS loading buffer. PageRuler Prestained Protein Ladder (Thermo Scientific) served as a protein molecular weight marker (Figure 11). Electrophoresis was carried out in a "Mini-Protean II" system (BIO-RAD) with initial 80 V for approximately 15-20 min until the marker bands preliminarily separated. The voltage was then increased to 120 V for around 1-1.5 h until each marker band was clearly divided.

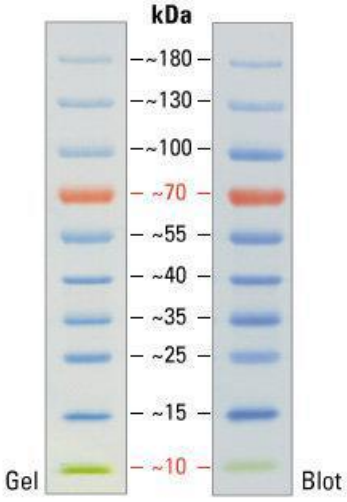

Figure 11: Correlation of different marker bands and molecular weight. The PageRuler Prestained Protein Ladder (Thermo Scientific) was used in SDS-PAGE to determine the size of proteins with a molecular weight between 10 kDa and 180 kDa.

Separating gel

	Gel concentration 10%	Gel concentration 15%
Rotiphorese Gel 30	4.0	5.9 ml
Tris-HCl/SDS	5.0	5.0 ml
Glycerine (79%)	2.0	2.0 ml
dH_2O	4.0	2.1 ml
APS (10%)	80 µl	80 µl
TEMED	25 µl	25 µl

APS should be prepared freshly. APS and TEMED were added last to start the polymerization.

Stacking gel

Rotiphorese Gel 30	1.6 ml
Tris-HCl / SDS	3.1 ml
dH_2O	7.8 ml
APS (10%)	80 µl
TEMED	25 µl

2xSDS Loading buffer

10% SDS	8 ml
0.5 M Tris/HCl	6 ml
100% glycerol	5 ml
Bromophenol blue	0.05%
dH_2O	to 20 ml

5xAnode buffer

Tris	1 M

HCl was added until pH reached 8.9, and solution was autoclaved

5xCathode buffer

Tris	0.5 M
Tricin	0.5 M
SDS	0.5% (w/v)

Solution was autoclaved.

2.11.2. Western blot analysis

After separation by SDS-PAGE, proteins were transferred from the gel to a polyvinylidene difluoride (PVDF) membrane for subsequent detection via Western blotting. Protein transfer was achieved by a semi-dry blotting approach. Therefore, the SDS gel and filter papers were equilibrated in transfer buffer for 10 min. PVDF membrane was pre-wetted for 1 min in 20% methanol and subsequently soaked in a transfer buffer for 10 min. Protein transfer was conducted using the "Trans-Blot Semi-Dry Electrophoretic Transfer Cell" (BIO-RAD) for 90 min at 15 V with a constant current intensity of 54 mA per gel. To prevent non-specific binding of antibodies, membranes were incubated overnight with a blocking buffer (5% nonfat dried milk powder or 3% BSA) at 4 °C. Then, blots were incubated with the primary antibody for 60 min at 20 °C. After washing the blots three times for 10 min with washing buffer, membranes were incubated for 60 min at 20 °C with a secondary antibody, which binds directly to the primary antibody and is conjugated to the horseradish peroxidase (HRP). Afterward, the membrane was washed three times. Finally, chemiluminescent substrates (SuperSignal West Femto, Thermo Scientific) for HRP were added to the membrane, based on the manufacturer's instructions. These substrates consist of a peroxide solution and an enhanced luminol solution. In the presence of peroxide, HRP catalyzes the oxidation of luminol to a product that emits light at 425 nm, which was detected with the Amersham Imager 600 (GE Healthcare Life Sciences).

Transfer buffer

Tris	3.03 g/l
Glycine	14.4 g/l
SDS	0.1% (w/v)
Methanol	20% (v/v)

Solution was stored at 4 °C.

Washing buffer

10x TBS	10% (v/v)
Tween 20	0.05%

Blocking buffer (Milk or BSA)

Nonfat dried milk powder	5%	BSA	3%

Milk or BSA were diluted in Washing buffer.

Antibodies used in this thesis are listed in Table 7.

Table 7. Antibodies used in this study

Antibody	Dilution	Source
anti-Pgk1p, mouse	1 : 1 000	LifeTechnologies (Novex)
anti-mouse-HRP	1 : 10 000	Sigma
anti-rabbit-HRP	1 : 10 000	Sigma
anti-rat-HRP	1 : 10 000	Cell signaling
anti-rabbit-Kar2p	1 : 1 000	Gift from Karin Römisch, Saarland University, Saarbrücken
anti-GFP, mouse	1 : 1 000	Roche
anti-V5, mouse	1 : 1 000	AbD SeroTec
anti-HA High affinity, rat	1 : 1 000	Roche
anti-FLAG High affinity, mouse	1 : 1 000	Sigma
anti-kAE1, mouse (BRIC170)	1 : 1 000	IBGRL (9450PA), epitope in aa region 368 to 382 is recognized

2.12. Determination of UPR activation via Kar2p expression

The UPR activity in yeast transformants expressing different kAE1 constructs was analyzed via Kar2p expression. Therefore, transformants were first cultivated in 5 ml of the appropriate d/o glucose medium for 18 h (30 °C, 220 rpm). Cells were then shifted to 5 ml galactose-containing d/o medium and grown to an OD_{600} of 0.6 to 0.8 to initiate protein expression. Cells corresponding to an OD_{600} of 5 were harvested and subsequently lysed using the optimized cell lysis protocol (see chapter 2.10.2). The amount of Kar2p was determined via SDS-PAGE and Western analysis using the appropriate anti-Kar2p antibody.

2.13.UPR-dependent lacZ reporter assay

Yeast cells were transformed with either an empty vector (pYES2.1) control or different kAE1 expression plasmids (pYES-kAE1^{HA}, pYES-kAE1^{FLAG}, or pYES-kAE1^{WT}), and pre-cultured for 18 h at 30°C at 220 rpm in 5 ml uracil d/o glucose medium. Induction of protein expression was initiated by inoculation of 5 ml uracil d/o galactose medium with 300-500 µl of the cell suspension. Cells were grown to OD_{600} 0.6-0.8 at 30°C and 220 rpm, harvested and lysed as described before (see chapter 2.12). Finally, cell debris was removed by centrifugation (4 °C, 14 000 rpm, 10 min), and 200 µl of the resulting supernatant were mixed with 100 µl

PBS buffer (pH 7.4) containing 500 µg/ml X-gal. After incubation at 30°C for 24 h, enzymatic activity of β-galactosidase was visually determined.

X-gal stock solution

5-bromo-4-chloro-3-indolyl-β-D-galactopyranoside (X-gal, Applichem) was dissolved in N, N-dimethylformamide (DMF) at a concentration of 20 mg/ml. Store in the dark at -20°C.

2.14. β-estradiol assay

2.14.1. GEV yeast strain construction and cultivation conditions

The yeast BY4742-GEV was generated via transformation of the linearized plasmid pACT1-GEV using *EcoR*V in BY4742 wild-type cells. Transformants were plated on leucine d/o agar to select colonies with successful homologous recombination events. Clones were then transformed with the plasmid pYES-kAE1^{WT,} yielding a yeast β-estradiol inducible kAE1-expressing yeast (BY4742-GEV [pYES-kAE1^{WT}]).

2.14.2. β-estradiol assay

kAE1 expression was stepwise induced via application of different concentrations of β-estradiol (0 nM, 1nM, 10 nM, 100 nM, 10^3 nM, 5×10^3 nM and 10^4 nM respectively). BY4742-GEV cells expressing an empty vector (BY4742-GEV [pYES-EV]) or HA-tagged kAE1 (BY4242-GEV [pYES-kAE1^{HA}]) were cultivated overnight. 300 µl of the respective overnight culture were transferred to 5 ml uracil d/o glucose-containing medium, supplemented with β-estradiol, and incubated for 18 h at 30 °C at 220 rpm. Cell suspension corresponding to an OD_{600} of 10 was harvested via centrifugation (5 min, 8 000 rpm, RT), and cells were subsequently washed twice with dH_2O. Finally, pellets were resuspended in 200 µl SDS sample buffer supplemented with 1×protease inhibitor cocktail (Roche), and cell lysis was conducted in a homogenisator after addition of glass beads (Precellys Evolution, Peqlab). Samples were incubated for 15 min at 37 °C, and after centrifugation (15 min, 13 000 rpm, 4 °C), supernatants were subjected to SDS-PAGE and immunoblotting.

β-estradiol stock solution

A 20 µg/ml β-estradiol stock solution was prepared by addition of 1 mg β-estradiol (Sigma-Aldrich, USA) in 1 ml 99% ethanol, solution was stored at -20 °C.

2.15. *HAC1* splicing reporter-based UPR detection assay

2.15.1. BY4741-SR-GFP strain preparation

The yeast strain BY4741-SR-GFP contains a splicing reporter (SR) consisting of *HAC1*-mRNA whose first exon has been replaced by a GFP-encoding exon. Cells of this reporter strain were transformed with either an empty vector (pYES-EV) control or different kAE1 expression plasmids (pYES-kAE1^{HA}, pYES-kAE1^{FLAG}, pYES-kAE1^{WT} and pYES-kAE1^{E681Q}). After cultivation of the transformants in 5 ml uracil d/o glucose medium, cells were shifted to 5 ml uracil d/o containing galactose to induce protein expression and incubated for 18 h at 30°C at 220 rpm.

2.15.2. *HAC1* splicing assay

10 µl aliquots of the previously prepared cell suspension (2.15.1) were spotted on poly-L-lysine-coated coverslips and incubated for 15 min (RT). UPR activation was determined by GFP fluorescence levels. The monitoring was conducted via fluorescence microscopy using a Keyence BZ-8000 microscope (100x Oil immersion Plan Apo VC objective [1.4 NA]) with pre-installed filter sets and the standard settings for GFP (Excitation at 488 nm). Yeast cells expressing the empty vector were used as a negative control (untreated), whereas cells incubated with 2.5 mM DTT or 2 µg/ml tunicamycin for 2 h incubation prior to microscopy served as positive control.

2.16. Indirect immunofluorescence assay

2.16.1. Cell fixation and spheroplasting

The protocol for the indirect immunofluorescence assay used in this thesis was adapted from the standardized manuals of the Gardner Lab. Briefly, yeast cells were grown to an OD_{600} of 10. 3.7 % formaldehyde (v/v) was added for fixation, and the cells were incubated on a roller drum at 20 °C for 1 h. After harvesting by centrifugation at 8 000 rpm for 4 min, cells were washed 3 times with 2 ml 1xPBS. Then, samples were washed once with 2 ml sorbitol (1.2 M) and once with 2 ml 1xPBS. Cells were resuspended in 1 ml sorbitol (1.2 M), 10 µl β-mercaptoethanol and 20 µl zymolyase (5 mg/ml zymolyase 100 T in 1.2 M sorbitol). Next, cells were put on a roller drum at 30 °C for spheroplastation, which was carefully monitored by observing the cells via bright-field microscopy. After approximately 45 min, cells were harvested by centrifugation at 3 000 rpm for 2 min and washed with 2 ml 1.2 M sorbitol. Spheroplasted cells were resuspended in 1.2 M sorbitol.

2.16.2. Cell permeabilization and antibody staining

Cell permeabilization was conducted by plunging the slide into -20°C methanol for 6 min, and immediately submerging it acetone for 30 s (RT). 200 µl of the block solution was added, and the slide was put in a humidity chamber. After 5 min, the block solution was removed, and 100 µl of the primary antibody (1:40 diluted in block solution) was added; samples were incubated at 30 °C overnight. Afterward, the cells were washed four times with block solution, and fluorescein isothiocyanate (FITC)-conjugated secondary antibody (1:160) was added. After incubation of 1 h (30°C, in the dark), cells were washed four times with block solution; eventually, 100 µl mounting medium was added to each well. Samples were analyzed with the fluorescence microscope Biozero BZ-8000 (Keyence) by using an oil-immersion objective (PlanApo, VC, 100x, NA: 1.40 (Nikon)), and the standard settings for GFP (Excitation at 488 nm)

<u>10xPhosphate buffer (100 ml)</u>

1 M K_2HPO_4	83.4 ml
1 M KH_2PO_4	16.6 ml

The pH was adjusted to 7.5, and the solution was autoclaved.

<u>Block Solution (10 ml)</u>

100 mg/ml BSA	1 ml
10xPhosphate buffer	500 µl
5 M NaCl	300 µl
NaN_3	1 mg

The pH was adjusted to 7.5. The block solution can be stored at 4 °C for extended periods of time.

<u>Mounting medium (100 ml)</u>

Phenylenediamine	100 mg
10xPhosphate buffer	10 ml
dH_2O	ad 100 ml

The pH was adjusted to 9 with NaOH. The mounting medium was stored at -20°C in the dark.

2.17. Transmission electron microscopy (TEM) analysis

Electron microscopy analyses were conducted as described in Sarder *et al.* (2020) in

cooperation with Dr. Charlotta Funaya (Electron Microscopy Core Facility, Heidelberg University). Briefly, BY4742 deletion mutants Δ*end3* or Δ*pep4* were transformed with the empty vector control (pYES2.1) or different kAE1 expression plasmids. Log phase cultures (OD_{600} = 0.6-0.8) of the respective transformants were cryo-immobilized on aluminum carriers under high pressure. Initial dehydration was achieved via freeze substitution in 0.1% (w/v) uranyl acetate dissolved in anhydrous acetone for 24 h at -90 °C. Afterward, the temperature was subsequently increased to -45 °C (5 °C/h), and samples were incubated for 5 h, followed by the final fixation in lowicryl HM20 embedding medium. Therefore, samples were washed three times with 100% acetone for 10 min followed by incubation in lowicryl-acetone solutions with incrementally increasing lowicryl concentrations (25%, 50%, 75%) for 2 h each. Lastly, samples were incubated three times in 100 % lowicryl for 10 h, respectively. Subsequent UV polymerization was conducted for 48 h at -25 °C before the temperature was increased to 20 °C (5 °C/h); samples were further exposed to UV at RT for 48 h. Microtome cuts (70 nm, Leica UC6 microtome) of each sample were prepared and collected on Formvar-coated copper slot grids followed by immunogold labeling. Therefore, grids were carefully placed on drops of blocking buffer (PBS with 1.5% BSA and 0.1% fish skin gelatin) for 30 min and transferred onto droplets containing the primary antibody (anti-kAE1 BRIC170, 1:100 in blocking buffer). After 30 min, samples were subsequently incubated with the appropriate secondary anti-mouse antibody (Dako, #Z025902-2) and 10 nm gold-conjugated Protein A (20 min incubation, respectively). The grids were washed five times in PBS between each incubation period. Fixation was conducted in 1% glutaraldehyde (in PBS) for 5 min, and samples were finally rinsed in water before the final post-staining via uranyl acetate and lead citrate. Eventually, samples were examined using a JEOL JEM-1400 electron microscope (JEOL, Tokyo) operating at 80 kV and equipped with a 4K TemCam F416 (Tietz Video and Image Processing Systems GmBH, Gautig). Gold particles within a 32 nm range of the plasma membrane or the vacuole were scored for PM- or vacuole-localized kAE1 proteins, respectively (Figure 12).

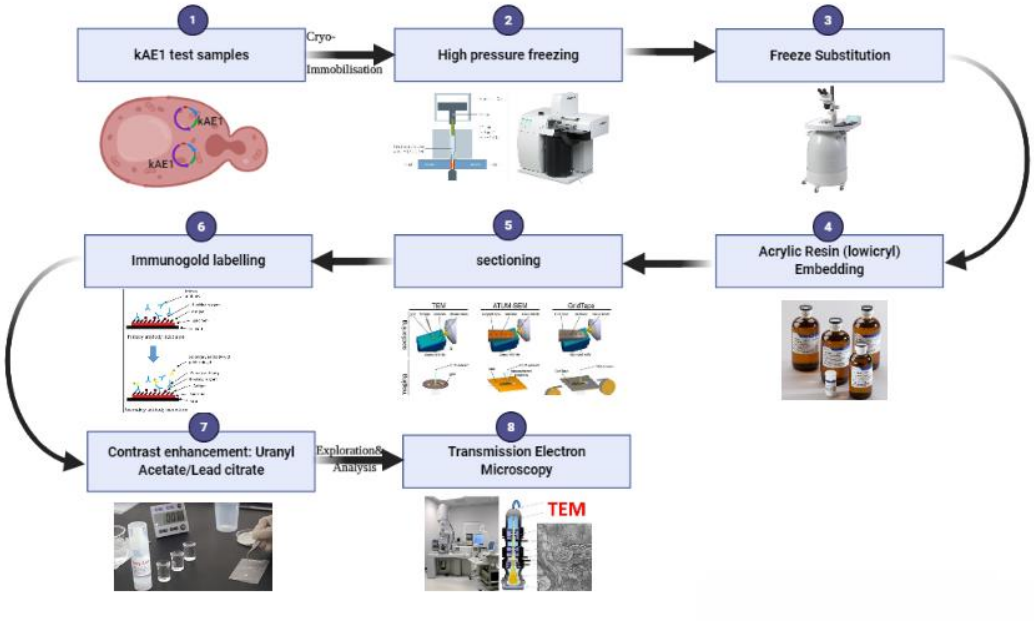

Figure 12: Overall workflow for the Transmission Electron Microscopy (TEM) study. 8 steps need to be prepared before starting the final TEM examination. The first step was to prepare kAE1 samples, the next step was to do cryo-immobilization through high-pressure freezing. The third step was to freeze by using 0.1% (w/v) uranyl acetate. The fourth step was to use lowicryl HM20 to rinse the samples. The fifth step was sectioning the samples. The sixth step was immunogold labeling by incubating firstly with anti-kAE1 antibodies and subsequently with an anti-mouse antibody and 10 nm gold-conjugated Protein A. The seventh step was to contrast enhancement via uranyl acetate/lead citrate. The last step was to examine cells under a TEM equipped with a 4K TemCam F416.

2.19. Structured illumination microscopy (SIM)

Yeast cells were placed on appropriate glass cover-slips (25 mm) and incubated for 1 h to inhibit cell movement. SIM was conducted in collaboration with Dr. Elmar Krause (Cellular Neurophysiology, Saarland University). Images were obtained using an inverted Elyra PS1 microscopy system (Carl Zeiss Microscopy, GmbH, Jena) with a 63x Plan-Apochromat objective lens (NA 1.4, Carl Zeiss). 488 nm (GFP) and 561 nm (mRFP) were applied as excitation wavelengths, respectively, and Zen12 software (Carl Zeiss) was used for image acquisition and super-resolution processing. Further image analysis was carried out with the Fiji software (Schindelin *et al.*, 2012), allowing the separate adjustment of image brightness and contrast of each fluorescence channel.

2.20. Statistical analysis

Statistical analysis was executed using the GraphPad Prism 8 Software. Mean values of the generated data (± SEM if not otherwise stated) were calculated, and the statistical

significance of sample sizes ($n \geq 3$) was evaluated using a One-way ANOVA-based approach (*, $p<0.05$; **, $p<0.01$; ***, $p<0.001$).

3. Results

Human kidney anion exchanger 1 (kAE1) is a bicarbonate transporter situated in the basolateral membrane of renal epithelial cells. It participates in the fine-tuning of the acid-base homeostasis by mediating electroneutral Cl^-/HCO_3^- exchange (Lashhab *et al.*, 2019). It has been shown that numerous autosomal mutations in the respective kAE1-encoding gene *SLC4A1* are associated with the misfolding, retention in the secretory pathway and/or premature degradation of the transporter, eventually cumulating in the development of a pathophysiological syndrome named distal renal tubular acidosis (dRTA) (Bonar & Casey, 2010). Some proteins involved in the trafficking of kAE1 have already been identified, however, the exact molecular mechanisms causing the development of dRTA remain unclear (Groves *et al.*, 1999; Lashhab *et al.*, 2019). *S. cerevisiae* is widely used as a model system for the study of various cellular pathways (e.g., trafficking, post-translational protein modifications, signaling pathways) because many essential processes are highly conserved between this unicellular organism and more complex eukaryotes (Winter & Chiang, 2016). Yeast offers rapid multiplication and consequently shorter experimental times, as well as plenty of manipulations tools, making it feasible to conduct large-scale screenings. Thus, *S. cerevisiae* is becoming a popular tool to answer many types of scientific questions (Kolb *et al.*, 2011; Berner *et al.*, 2018). In this study, yeast was employed to analyze the intracellular kAE1 trafficking to the plasma membrane and the turnover of the transporter and to identify potentially involved proteins. To start the project, HA- and FLAG-tagged yeast codon-optimized kAE1 were firstly expressed in yeast, and cellular localization was checked subsequently via electron microscopy and super-resolution microscopy (SIM). Additionally, the growth behavior and the activation of the UPR were investigated in kAE1 overexpressing yeast cells. Finally, various pathways were analyzed (e.g., those that increase ER folding capacity) to potentially reduce this UPR activation.

3. 1. Expression of codon-optimized kAE1 variants in yeast

3.1.1. Expression codon-optimized HA-, V5- and FLAG-tagged kAE1 variants in yeast

Previous studies have already reported that the heterologous expression of various truncated versions of AE1 or kAE1 in *S. cerevisiae* is generally possible. However, a partial transport to the plasma membrane as well as *in vivo* activity could only be shown for the

truncated derivative AE1$^{361-911}$; all other shortened variants were accumulated in various intracellular membranes (Sekler *et al.*, 1995; Groves *et al.*, 1996). In addition, attempts to express full-length versions of human AE1 in yeast failed because AE1 was not only unable to reach the yeast cell surface but was also not functional (Bonar & Casey, 2010). However, a recent report demonstrated that a full-length variant of yeast codon-optimized kAE1 was successfully expressed in *S. cerevisiae*, partially reached the cell surface, and showed anion transport activity (Sarder *et al.*, 2020; Li *et al.*, 2021). In mammalian cells, it has been already described that modification of the N-terminus and/or integration of an epitope-tag into the third extracellular loop does not affect kAE1 function and trafficking (Toye *et al.*, 2004). Based on these findings, HA-, V5- and FLAG- tags were integrated into the third extracellular loop of yeast codon-optimized kAE1 (ykAE1) between the amino acids Val^{557} and Lys^{578} (Figure 13).

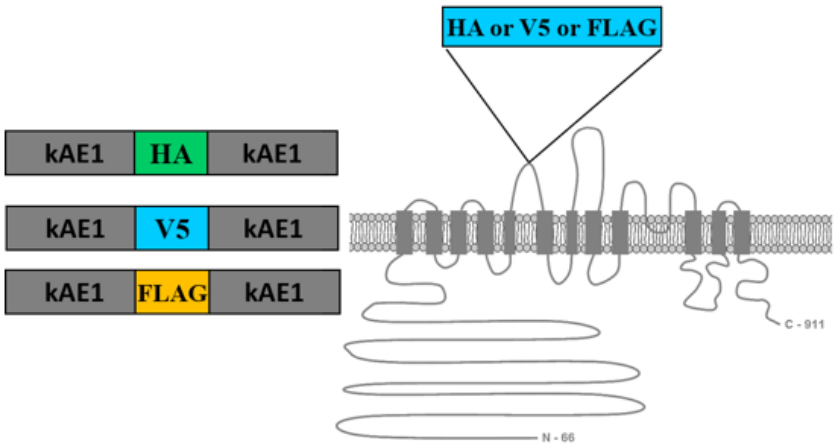

Figure 13: Expression of tagged kAE1 variants in *S. cerevisiae*. Schematic overview of full-length kAE1 with epitope-tags (HA, V5 or FLAG) in the third extracellular loop between amino acids Val^{557} and Lys^{558}. kAE1 variants were cloned into the vector pYES2.1 and transformed into different *S. cerevisiae* strains to obtain galactose-inducible kAE1 expression strains.

cDNA sequences of the three full-length kAE1 variants were ordered, and the fragments were ligated into the vector pYES 2.1. In the first step, the three variants were transformed into wild-type BY4742 cells obtaining BY4742 [pYES-kAE1^{HA}], BY4742 [pYES-kAE1^{V5}], and BY4742 [pYES-kAE1^{FLAG}]. In addition, constructs were also transformed into the BY4742 deletion mutant Δ*end3* which shows significantly reduced endocytosis rates compared to wild-type cells. Finally, kAE1 expression was validated via Western analysis using an appropriate

anti-HA, anti-V5, and anti-FLAG antibody, respectively (Figure 14).

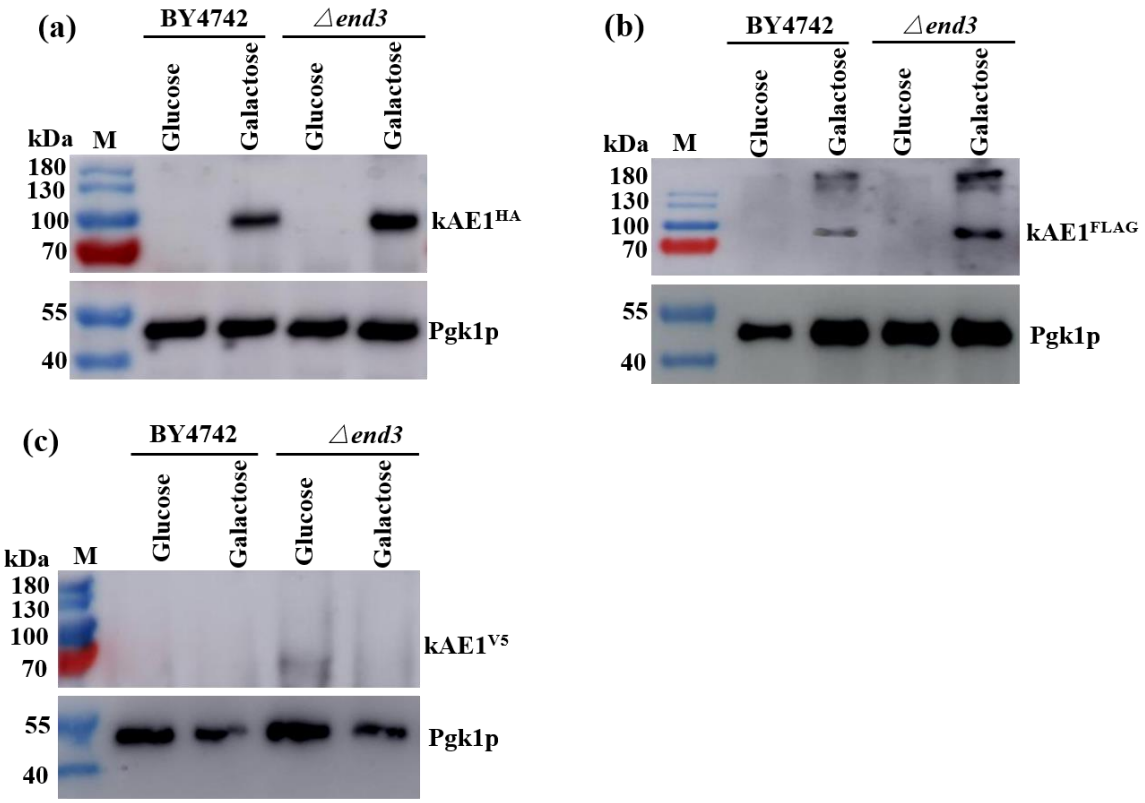

Figure 14: Expression levels of HA-, V5- and FLAG-tagged versions of yeast codon-optimized kAE1 (kAE1^{HA}, kAE1^{V5}, and kAE1^{FLAG}) in *S. cerevisiae* under inducing (galactose) and non-inducing (glucose) conditions. (a, b) kAE1^{HA} and kAE1^{FLAG} expression could be verified in wild-type BY4742 as well as Δ*end3* cells by Western blots. (c) No expression was detected in cells expressing the V5-tagged kAE1 construct. A protein standard (M) served as a molecular weight marker, and detection of phosphoglycerate kinase 1 (anti-Pgk1p) was applied as a loading control.

As shown in Figure 14, the results indicated that of the three tagged codon-optimized kAE1 variants, only kAE1^{HA} and kAE1^{FLAG} expression could be detected based on Western blot analysis; no expression was detectable in cells transformed with pYES-kAE1^{V5}. Furthermore, kAE1^{HA} and kAE1^{FLAG} protein levels were more pronounced in BY4742 Δ*end3* cells compared to wild-type cells.

3.1.2. Expression of kAE1^{HA}, kAE1^{V5}, kAE1^{FLAG} in an β-estradiol inducible expression strain

The integrative GEV plasmid, containing a β-estradiol inducible GEV promoter for dose-dependent regulation of protein expression, is a gift from Prof. Dr. David Botstein (McIsaac *et al.*, 2011). To generate the strain BY4742-GEV, the plasmid pACT1-GEV was digested with *EcoR*V, transformed into BY4742 cells, and selection occurred on leu d/o plates. Colonies of yeast after successful homologous recombination were subsequently transformed with the plasmids pYES-kAE1^{HA}, pYES-kAE1^{V5}, pYES-kAE1^{FLAG}, respectively (Figure 15).

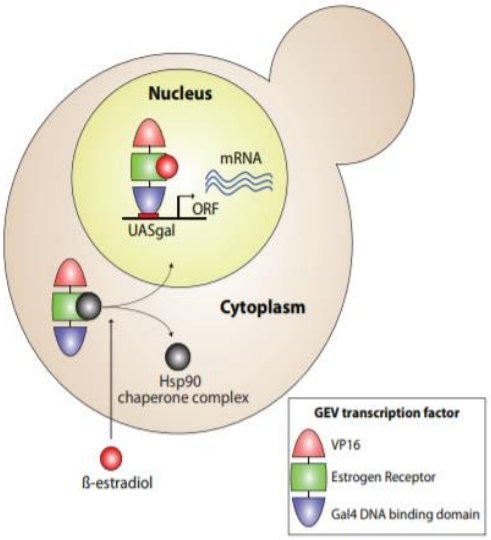

Figure 15: Principle of the GEV expression system. The system is based on the constitutively expressed transcriptional activator (GEV), which is inactively present in the cytoplasm associated with the chaperone Hsp90. After application of β-estradiol, the hormone binds to its respective binding domain, leading to dissociation of GEV from Hsp90. The activated GEV enters the nucleus and binds to specific UAS_{GAL} consensus sequences, thereby strongly inducing the transcription of P_{Gal}-dependent genes (McIsaac *et al.*, 2011).

In the first experiment, cells from a fresh overnight culture were incubated in the presence of 100 nM β-estradiol, and the expression of different kAE1 variants was analyzed via Western blot. As already seen in BY4742 wild-type cells, no expression was detectable for kAE1^{V5} (Figure 16a), whereas a signal was detected at the correct size (approximately 95 kDa) for both kAE1^{HA} and kAE1^{FLAG} (Figure 16b, c). Interestingly, the expression in kAE1^{HA} was much stronger than kAE1^{FLAG} after 100 nM β-estradiol supplementation (Figure 16a).

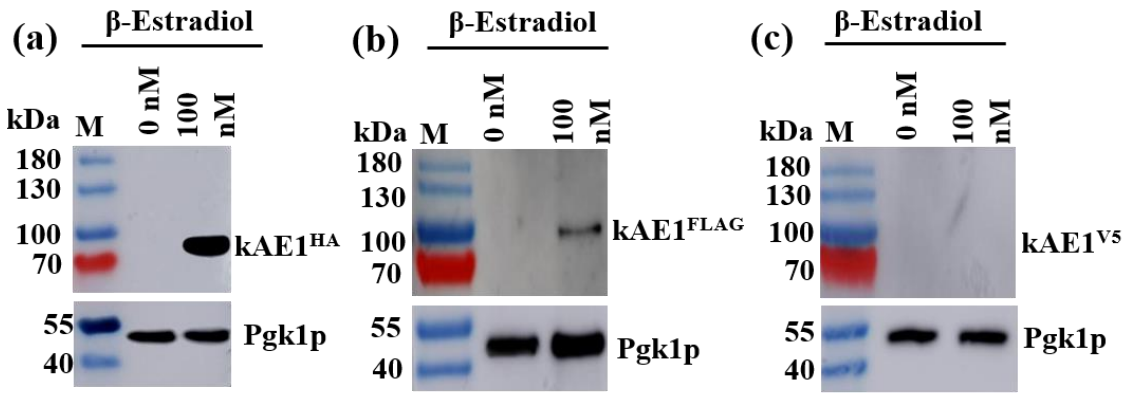

Figure 16: Expression of various kAE1 variants in a BY4742-GEV strain. kAE1 was detectable in BY4742-GEV [pYES-kAE1^{HA}] and BY4742-GEV [pYES-kAE1^{FLAG}], whereas no expression was observed in the BY4742-GEV [pYES-kAE1^{V5}]. A molecular weight marker (M) was used for protein size determination. Phosphoglycerate kinase 1 (Pgk1p) served as a loading control.

3.1.3. Optimization of the cell lysis protocol to facilitate kAE1 membrane extraction

Detergents are often added to cell lysis buffers to facilitate the release of transmembrane proteins or improve cell disruption (Hopkins, 1991). The amphiphilic properties of these chemicals allow the breakage of protein-protein, protein-lipid, and lipid-lipid associations, the denaturation of proteins, and the prevention of non-specific bindings in immunochemical assays and protein crystallization (Moraes *et al.*, 2014). Triton X-100 (TX100) is a widely utilized anionic surfactant often used in protein extraction protocols due to its potential to lyse cells and solubilize membrane-bound proteins (Koley & Bard, 2010). In this study, three different concentrations of TX100 (0.3%, 1%, and 2%, respectively) were added to the lysis buffer to enhance the efficiency of kAE1 extraction from the cell membrane. The Western analysis results showed that TX100 supplementation significantly improved the separation of kAE1 from the rest of the membrane structures (Figure 17a). Densiometric evaluation of the visualized Western blot signals was conducted to compare the kAE1 protein levels of the pellet fraction (P) and the supernatant (S) (Figure 17b). When TX100 was used at concentrations of 0.3% or 1%, kAE1 protein levels in the supernatant significantly increased compared to no TX100 supplementation. The use of 2% TX100 was slightly less efficient than 1% TX100 resulting in only a 10.5% increase compared to the 0% TX100 condition. However, the overall

kAE1 protein levels in the pellet fraction in all samples were much higher than in the supernatant.

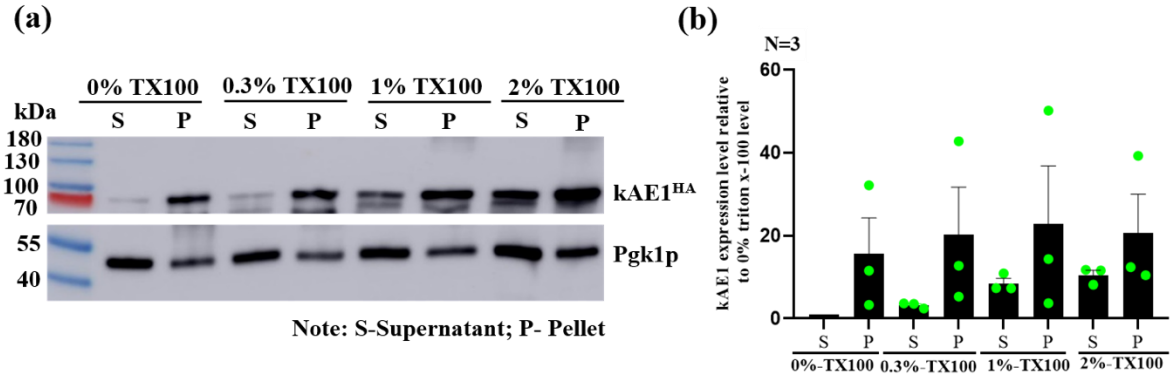

Figure 17: Triton X-100 improves kAE1 separation from yeast membrane structures. As the TX100 concentration in the cell lysis buffer increased from 0% to 2%, kAE1 protein level in the supernatant increased consistently from 1% to 10.5%. In contrast, the cell pellet fraction showed the highest kAE1 level (22.8%) at 1% TX100 concentration. Increased concentrations of TX100 appeared to reduce the recovery of kAE1. Phosphoglycerate kinase 1 (Pgk1p) was used as a loading control.

3.2. Full-length kAE1 localization in yeast

3.2.1. Localization of HA- and FLAG-tagged kAE1 in yeast

In mammalian cells and under normal physiological conditions, kAE1 localizes in the basolateral membrane of the α-intercalated cells to regulate the acid-base balance by mediating Cl^-/HCO_3^- exchange. The prerequisite for using yeast as a model system for kAE1 is that the anion transporter is correctly trafficked to the yeast plasma membrane (PM) (Sarder *et al.*, 2020). Therefore, $kAE1^{HA}$ and $kAE1^{FLAG}$ were constructed and transformed into the wild-type strain BY4742 to check the localization of both kAE1 variants using indirect-fluorescence microscopy. As shown in Figure 18, no fluorescence signal could be detected under non-inducing conditions (glucose) after FITC-coupled antibody staining. In contrast, green signals were visualized in cells cultivated in galactose medium, inducing the expression of kAE1 in *S. cerevisiae*. Furthermore, the results also showed that faint green kAE1 signals are partially localized at the yeast plasma membrane. However, the majority of kAE1 signals was mainly located in ER-like structures (Figure 18). Unfortunately, it is difficult to accurately confirm kAE1 localization based on only indirect-fluorescence microscopy results as yeast cortical ER structures are spatially close to the plasma membrane hindering the discrimination between these subcompartments. Therefore, other microscopy techniques with higher resolution (i. e. electron

microscopy or super-resolution microscopy) are needed to analyze kAE1 localization in yeast further.

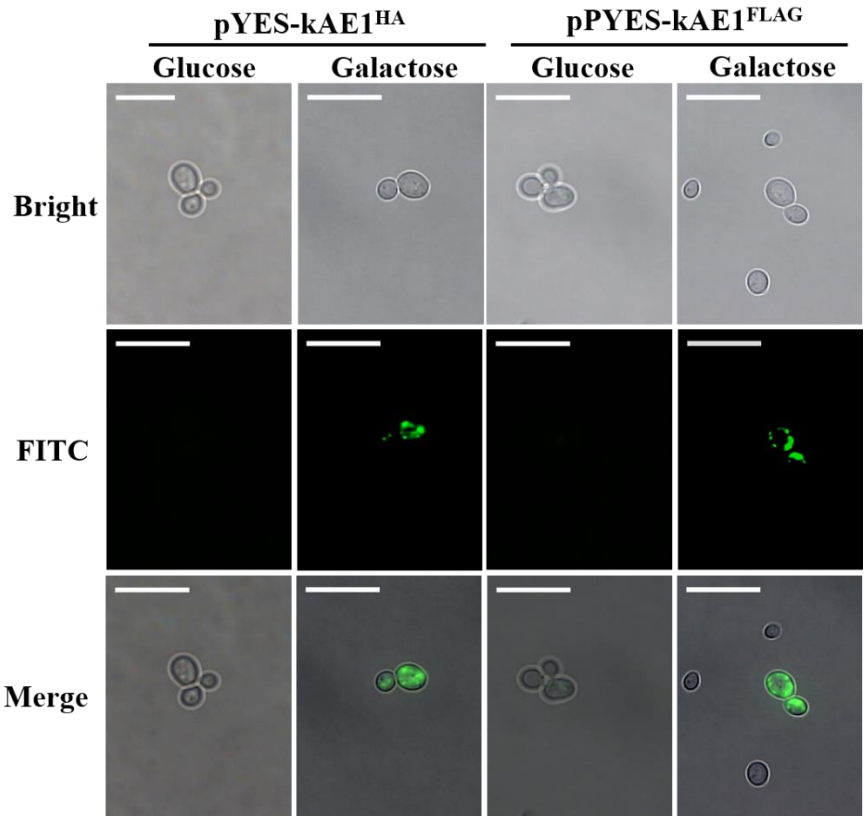

Figure 18: Detection of kAE1^{HA} and kAE1^{FLAG} localization in *S. cerevisiae* via indirect immunofluorescence Galactose supplementation induced the expression of kAE1^{HA} and kAE1^{FLAG}; samples were probed with primary anti-HA and anti-FLAG, respectively, and secondary FITC-coupled anti-rat antibodies. Green fluorescence was detected for both, kAE1^{HA} and kAE1^{FLAG}. Yeast cells grown under non-inducing conditions (glucose) were used as negative control. Scale bar: 10 µm.

3.2.3. Full-length kAE1 partially localizes at the yeast plasma membrane

To check kAE1 localization in yeast in more detail, the intracellular kAE1 localization was determined by transmission electron microscopy (TEM) and immunogold labeling. Galactose-inducible expression plasmids pYES2.1 containing three different kAE1 variants (kAE1^{HA}, kAE1^{WT}, and kAE1^{B3Mem}) were transformed into BY4742 Δ*end3* and BY4742 Δ*pep4* (deficient in vacuolar degradation). Transformants were picked from the plates, and the expression was verified before the conduction of the TEM study. Western analysis indicated that kAE1^{HA}, kAE1^{WT}, and kAE1^{B3Mem} were all expressed in both BY4742 Δ*end3* and Δ*pep4* cells (Figure 19).

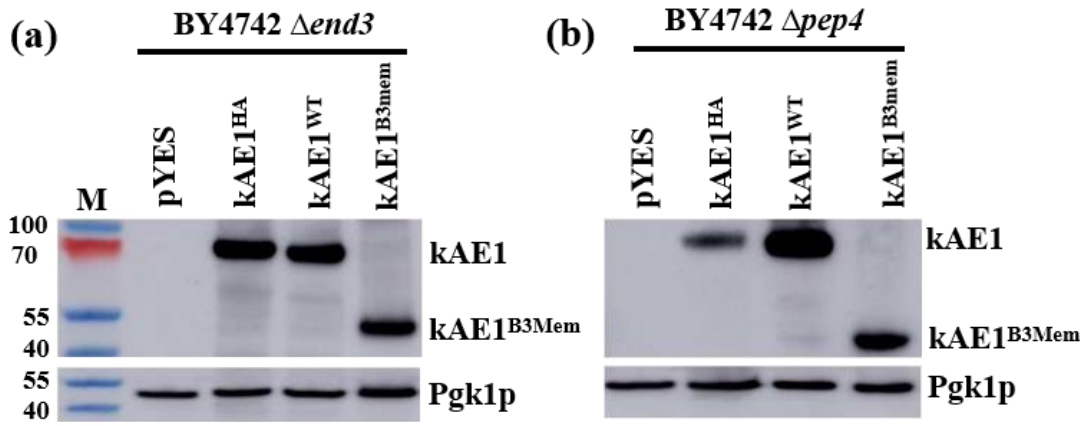

Figure 19: Expression level of kAE1 derivatives in BY4742 Δ*end3* and Δ*pep4* mutants. Signals of the indicated kAE1 variants ($kAE1^{HA}$, $kAE1^{WT}$ and $kAE1^{B3Mem}$) were visualized using an anti-kAE1 antibody (BRIC170), and the appropriate secondary HRP-coupled secondary antibody; detection of phosphoglycerate kinase 1 (Pgk1p) was used as a loading control. Mutants were additionally transformed with the empty vector (pYES, negative control). An appropriate protein standard (M) served as a molecular weight marker.

For the following TEM assay, $kAE1^{B3Mem}$ was used as a positive control as previous studies could already verify its targeting to the yeast plasma membrane (Toye *et al.*, 2004); cells transformed with an empty vector served as negative control. The overall cell structure for BY4742 Δ*end3* and Δ*pep4* cells expressing $kAE1^{HA}$ is shown in Figure 20. Theoretically, more kAE1 should traffic to the yeast plasma membrane in BY4742 Δ*end3* strain due to the deletion of the *END3* gene impairing both receptor-mediated and fluid-phase endocytosis (Giardina *et al.*, 2014). In the BY4742 Δ*pep4* strain, more kAE1 should be localized in the vacuole due to the absence of several Pep4p-maturated vacuolar hydrolases affecting the kAE1 degradation process (Ammerer *et al.*, 1986).

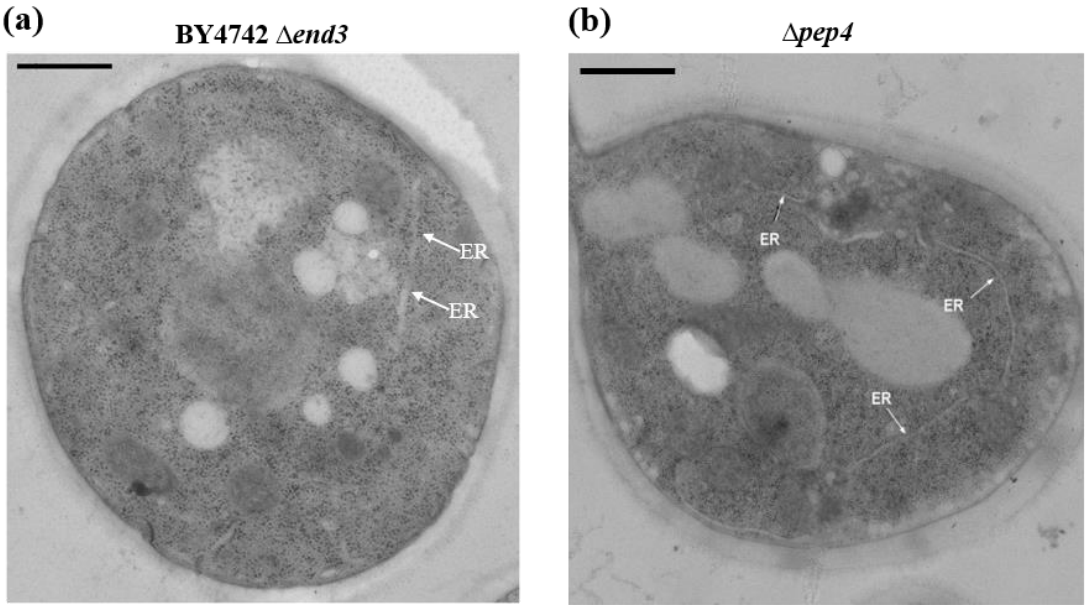

Figure 20: Depiction of cellular structures of BY4742 Δ*end3* and Δ*pep4* cells visualized via TEM. The white arrow indicates yeast cell endoplasmic reticulum (ER) structure. Scale bars: 500 nm.

As shown in Figure 21, after using immunogold labeling with primary antibodies (anti-BRIC170) against kAE1, it could be shown that the gold particles were localized in the yeast plasma membrane in Δ*end3* and Δ*pep4* cells, expressing the different kAE1 variants. Notably, in almost all cells, no cortical ER structures were visible close to the labeled sites (~ 35 nm). Therefore, it was proposed that the gold particles are indeed localized in the yeast cell plasma membrane instead of cortical ER structures (Figure 21). In contrast, no gold particles were visible in the negative control cells.

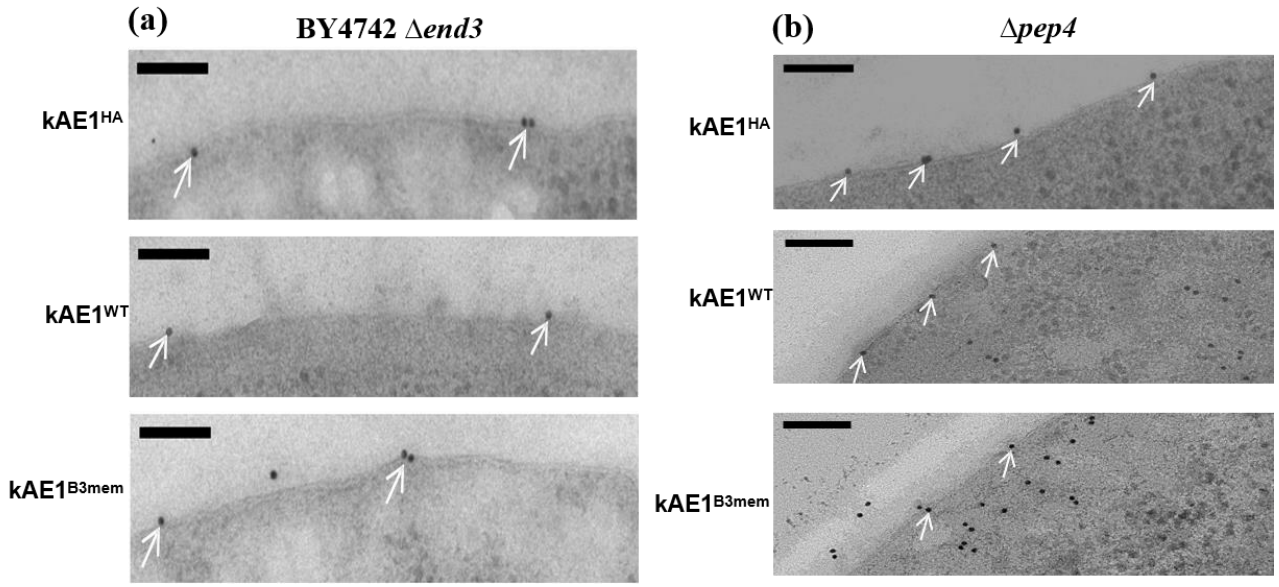

Figure 21: Transmission electron microscopy (TEM) of Δ*end3* and Δ*pep4* cells after immunogold staining. Yeast cells were transformed with yeast codon-optimized versions of kAE1^{HA}, wild-type kAE1 (kAE1^{WT}), or truncated kAE1 (kAE1^{B3Mem}). kAE1 localization is indicated by white arrows; Scale bar: 100 nm.

Furthermore, PM-localized gold particles were counted (n = 33 cells/sample) in both Δ*end3* and Δ*pep4* cells to calculate potential differences in the localization of the kAE1 derivatives. The results indicated a significant increase for PM-localized kAE1 in all kAE1-expressing cells compared to empty vector control cells. In case of Δ*end3* cells, kAE1^{HA} showed the highest number of PM-localized kAE1 signals (2.6/µm), followed by kAE1^{B3mem} (1.5/µm) and kAE1^{HA} (1.1/µm) (Figure 22a). Regarding Δ*pep4* cells, kAE1^{HA} expression again showed the highest number of PM-localized kAE1 signals with 2.2 particles per 1 µm PM, whereas the same amount of gold particles was observed for kAE1^{B3mem} and kAE1^{HA} (1.7/µm PM, respectively) (Figure 22b). This may be caused by a difference in the expression levels of kAE1 variants.

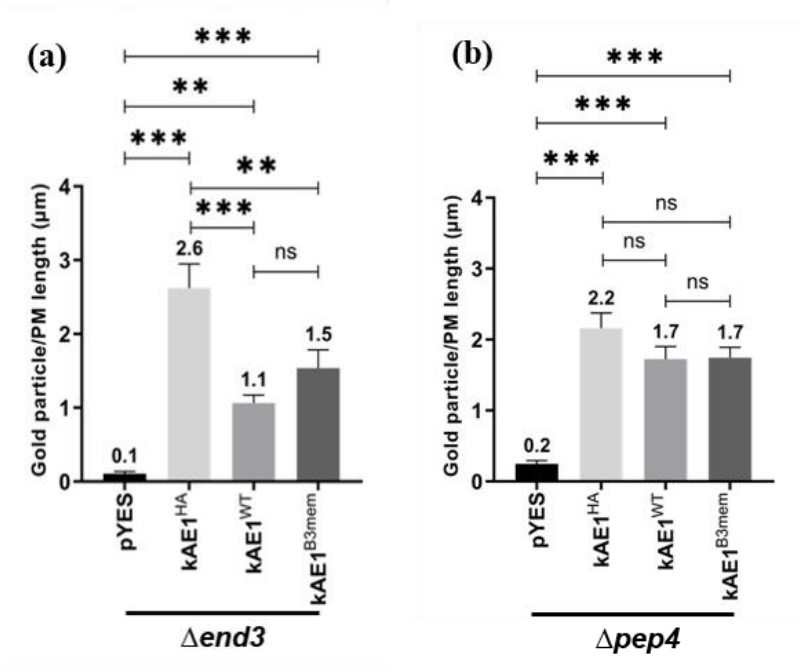

Figure 22: Distribution of immunogold-stained kAE1 at the plasma membrane. kAE1 localization at the plasma membrane was determined via transmission electron microscopy in the yeast deletion mutants Δ*end3* (a) and Δ*pep4* (b) expressing kAE1WT, kAE1HA, or kAE1^{B3Mem}. Statistical analysis was conducted by counting the number of gold particles per µm, and depicted is the respective mean average ± SEM (n = 33 cells/sample); One-Way ANOVA: $^{**}p < 0.01$ and $^{***}p < 0.001$; ns = not significant. Yeast expressing the empty vector pYES were used as a control.

Based on the kAE1^{HA}, kAE1^{B3Mem,} and kAE1^{WT} localization results, further experiments were conducted to assess whether N-terminal addition of enhanced green fluorescent protein (eGFP) affects kAE1 targeting to the yeast cell surface. To do so, eGFP-kAE1 and the PM marker Pma1p-mRFP were co-expressed in BY4741 Δ*ist2* cells in which yeast cortical ER structures are clearly separated from the plasma membrane. Using fluorescence-based SIM imaging, kAE1 was found to partially co-localize with the yeast plasma membrane, which is indicated as a yellow color after figure merging (Figure 23). Therefore, the N-terminal addition of eGFP in kAE1 presumably does not alter plasma membrane-targeting of kAE1 in yeast.

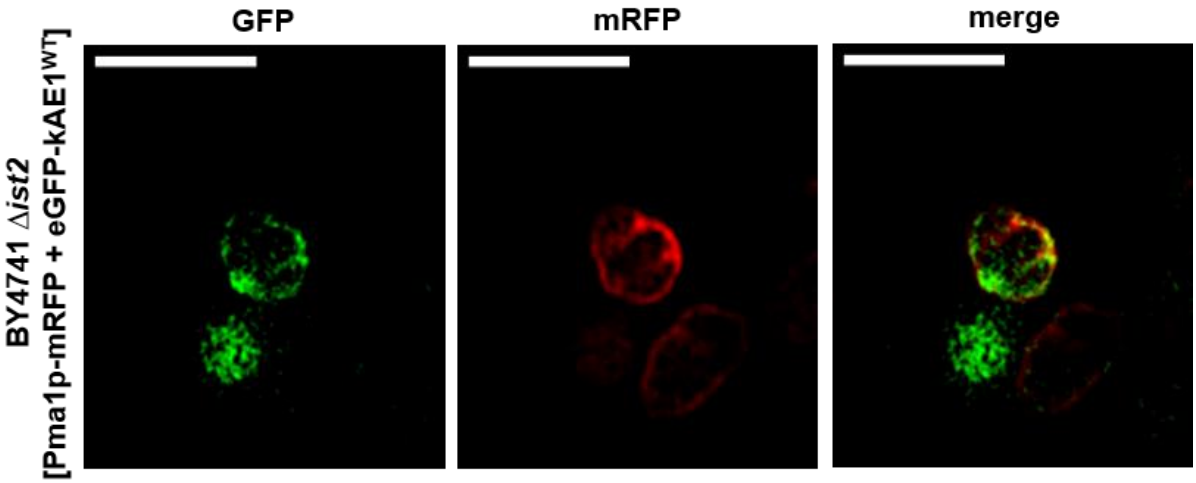

Figure 23: SIM analysis of cells co-expressing eGFP-kAE1^{WT} and the mRFP-tagged PM marker Pma1p. BY4741 Δ*ist2* cells with a chromosomally integrated mRFP-tagged *PMA1* were transformed with N-terminally eGFP-coupled kAE1 (eGFP-kAE1^{WT}) and analyzed using SIM. The results indicate a partial co-localization (Merge) of eGFP-kAE1 (GFP) and the PM marker Pma1p-mRFP (mRFP); Scale bar: 5 µm.

The results of the different microscopy techniques showed for the first time that not only the truncated kAE1 variant kAE1^{B3mem} but also untagged (kAE1^{WT}) and tagged (kAE1^{HA}) full-length kAE1 derivatives can reach the yeast plasma membrane. Additionally, it was demonstrated that the N-terminal fusion of eGFP to kAE1 does not completely inhibit its correct trafficking to the PM. Taken together, these data underline the potential of yeast as a suitable model system for the study of human kAE1.

3.2.4. Full-length kAE1 partially localizes in the yeast ER, vacuole and MVBs

The endoplasmic reticulum (ER) and other secretory compartments of *S. cerevisiae* have biochemical similarities with higher eukaryotic cells (Kimata & Kohno, 2011). In *S. cerevisiae*, the ER can mainly be divided into three different types: cortical ER (cER), rough endoplasmic reticulum (RER), and perinuclear ER. Out of these, cER comprises the largest subdomain of the yeast ER system and comes in close contact with the yeast PM (Lewis *et al.*, 1996). RER and perinuclear ER, in contrast, are primarily localized in the outer membrane of the nucleus, where they are involved in protein synthesis (Shen *et al.*, 2004; Kim *et al.*, 2008). TEM data analysis indicated that kAE1^{WT}, kAE1^{HA}, and truncated kAE1^{B3Mem} are mainly retained in ER

structures, especially the cortical ER. In contrast, cells used as a negative control (pYES-EV) showed the highest amount of gold particles in the vacuole, nucleus, or cell wall, which can probably be attributed to the unspecific binding of the antibody (Figure 24).

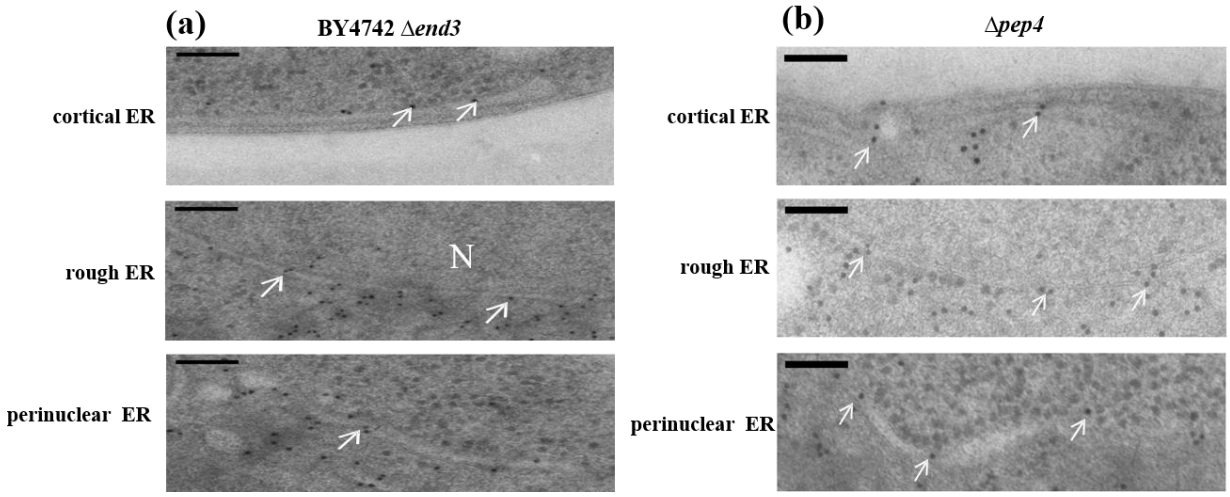

Figure 24: Immunogold labeling verified localization of kAE1 in cortical ER, rough ER, and perinuclear ER of both, Δ*end3* and Δ*pep4* cells expressing yeast codon-optimized kAE1. N indicates nucleus. Scale bar: 100 nm

In addition to the different ER structures and the PM, kAE1 could also be found in other cell organelles, such as multivesicular bodies (MVBs) and vacuole (Figure 25). Yeast MVBs can be defined as a pre-vacuolar compartment essential for protein sorting, either recycling endocytosed proteins back to the PM or transfer them to the vacuole for degradation via the so-called 'endosomal sorting complexes required for transport' (ESCRT) pathway (Katzmann, 2004). The TEM analysis results showed that at least part of the kAE1 fraction is trafficked to the vacuole after MVBs sorting.

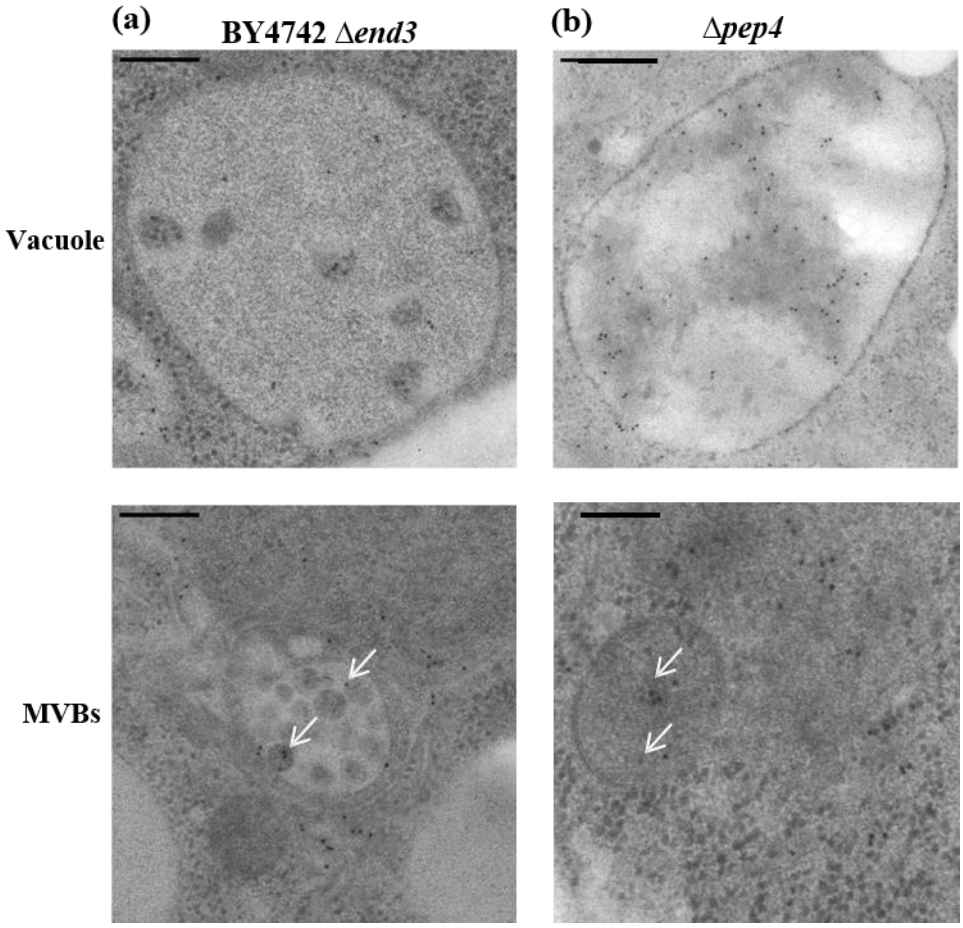

Figure 25: Localization of kAE1 in the vacuole and multivesicular bodies (MVBs) detected after immunogold labeling (white arrows). EM images showing results of cells expressing $kAE1^{HA}$. Scale bar: 100 nm.

The number of gold-labeled kAE1 in the vacuole was evaluated via counting, and the results indicated that significantly more kAE1 could be detected in BY4742 Δ*pep4* cells compared to Δ*end3* cells. In the latter, the derivatives $kAE1^{HA}$ (81.5) and $kAE1^{B3mem}$ (85.2) were enriched considerably in the vacuole compared to the empty vector control (Figure 26b). In case of all analyzed kAE1 derivatives, significantly increased numbers of gold particles could be detected in the vacuole after expression of the constructs in Δ*pep4* compared to the empty vector control (Figure 26b). Notably, the number of gold particles in $kAE1^{B3mem}$ (288.2) expressing cells was much higher compared to $kAE1^{HA}$ (122.1) and $kAE1^{WT}$ (151.3), pointing to different degradation rates of the truncated kAE1 variant.

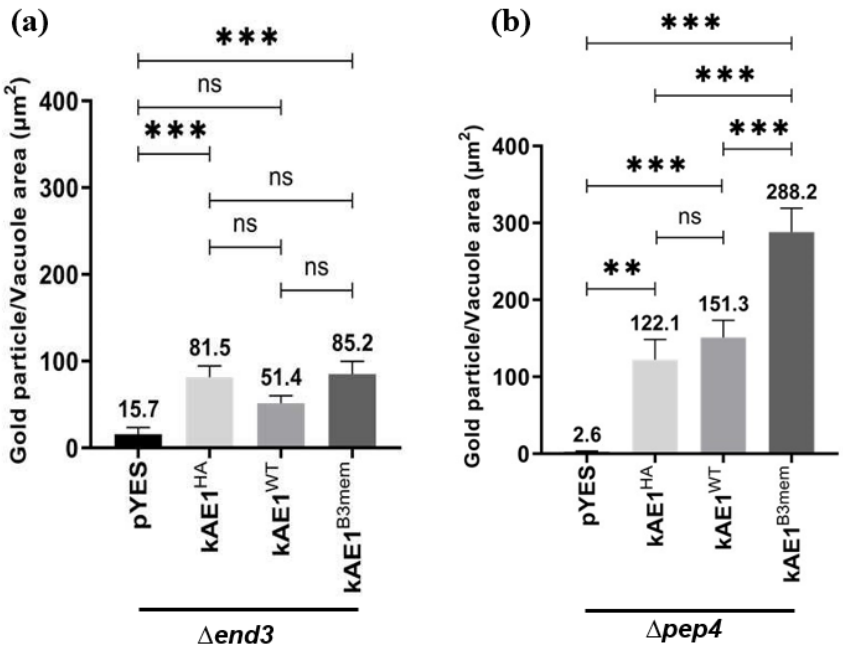

Figure 26: Distribution of immunogold-labeled kAE1 in the vacuole of Δ*end3* (a) and Δ*pep4* (b) cells expressing kAE1WT, kAE1HA, or kAE1^{B3Mem}. kAE1 localization was analyzed via transmission electron microscopy, and statistical analysis was performed by counting the number of gold particles per µm^2; depicted is the respective mean average ± SEM ($n_{\Delta end3}$ = 26 cells/sample; $n_{\Delta pep4}$ = 27 cells/sample); One-Way ANOVA: $^{**}p < 0.01$ and $^{***}p < 0.001$; ns = not significant. Yeast cells expressing the empty vector pYES were used as negative control.

3.2.5. kAE1 mainly accumulates in membrane-like structures derived from the ER

TEM data showed that only faint amounts of all analyzed kAE1 variants localized at the yeast plasma membrane, while the majority of kAE1 protein was retained in parts of the secretory pathway of the cells, such as ER, vacuole, and MVBs. More precisely, kAE1 variants accumulated in condensed accumulates in intracellular membrane/vesicle-like (MV) structures, evidently detectable after kAE1 expression in Δ*end3* or Δ*pep4* cells (Figure 27, Figure 28).

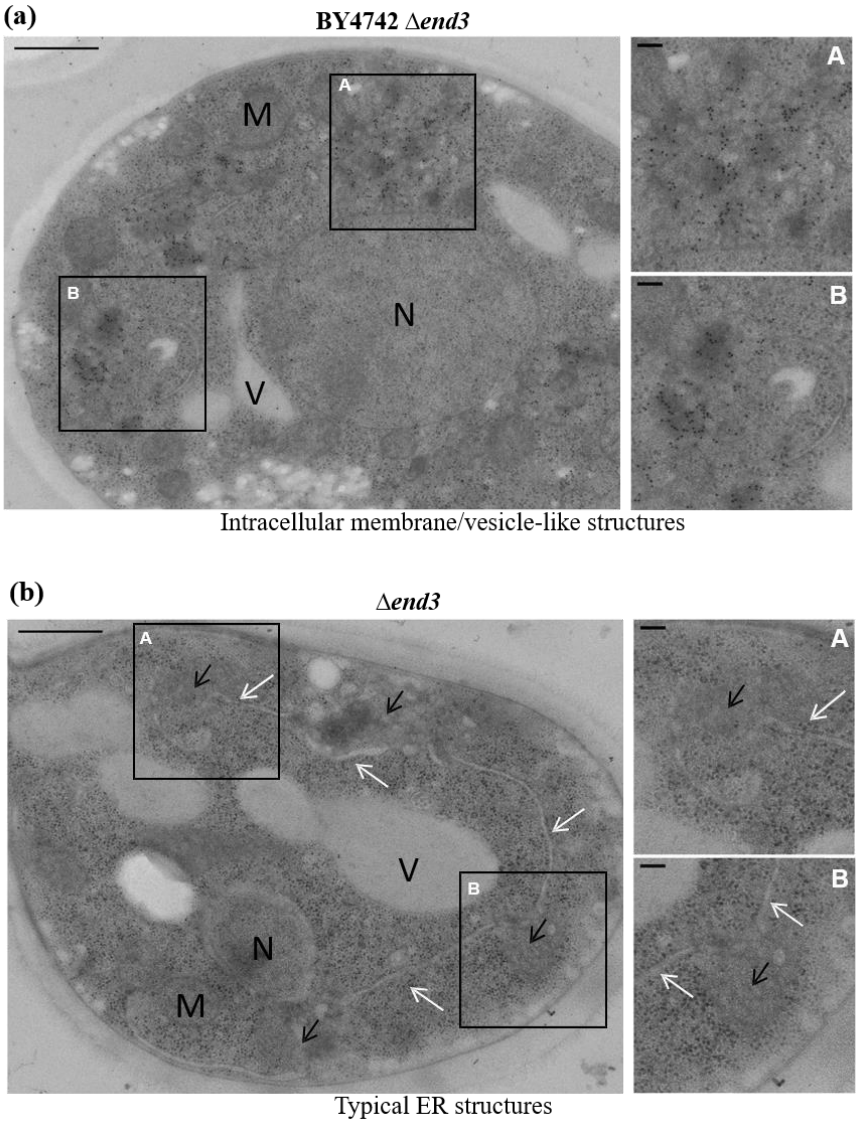

Figure 27: Accumulation of kAE1 in intracellular membrane/vesicle-like structures after expression in BY4742 Δ*end3* cells. HA-tagged kAE1 was visualized via immunogold labeling following TEM. (a) kAE1 localization in typical MV-like structures. (b) Association of MV-like structures (black arrows) with ER structures (white arrows). Inlets A and B indicate the magnified area of the respective regions (black box); Scale bar: 500 nm and 100 nm.

The TEM analysis of BY4742 Δ*end3* and Δ*pep4* cells showed that in some cellular sections, MV-like structures and the ER were connected (Figure 27), indicating their potential attribution to the yeast ER (e. g. cortical ER, rough ER, or perinuclear ER) (Figure 28). However, the kAE1 accumulations could also be located in the Golgi apparatus or endosomal structures, which cannot be ascertained without the use of marker proteins. Therefore, additional experiments were conducted to check the kAE1 co-localization with different marker proteins in yeast.

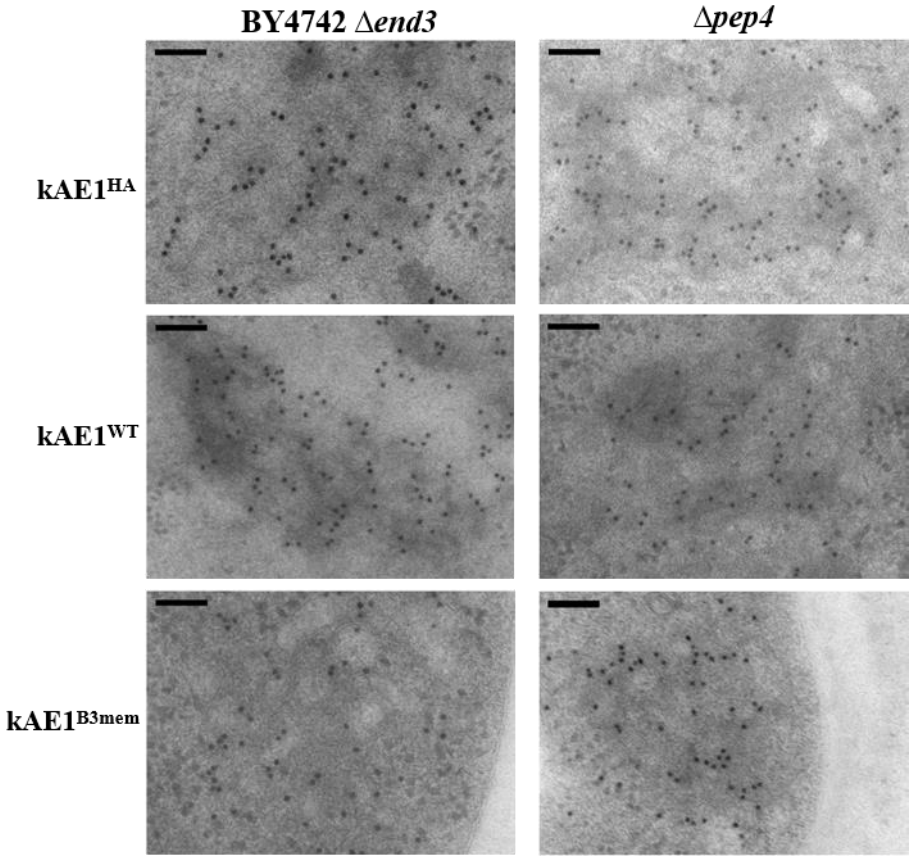

Figure 28: Accumulation of various kAE1 derivatives in BY4742 Δ*end3* and Δ*pep4* cells. Both full-length (kAE1^{HA} and kAE1^{WT}) and truncated versions (kAE1^{B3mem}) accumulated in membrane-like structures derived from the ER.

3.2.6. kAE1 localization in the secretory pathway of *S. cerevisiae*

The results of the electron microscopy-based study indicated that most kAE1 is aggregated in membrane and vesicle structures, most likely belonging to the intracellular ER network. Due to experimental limitations, a clear distinction between ER or Golgi or endosomal structures was difficult, impeding the exact localization of the anion transporter. For a more precise determination, the eGFP-tagged kAE1 variant (eGFP-kAE1) was transformed into cells of the yeast strain S228C, which chromosomally expressed different mCherry-tagged organelle-specific marker proteins, and respective transformants were analyzed using SIM imaging (Figure 29).

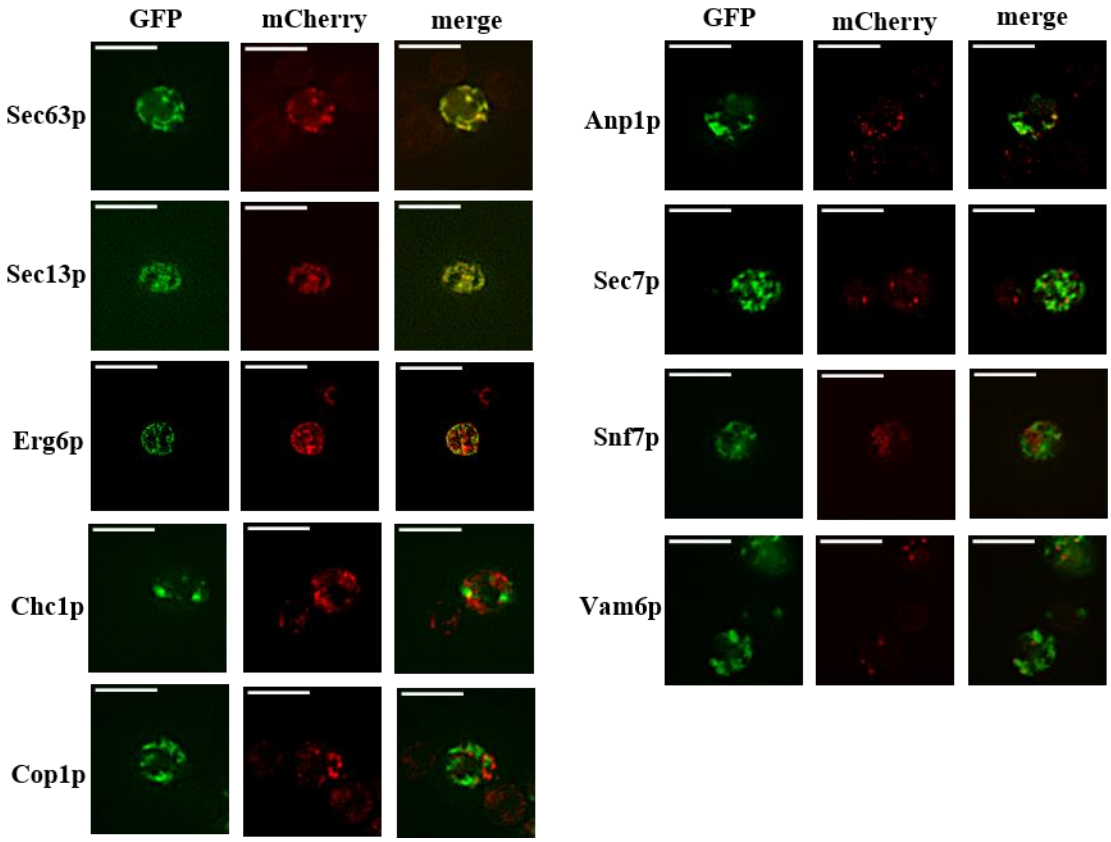

Figure 29: kAE1 localization in the secretory pathway of *S. cerevisiae*. Structure illumination microscopy (SIM) images of *S. cerevisiae* S288C cells expressing an eGFP-tagged full-length kAE1 derivative (GFP) together with the indicated mCherry-tagged organelle marker proteins (mCherry). Potential signal overlay is depicted in yellow (merge). Scale bar: 5 µm.

The SIM data pointed to a partial co-localization of kAE1 with Sec63p (ER marker), Sec13p (COPII vesicle marker), and Erg6p (cortical ER marker), as well as an overlap with the early Golgi marker Anp1p. However, no co-localization of the GFP-tagged anion transporter with other compartment markers (Sec7p, Vam6p, Snf7p, Cop1p, and Chc1p) was detected. Although the majority of kAE1 signals overlapped with Sec63p, no ring-like ER structure around the yeast nucleus was visible (Figure 29). Comparing the obtained results of these experiments with electron microscopy data of kAE1 expressing yeast cells, the fluorescence patterns show striking similarities with multivesicular bodies (Sarder *et al.*, 2020; Li *et al.*, 2021). Therefore, it could be proposed that kAE1 accumulation disturbs and/or affects the native structure of the yeast ER. In summary, all the kAE1 variants were predominantly located in ER structures, indicating that kAE1 was not efficiently released from the ER. To further analyze this accumulation of heterologously expressed kAE1, additional studies are needed to explore some potential reasons behind this phenotype.

3.3. kAE1 induces yeast unfolded protein response

3.3.1. Expression of kAE1 variants in yeast causes cell growth defects

The heterologous expression of proteins can lead to growth defects in the expressing cell and is often accompanied by high ER stress levels (Schröder, 2008). Therefore, potential effects of kAE1 expression on the yeast growth behavior were analyzed, determining the growth rates of BY4742 cells expressing untagged or tagged kAE1 derivatives. In addition to untagged and HA-tagged kAE1 (pYES-kAE1^{WT} and pYES-kAE1^{HA}) and the N-terminally truncated kAE1 variant kAE1^{B3mem} (pYES-kAE1^{B3mem}), also the mutant kAE1^{E681Q} (pYES-kAE1^{E681Q}) was transformed into wild-type BY4742 cells. Based on an alteration in the membrane domain of kAE1, the latter is a kAE1 mutant with defects in the anion transport capacity and is often used as a control in various studies. Previous studies were able to show that the overexpression of the H/KDEL receptor Erd2p in yeast leads to a strong induction of the UPR. Therefore, yeast cells expressing V5-tagged Erd2p were used to compare the severity of the UPR induction by the kAE1 derivatives. Untreated cells transformed with the empty vector were used as negative control (pYES-EV), whereas cells supplemented with DTT (EV-DTT) were used as positive control. To exclude artificial effects of the dissolvent, empty vector carrying cells were cultivated with DMSO alone as a second control (EV-DMSO). As depicted in Figure 30, untreated and DMSO-treated empty vector cells as wells as cells overexpressing the HDEL receptor Erd2p (ERD2) showed the highest growth rates. In contrast, cell growth of yeast expressing the different kAE1 variants was considerably reduced and similar to the growth pattern of DTT-treated cells. Notably, neither the truncated kAE1 variant kAE1^{B3Mem} nor the mutant kAE1^{E681Q} showed a significantly different growth pattern compared to kAE1^{WT}. This might indicate that the N-terminus and the bicarbonate exchange function of kAE1 are not directly involved in the growth defect of kAE1 expressing yeast cells.

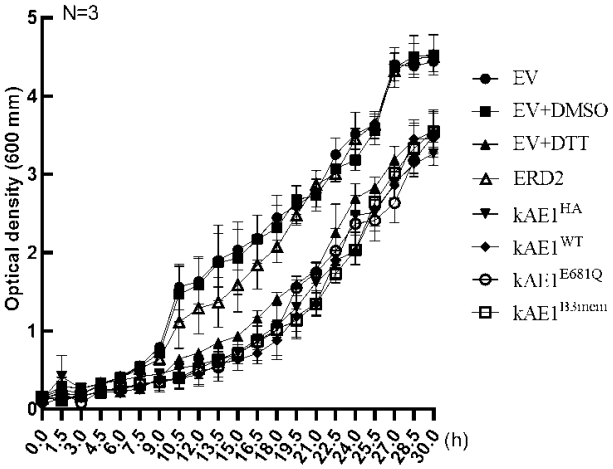

Strain	OD_{600}/h
EV	**0.21±0.01**
EV+DMSO	**0.21±0.03**
EV+DTT	**0.11±0.03***
ERD2	**0.17±0.05**
$kAE1^{HA}$	**0.12±0.03***
$kAE1^{WT}$	**0.09±0.04****
$kAE1^{E681Q}$	**0.09±0.05****
$kAE1^{B3mem}$	**0.10±0.04****

Figure 30: Cellular growth rates after expression of various kAE1 variants in yeast. Growth rates of wild-type BY4742 cells expressing the indicated kAE1 variants ($kAE1^{HA}$, $kAE1^{WT}$, $kAE1^{E681Q}$, $kAE1^{B3mem}$) were measured via OD_{600} determination over 30 h. Untreated (EV) and DMSO-treated (EV+DMSO) yeast transformed with the empty pYES2.1 vector were used as negative control. Empty vector cells incubated with 2.5 mM DTT (EV+DTT) as well as yeast cells overexpressing the HDEL receptor Erd2p (ERD2) served as positive controls. Depicted are the mean values ± SD; n = 3.

3.3.2. kAE1 expression induces yeast ER-stress

Proteins must be correctly folded, assembled, and located to fulfill their designated cellular functions. However, unfolded or misfolded proteins may aggregate in the lumen of the ER, thereby inducing ER stress. Consequently, UPR-related mechanisms are activated to deal with these accumulations by either assisting in folding or degradation of the proteins (Shamu *et al.*,1994; Okamura *et al.*,2000). Based on the electron microscopy data and the analysis of the cellular growth patterns, it was preliminary hypothesized that expression of kAE1 variants leads to folding problems and potentially induces cellular ER-stress. To further test this hypothesis, the kAE1 variants pYES-$kAE1^{WT}$, pYES-$kAE1^{HA}$, pYES-$kAE1^{FLAG}$, pYES-$kAE1^{B3mem}$, and pYES-$kAE1^{E681Q}$ were transformed into BY4742 cells. Yeast cells overexpressing the H/KDEL receptor Erd2p (pYES2.$1^{ERD2\text{-}V5}$) served as control. ER stress of the transformants was monitored by measuring the UPR activation with different biochemical approaches.

UPR activation in yeast can be monitored via the expression level of Kar2p since the final step of the UPR signaling pathway includes the Hac1p-dependent upregulation of ER-luminal chaperones such as Kar2p or Pdi1p, to generally increase the folding capacity of the ER (Lajoie *et al.*, 2012). Therefore, Western analyses were conducted to determine the intracellular protein level of Kar2p. As shown in Figure 31, a massive increase in the amount of Kar2p could be observed after overexpression of the indicated kAE1 variants ($kAE1^{WT}$, $kAE1^{HA}$, $kAE1^{FLAG}$,

and kAE1^{E681Q}), correlating with the growth rate analysis. As expected, the presence of the UPR activators DTT and tunicamycin led to a substantial elevation of intracellular Kar2p level. Negative controls (EV, EV+DMSO) showed only minor amounts of the chaperone. Interestingly, no significant difference was detected between cells overexpressing the yeast HDEL receptor Erd2p and empty vector control cells.

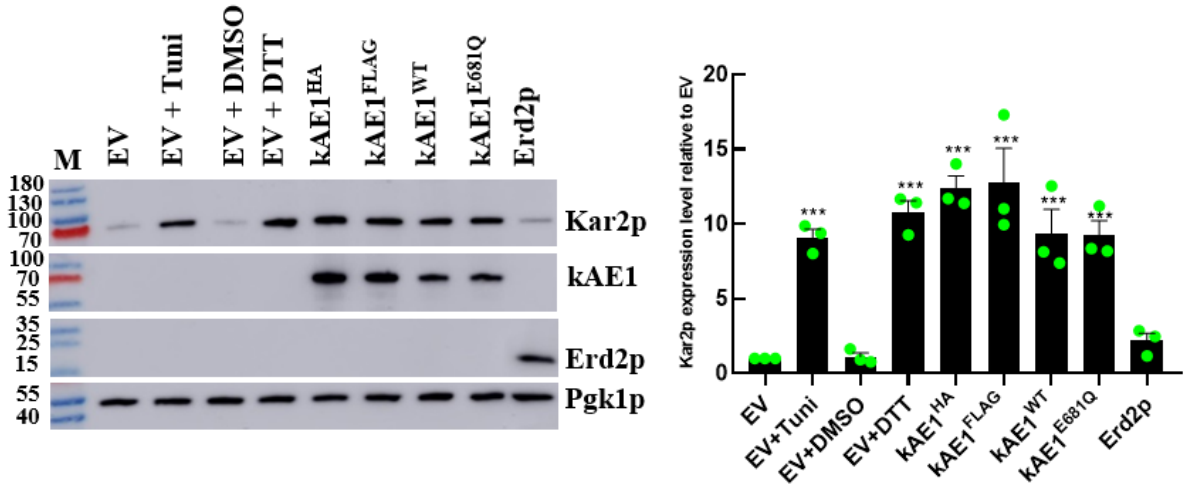

Figure 31: kAE1 expression induces UPR activation in yeast. Kar2p levels of BY4742 cells expressing empty pYES2.1 vector (EV), HA- or Flag-tagged kAE1 (kAE1^{HA} or kAE1^{FLAG}), wild-type kAE1 (kAE1^{WT}) or an inactive kAE1 variant (kAE1^{E681Q}) were determined via Western blot analysis. Yeast transformed with the empty vector were incubated for 6 h with tunicamycin (EV+Tuni) or DTT (dissolved in DMSO, EV+DTT) and used as positive control. Untreated (EV) and DMSO-treated empty vector cells (EV+DMSO) served as negative control. Western blots were incubated with the appropriate primary antibodies against Kar2p, kAE1 (anti-BRIC170), Erd2p (anti-V5), and the loading control Pgk1p; secondary antibodies were HRP-conjugated, and signals were visualized via chemiluminescence (Left). Relative Kar2p protein levels were determined via densitometric analysis of the corresponding signals and normalized to Pgk1p, and the empty vector, depicted are the respective mean values (±SEM), n = 3, ***$p < 0.001$ (One-Way ANOVA), (Right).

To further address the correlation between kAE1 expression and yeast UPR activation, Kar2p levels were determined in the β-estradiol inducible yeast strain BY4742-GEV expressing kAE1. As shown in Figure 32a, cells transformed with the empty vector showed no significant alterations in the intracellular Kar2p level. However, when BY4742-GEV cells were transformed with kAE1^{HA}, the protein level of kAE1 steadily increased, corresponding to the rising β-estradiol concentrations in the cell culture medium (0 nM, 1 nM, 10 nM, 10^2 nM, 10^3 nM, 5x10^3 nM and 10^4 nM), as well as the amount of intracellular Kar2p (Figure 32b). These results highlight the correlation between kAE1 overexpression and the increase in ER stress

resulting in the activation of the UPR.

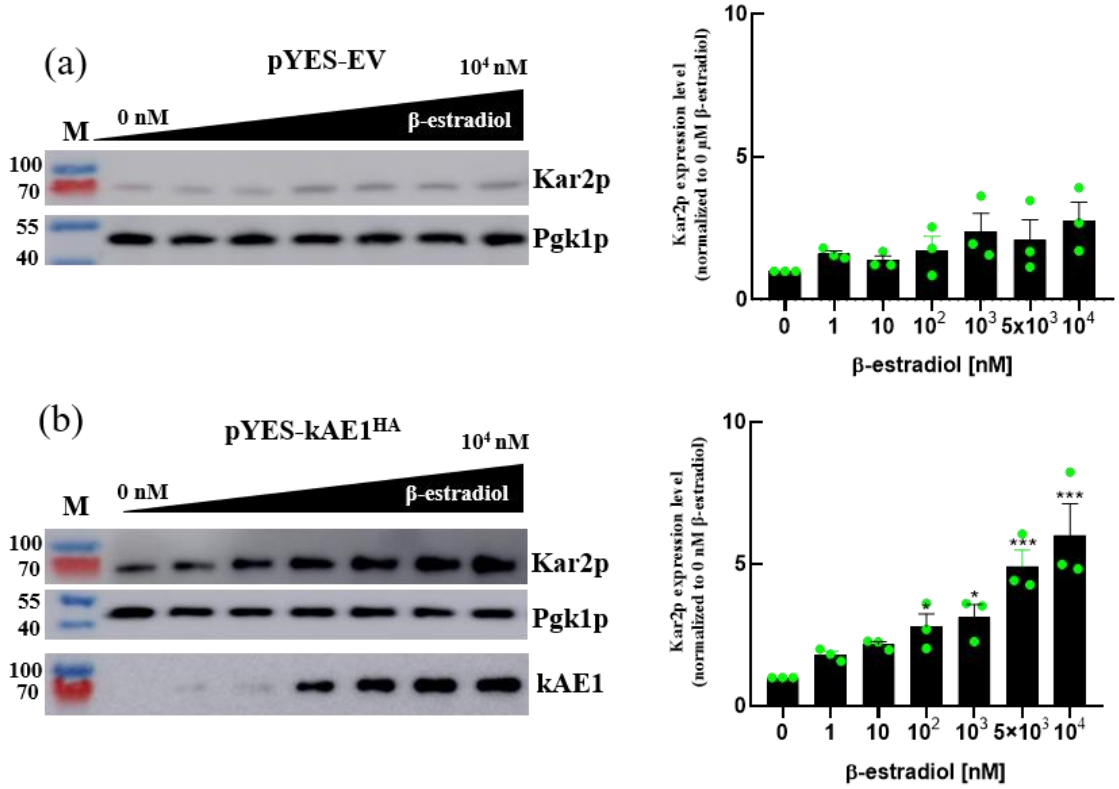

Figure 32: UPR activation directly correlates with gradual kAE1 expression in the BY4742-GEV system. BY4742-GEV cells were transformed with the empty vector (pYES2.1, a) or pYES-kAE1^{HA} (b). Kar2p protein level was determined via Western blot after application of different concentrations of β-estradiol (0 nM, 1 nM, 10 nM, 10^2 nM, 10^3 nM, 5x10^3 nM and 10^4 nM). Relative Kar2p expression level is compared to EV (normalized to Pgk1p, and 0 µM β-estradiol). Mean value ± SEM (n = 3) are indicated (*$p < 0.05$; and ***$p < 0.001$, One-Way ANOVA).

3.3.3. UPR is activated in response to the accumulation of ER-stress after kAE1 expression

To further analyze kAE1-induced UPR induction, the UPRE-LacZ reporter system was used. In this approach, the transcription factor Hac1p binds to copies of the unfolded protein response element (4xUPRE) and induces the expression of the reporter gene *lacZ* coding for β-galactosidase. This enzyme is capable to hydrolyze supplemented X-Gal resulting in a blue coloration that directly correlates to β-galactosidase activity and thereby to the level of UPR activation (Figure 33a).

BY4742 cells were transformed with the plasmid pJC104 carrying the UPRE-LacZ system and subsequently with EV, kAE1^{HA}, kAE1^{FLAG}, kAE1^{WT}, respectively. After selection of the transformants and induction of gene expression, yeast cells were lysed using a standard cell

lysis protocol. Afterward, SDS-PAGE followed by Western analysis was performed to verify kAE1 expression. Strong signals could be detected for $kAE1^{HA}$, $kAE1^{FLAG}$, and a faint signal was visible for $kAE1^{WT}$. Yeast cells transformed with the empty vector were treated with tunicamycin (EV+Tuni) or DTT (EV+DTT) and served as positive controls. Untreated (EV) and DMS-treated (EV+DMSO) empty vector containing cells were used as negative controls. All controls were also routinely analyzed via Western blot (Figure 33b).

(a)

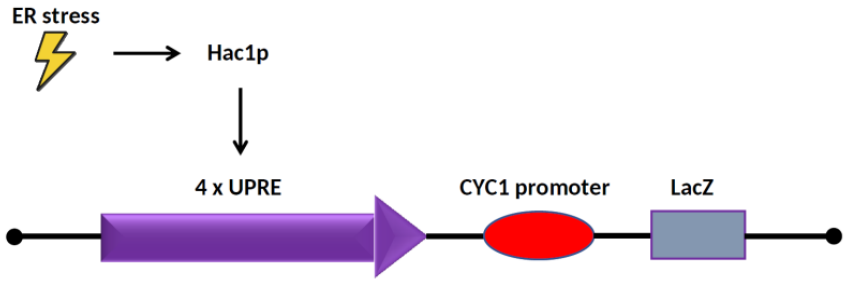

(b)

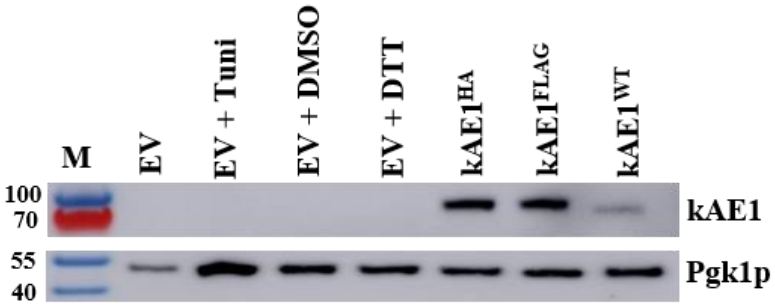

Figure 33: (a) Schematic depiction of the UPRE-LacZ reporter system. After UPR activation, the transcription factor Hac1p is activated and binds to the 4xUPRE elements, triggering the *lacZ* gene expression. The translated gene product, β-galactosidase, is capable to cleave supplemented X-Gal resulting in a blue color change (adapted from Lee *et al.*, 2008). **(b) Verification of kAE1 expression in BY4742 cells co-transformed with pJC104**. Western blot analysis showed strong kAE1 expression of yeast transformed with $kAE1^{HA}$ and $kAE1^{FLAG}$. A signal with weak intensity was visualized for $kAE1^{WT}$, no signals were detected in the empty vector control samples (EV, EV+Tuni, EV+DMSO, EV+DTT). Anti-kAE1 (BRIC170) and anti-mouse HRP-conjugated antibodies were used as primary and secondary antibodies, respectively. Pgk1p was used as a loading control and was detected via anti-Pgk1.

After confirming the kAE1 expression, X-gal was added to the cell lysates, and the color change was documented (Figure 34). Whereas no color change occured in the negative controls

(EV and EV+DMSO), coloration of the positive controls shifted to blue (EV+DTT, EV+Tuni), indicating UPR activation in these cells. Interestingly, the blue color was also observed in cell lysates of yeast expressing the various kAE1 derivatives, demonstrating that kAE1 expression also induces UPR in BY4742 cells (Figure 34).

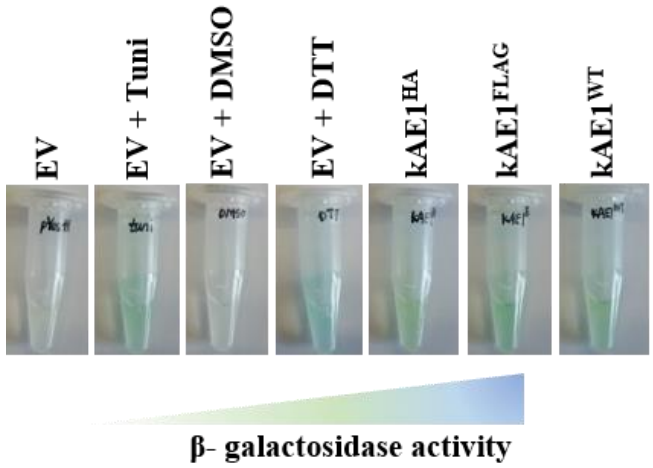

Figure 34: Activation of UPR after kAE1 expression. UPR-dependent *lacZ* reporter assay of BY4742 cells expressing empty pYES2.1 vector or the indicated kAE1 variants as well as the UPR reporter plasmid pJC104-UPRE-LacZ. Color shifts of cell lysates are illustrated after X-gal supplementation. Tunicamycin (Tuni) or DTT treatment was performed to mimic ER stress, and the respective cell lysates served as positive controls.

In addition to UPRE-LacZ, a second reporter assay was used to confirm the observed kAE1-induced UPR activation. By replacing the first exon of *HAC1* with GFP, the Ire1p-dependent splicing and activation of the transcribed mRNA leads to GFP expression, allowing a direct correlation of UPR activity and fluorescence intensity (Lajoie *et al.*, 2012, Figure 35).

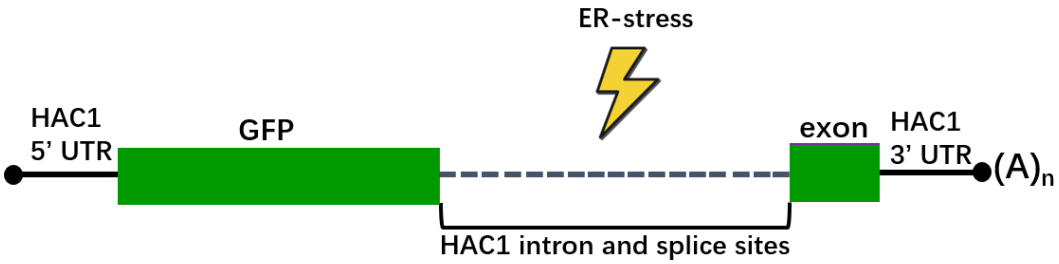

Figure 35: Schematic diagram for the HAC1-GFP construct. GFP signal intensity indirectly indicates UPR activation level via Ire1p-mediated removal of the intron sequence of the transcribed *HAC1* mRNA.

In this study, the yeast strain BY4741-SR-GFP was used in which the HAC1-GFP

construct is already genomically integrated. To start the experiment, cells of the reporter strain were transformed with kAE1^{HA}, kAE1^{FLAG}, kAE1^{WT}, and kAE1^{E681Q}, and fluorescence was directly checked via microscopy. GFP signals could be detected in all cells transformed with the kAE1 variants. However, the overall GFP intensity was weaker compared to cells treated with ER stress-inducing chemicals (Tuni, DTT), and no fluorescence was detected in the negative control pYES-EV (Figure 36).

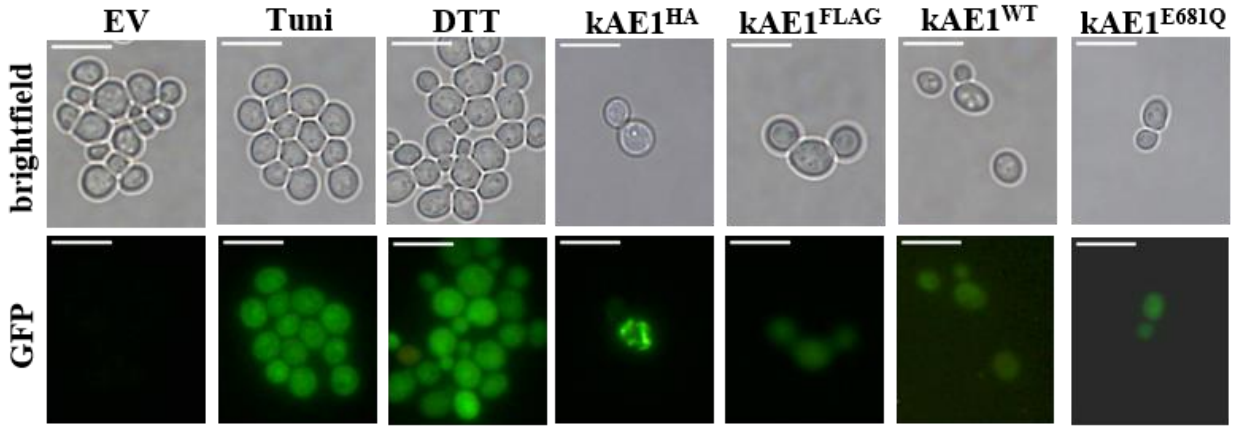

Figure 36: Fluorescence microscopy images of BY4741 SR-GFP cells expressing different kAE1 derivatives. Tunicamycin or DTT was used as positive control, untreated cells transformed with the empty vector (EV) served as negative control; Scale bar: 10 µm.

To further validate the results of the reporter assays, Kar2p expression was finally validated in BY4742 Δ*ire1* and Δ*hac1* cells. Deletion of *IRE1* or *HAC1* should prevent UPR activation in yeast and thereby inhibit UPR-related upregulation of Kar2p. Therefore, kAE1^{HA} was expressed in both deletion mutants, respectively, and Kar2p protein levels were analyzed via Western blot (Figure 37). In contrast to wild-type, Δ*ire1* and Δ*hac1* cells showed no upregulation of Kar2p after overexpression of the kAE1 variant, thus linking the Ire1p-mediated UPR induction directly to the heterologous expression of the transporter.

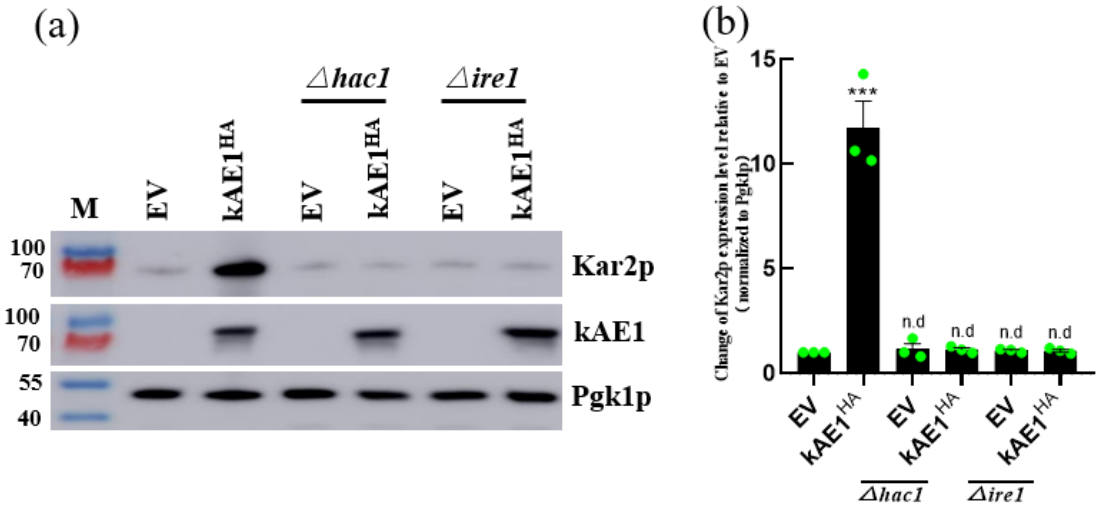

Figure 37: Correlation of Kar2p upregulation and kAE1 expression in wild-type, Δ*hac1,* and Δ*ire1* BY4742 cells. Yeast were either transformed with the empty vector (EV) or kAE1^{HA}, and protein levels of kAE1 and Kar2p were analyzed via Western blot (a); detection was conducted using appropriate antibodies, Pgk1 served as loading control. Densiometric analysis of the respective signals was performed, and Kar2p levels were normalized to the empty vector (b). Depicted are the mean value ± SEM (n = 3), ***$p < 0.001$ (One-Way ANOVA), n.d.: not determined

3.3.4. Structural kAE1 yeast homolog Bor1p shows striking similarities in UPR induction

The results of the previous experiments clearly point to a correlation of the activation of UPR as cellular defense mechanism and the overexpression of kAE1 derivatives. Similar effects of heterologously expressed proteins have already been described and are presumably caused by an overload of the ER machinery (Romanos *et al.*,1992; Momcilovic *et al.*, 2006; Xu & Reed, 1998). However, the consequence of kAE1 overexpression was significantly more substantial compared to the overexpression of the HDEL receptor Erd2p. It could be possible that the strong discrepancy observed might be explained by the exogenous nature of kAE1 as a human protein, whereas Erd2p is an endogenous protein of yeast. To further analyze this hypothesis, several other yeast membrane proteins, including the structural kAE1 homolog Bor1p, were overexpressed and Kar2p protein levels were determined. Western analyses indicated a considerable upregulation of Kar2p after induction of the expression of all yeast endogenous membrane proteins except for the yeast HDEL receptor Erd2p (Figure 38). These findings correlate with previous studies and demonstrate the significant UPR activation after overexpression of complex proteins (Romanos *et al.*,1992; Llewellyn *et al.*, 1997).

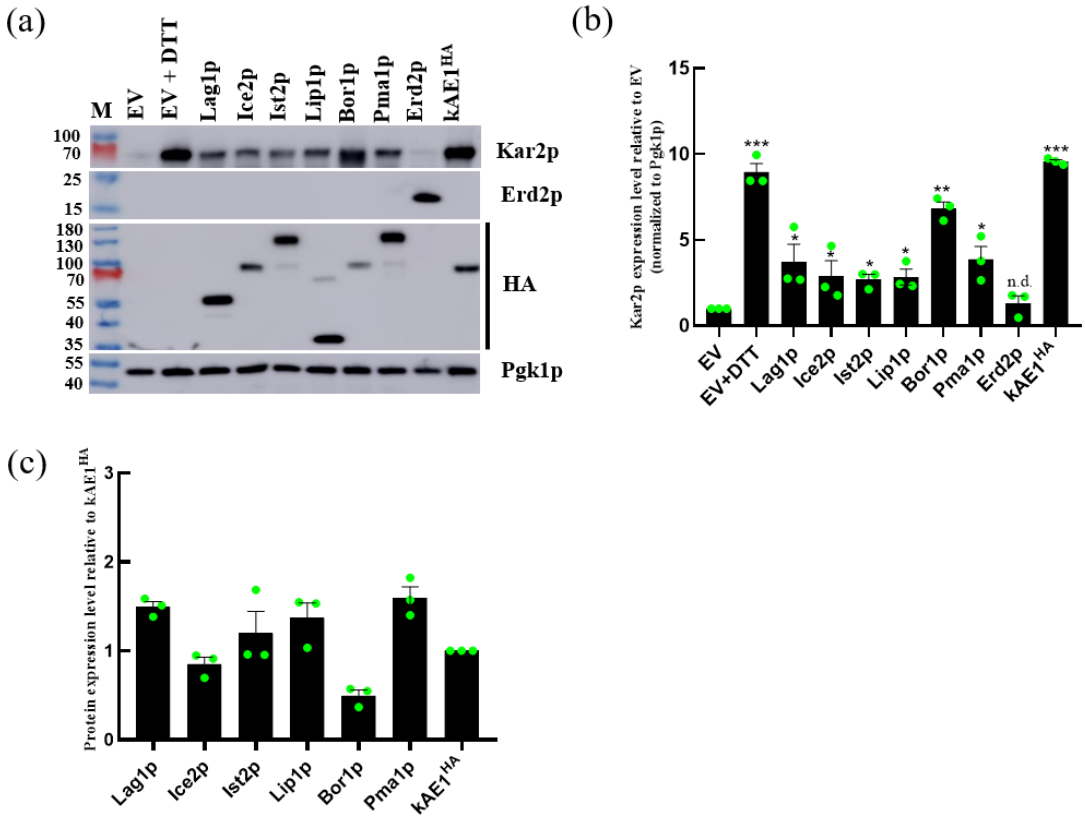

Figure 38: Effect of the overexpression of different membrane proteins on UPR activation in yeast. BY4742 cells were transformed with various HA-tagged yeast membrane proteins (pBG1805 vector), pYES-Erd2-V5 or kAE1^{HA}, empty vector expressing cells were used as negative control (EV). For a positive control EV transformants were pre-cultivated with DTT for 6 h (EV+DTT). (a) Western blots analyses were conducted with the indicated primary antibodies (anti-Kar2p, anti-V5, anti-HA). Pgk1p served as a loading control. Relative Kar2p expression levels were calculated after densitometric analysis of the obtained protein signals and either compared to the negative control (b; normalized to Pgk1p) or to kAE1^{HA} (c). Illustrated are the mean values (± SEM) of 3 replicates, *$p < 0.05$; **$p < 0.01$ and ***$p < 0.001$ (One-Way ANOVA), n.d.: not determined.

The overexpression of Bor1p led to the strongest upregulation of Kar2p of all endogenous yeast membrane proteins, although kAE1^{HA} expressing cells showed the highest level of the ER chaperone overall, similar to the positive control (DTT-treated cells, Figure 38). However, the protein level of kAE1^{HA} was two times higher than Bor1p (Figure 38c). Remarkably, elevated expression levels might not be the sole contributing factor to the immense UPR activation because the UPR-activating effect of both, Bor1p and kAE1^{HA} was only slightly different (Figure 38b). Based on these findings, it would be interesting to analyze the relationship between the overexpression of yeast exogenous and/or endogenous proteins and the UPR induction in the future.

3.3.5. Structural features of kAE1 in its C-terminal region contribute to UPR induction in yeast

The previous results could show that kAE1 function (kAE1^{E681Q}) does not play a role in UPR induction in yeast and that the protein level itself may not be the sole reason for higher ER stress reactions. Therefore, further studies were conducted to determine the involvement of specific structural features of kAE1 in the Ire1p-mediated UPR activation. Therefore, various truncated versions of kAE1 were constructed, lacking different transmembrane fragments (Figure 39).

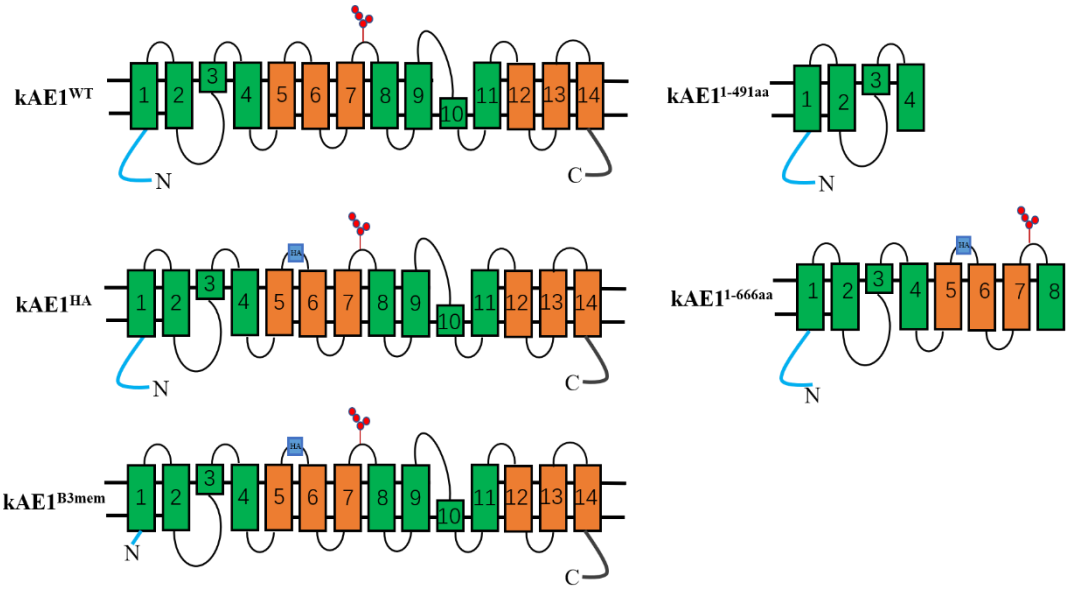

Figure 39: Structural composition of truncated kAE1 derivatives. Schematic outline of wild-type kAE1 (kAE1^{WT}), HA-tagged kAE1^{HA}, and the already described N-terminally truncated kAE1^{B3mem}. Additionally, kAE1$^{1-499}$ (missing the N-glycosylation site at position Asn^{577} and TMD 5 to 14) and kAE1$^{1-666}$ (lacking the cytosolic C-terminus and TMD 10 to 14) were constructed. The core domain consisting of TM1, 2, 3, 4, 8, 9, 10, and 11 and containing the anion-binding site is colored in green. The gate domain consisting of TM 5, 6, 7, 12, 13, and 14 is illustrated in orange. The single N-glycosylation site is located at Asn^{577} (red dot), the HA-tag in the third extracellular loop is depicted in blue.

The different kAE1 variants, as well as kAE1^{WT}, kAE1^{B3Mem,} and kAE1^{HA}, were transformed into BY4742 cells, and Kar2p protein levels were determined (Figure 40). Although the expression of all constructs led to an increase in Kar2p levels compared to the empty vector, kAE1$^{1-491}$ and kAE1$^{1-666}$ expressing cells displayed a considerably reduced intracellular amount of Kar2p compared to both kAE1^{WT} and kAE1^{HA} expressing cells.

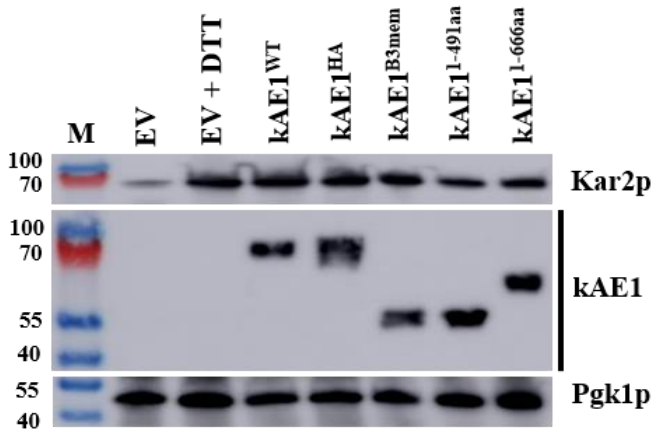

Figure 40: Western analysis of BY4742 cells expressing various C- or N-terminal truncated kAE1 variants. BY4742 cells were transformed with the indicated kAE1 derivatives ($kAE1^{HA}$, $kAE1^{WT}$, $kAE1^{B3mem}$, $kAE1^{1-491aa}$, and $kAE1^{1-666aa}$), and Kar2p protein levels were determined after expression of the constructs. Untreated (EV) and DTT-treated empty vector cells (EV+DTT) served as negative and positive control, respectively. Western blots were probed with primary antibodies against Kar2p, kAE1 (anti-BRIC170), and the loading control Pgk1p.

Further statistical analysis of relative Kar2p expression levels showed no significant difference ($p > 0.05$) between $kAE1^{B3Mem}$ and $kAE1^{HA}$ (Figure 41a), indicating that the cytosolic N-terminus is not responsible for UPR activation in yeast cells. In contrast, UPR activation levels in $kAE1^{1-491}$ and $kAE1^{1-666}$ decreased by almost half when compared with $kAE1^{HA}$. One-Way ANOVA analysis showed significant differences in the Kar2p level compared to $kAE1^{HA}$ (Figure 41a), indicating that the lack of TMD 10-14 and/or the cytosolic C-terminus in $kAE1^{1-666}$ may play a crucial role in UPR induction in yeast. Notably, the expression level of all truncated versions did not dramatically differ from unmodified $kAE1^{WT}$. Variations in protein levels could therefore be excluded as the origin of reduced UPR activation levels in $kAE1^{1-491}$ and $kAE1^{1-666}$ expressing cells (Figure 41b). Interestingly, both $kAE1^{1-491}$ and $kAE1^{1-666}$ did not entirely prevent Kar2p upregulation (reduction by around 50 % compared to $kAE1^{WT}$). Both derivatives induced a similar upregulation of Kar2p, indicating that removal of TMD 5-9 and Asn^{577} has no further effect on UPR activation (Figure 41a). In the future, it would be interesting to construct additional truncated versions (e.g. kAE1 lacking the cytosolic C-terminal part) to assess more accurately which parts of the different regions are responsible for the massive UPR response when overexpressed in yeast cells.

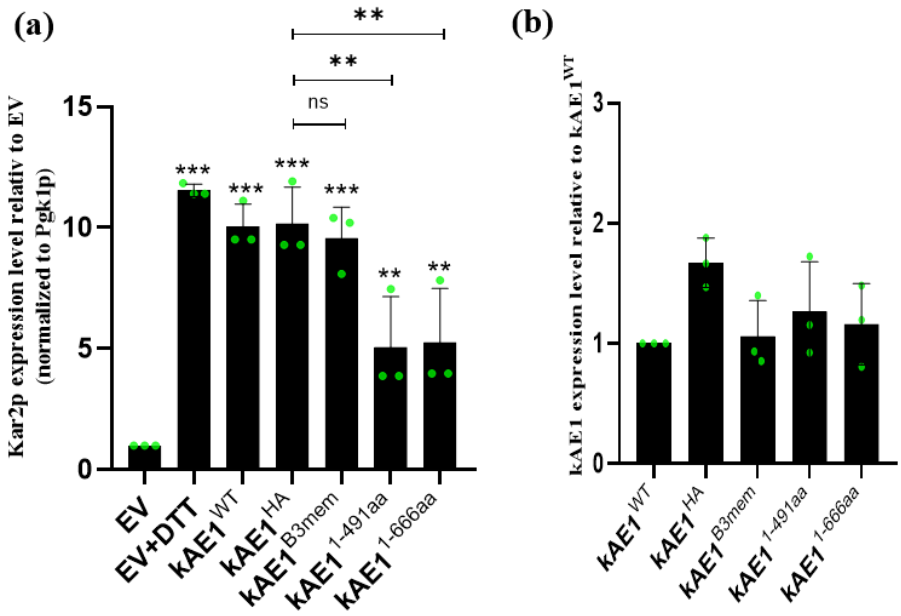

Figure 41: Relative Kar2p expression level compared to empty vector control cells (a). kAE1$^{1\text{-}491}$ and kAE1$^{1\text{-}666}$ showed significantly lower Kar2p protein levels when compared with kAE1^{HA} and EV+DTT. Kar2p expression levels were normalized to Pgk1p. (b) kAE1 expression levels show no significant differences among all tested kAE1 variants. kAE1 expression levels are relative to kAE1^{WT}. Mean value ± SEM (n = 3) are indicated ($^{**}p < 0.01$ and $^{***}p < 0.001$, One-Way ANOVA).

3.3.6. Increased ER folding capacity reduces UPR activation in kAE1 expressing cells

Based on the previous data, different experimental approaches were employed to counteract the increasing ER stress and UPR activation following the overexpression of kAE1 variants. Various strategies could already be established in yeast, enhancing the folding the ER, thereby improving general protein secretion and proper targeting (Morishima *et al.*, 2004; Kim *et al.*, 2008). Therefore, additional copies of single ER-luminal proteins (Pdi1p, Emc1p, Emc4p, Emc5p, Mpd2p, Eug1p, Scj1p, Ero1p) were expressed in the wild-type strain BY4742 to check whether they can effectively reduce ER stress during simultaneous overexpression of kAE1.

To start the experiment, pESC$_{HIS}$-yeGFP-kAE1^{WT} was co-transformed with pBG1805 vector variants expressing either Pdi1p, Emc1p, Emc4p, Emc5p, Mpd2p, Eug1p, Scj1p, or Ero1p. Kar2p protein levels in each transformant were assessed by Western blot analysis and subsequent statistical analysis. The results showed that even strong expression of each ER chaperon did not affect Kar2p expression levels (Figure 42).

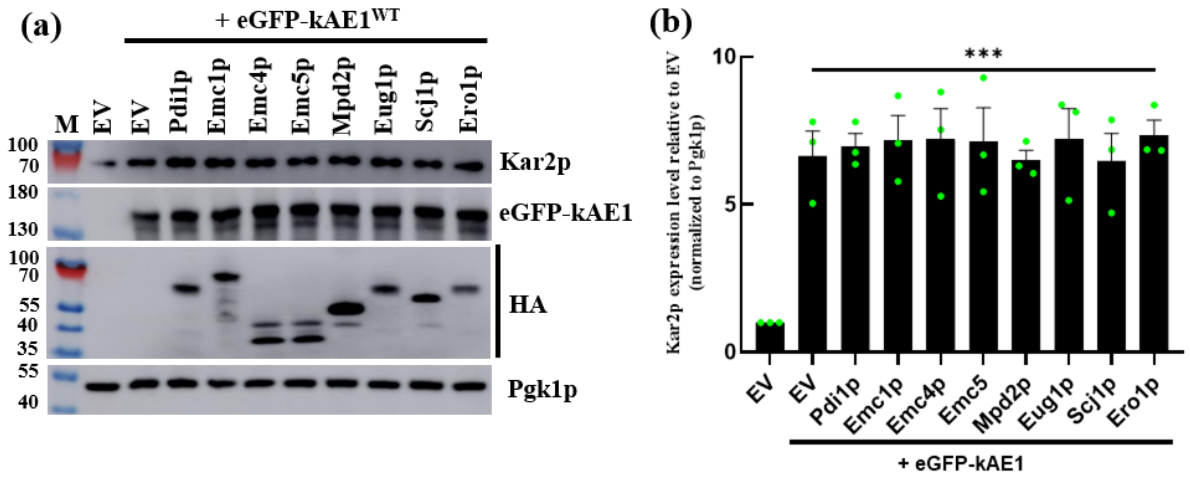

Figure 42: Western blot analysis of BY4742 cells expressing eGFP-kAE1^{WT} together with the empty vector pBG1805 (EV) or the same vector coexpressing the indicated yeast ER chaperone. EV cells served as negative controls. (a) Western analysis was conducted using primary antibodies against Kar2p (anti-Kar2p), kAE1 (anti-BRIC170), and the different HA-tagged ER chaperones (anti-HA), as well as the loading control Pgk1p (anti-Pgk1p). (b) Kar2p expression level were compared to EV after normalization to Pgk1p signals, and the mean values ± SEM (n = 3) are indicated ***$p < 0.001$, One-Way ANOVA.

Because the expression of the various ER proteins did not alter the severity of the UPR activation, and in correlation with the electron microscopy data conducted in this study, it was hypothesized that the pronounced accumulation of kAE1 protein in the different subcompartments of the secretory pathway is irreversibly leading to cellular ER stress. Therefore, overexpression of a single ER-luminal protein might not be sufficient to improve ER folding capacity at an adequate level to significantly reduce cellular UPR activation. Therefore, the experiments were repeated using the BY4742-GEV system, allowing a dose-dependent kAE1 expression via β-estradiol supplementation. BY4742-GEV cells were co-transformed with pESC$_{HIS}$-yeGFP-kAE1^{WT} and pBG1805 variants expressing either Pdi1p, Emc1p, Emc4p, Emc5p, Mpd2p, Eug1p, Scj1p, or Ero1p. The empty vector pBG1805 served again as negative control, and kAE1 expression was induced by the addition of 30 nM β-estradiol. Additionally, co-transformed yeast (pBG1805-EV+pESC$_{HIS}$-yeGFP-kAE1^{WT}) were incubated in galactose-containing medium to ensure a strong kAE1 overexpression (+Gal). As shown in Figure 43, kAE1 expression was verified for all analyzed transformants via Western blot. Additionally, intracellular Kar2p levels were determined.

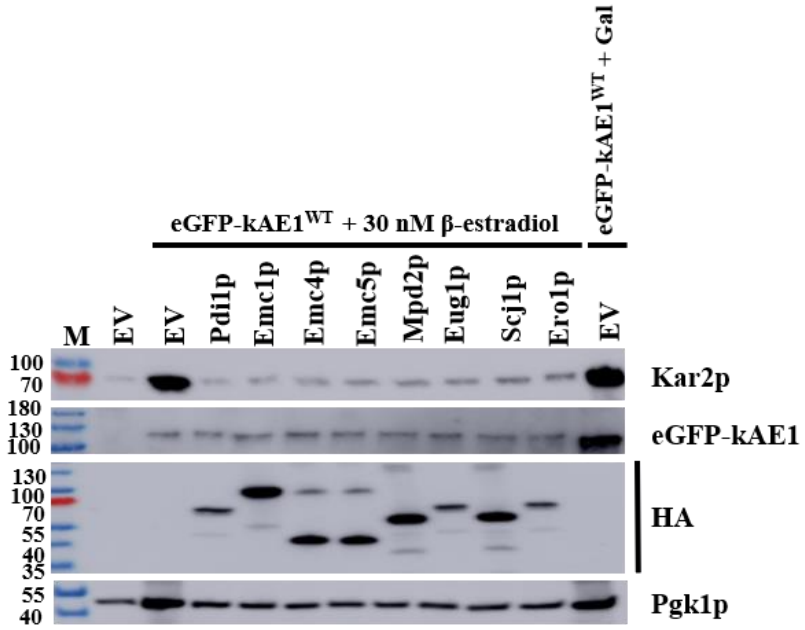

Figure 43: Western analysis of BY4742-GEV cells after co-expression of eGFP-kAE1^{WT} and the indicated yeast ER chaperone. BY4742-GEV cells were co-transformed with pESC$_{HIS}$-yeGFP-kAE1^{WT} and the indicated ER proteins (in the vector pBG1805). Cells only transformed with the empty pBG1805 vector (EV) served as negative control. Expression was induced by addition of 30 nM β-estradiol. As a positive control, eGFP-kAE1 expression was induced by galactose (+Gal) to generate a strong kAE1 overexpression. Significantly reduced Kar2p expression was observed in the different ER chaperone expressing yeast strains compared to the control. Western blots were incubated with the appropriate primary and secondary antibodies.

Subsequent statistical analysis showed that the overexpression of the indicated ER-luminal chaperone gene dramatically decreased the Kar2p level compared to the appropriate empty vector control (pESC$_{HIS}$-yeGFP-kAE1^{WT}+pBG1805 EV) (Figure 44a). Notably, kAE1 expression level in the presence of 30 nM β-estradiol was approximately eight times lower than the expression level after incubation in standard galactose-containing medium (Figure 44b). This shows that the expression of one additional chaperone could significantly reduce ER stress in the cell if the kAE1 protein load is relatively low, thus preventing kAE1-mediated UPR induction in yeast.

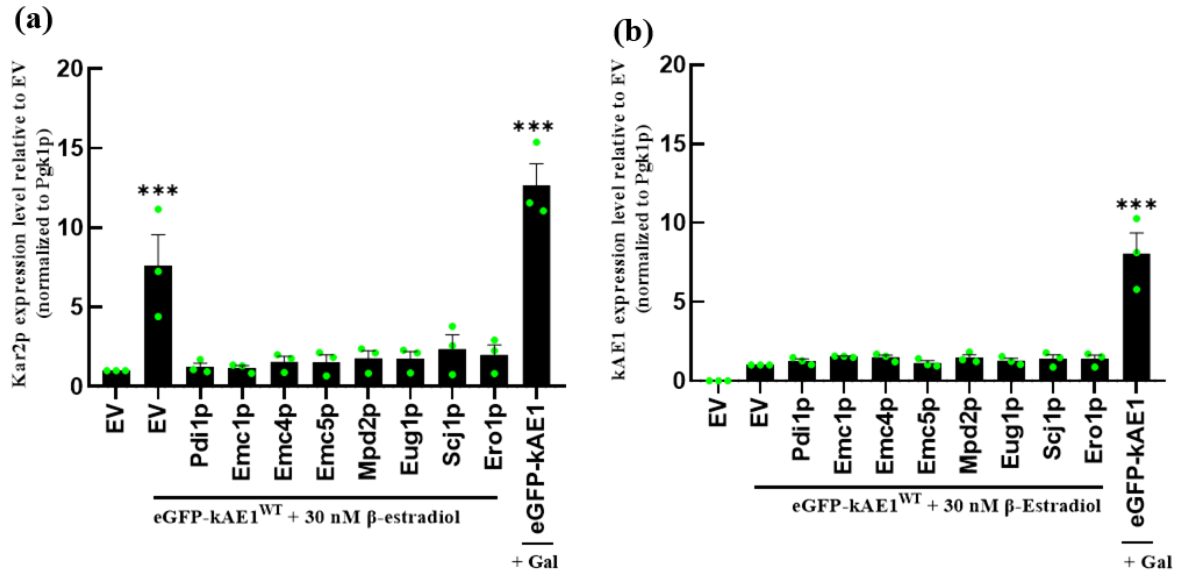

Figure 44: Densiometric analysis of Kar2p levels after co-expression of eGFP-kAE1^{WT} and the indicated yeast ER chaperones. (a) Kar2p protein level dramatically decreased compared to EV (pESC$_{HIS}$-yeGFP-kAE1^{WT}+pBG1805 empty vector). Relative Kar2p levels were normalized to the loading control Pgk1p and the EV control (cells solely transformed with pBG1805). (b) No significant difference in the kAE1 expression level was detectable between all samples expressing eGFP-tagged kAE1. kAE1 protein levels were normalized to Pgk1p, and the appropriate EV control (pESC$_{HIS}$-yeGFP-kAE1^{WT}+pBG1805 empty vector). Depicted are the mean values ± SEM (n = 3); ***$p < 0.001$ (One-Way ANOVA).

In further studies, yeast cells expressing the mCherry-tagged ER marker Sec63p (mCherry) and eGFP-tagged kAE1 (GFP), as well as different untagged ER chaperones, were used to localize kAE1 by SIM imaging. The results showed that cells co-expressing a single ER-luminal chaperone gene with eGFP-kAE1 led to a distinct redistribution of kAE1 signals (green) to ring-like structures at the cell periphery compared to the empty vector control (Figure 45). This was especially visible after overexpression of Eug1p and Mpd2p. This drastic shift in the localization of kAE1 connotes that the overexpression of single ER-luminal chaperone genes assists the folding of kAE1, thereby reducing ER-stress and improving kAE1 trafficking to the yeast PM.

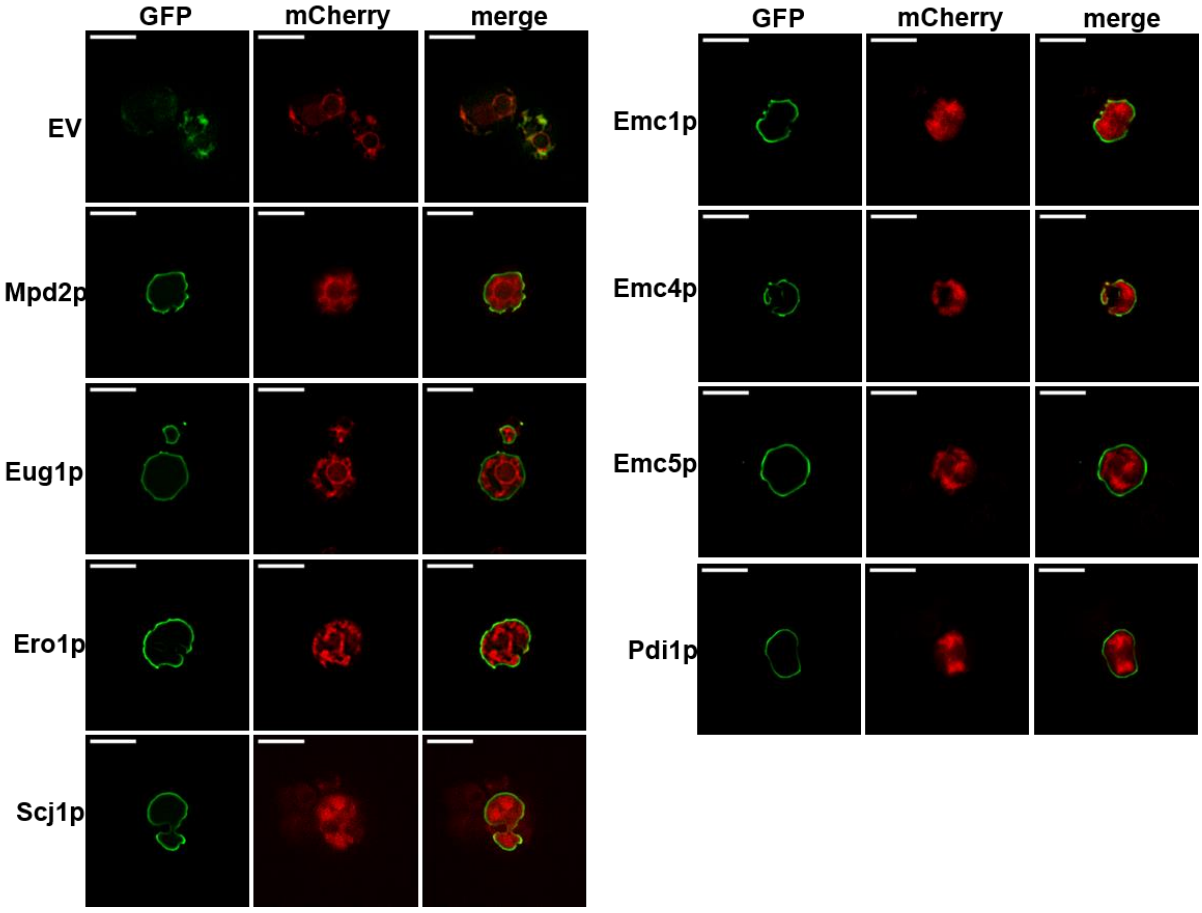

Figure 45: Redistribution of kAE1 to the PM after co-expression of ER chaperones. SIM images were obtained of yeast cells co-expressing the mCherry-tagged ER marker Sec63p (mCherry), eGFP-tagged kAE1 (GFP), as well as the indicated ER chaperone. Cells carrying the empty vector pBG1805 (EV) served as negative control; potential overlap of fluorescent signals is illustrated in yellow (merge), Scale bar: 5 µM.

In addition to the co-localization with the yeast ER-marker Sec63p, co-localization of kAE1 and the PM marker Pma1p was further analyzed via SIM. As illustrated in Figure 46, the results clearly indicated that yeast cells co-expressing mRFP-coupled Pma1p (mRFP), as well as the eGFP-tagged kAE1 derivative (GFP) and the indicated ER chaperones, showed ring-like structures at the cell periphery with clear and strong co-localization of the peripheral GFP signals with the yeast PM. Only limited co-localization was detected in the EV strain.

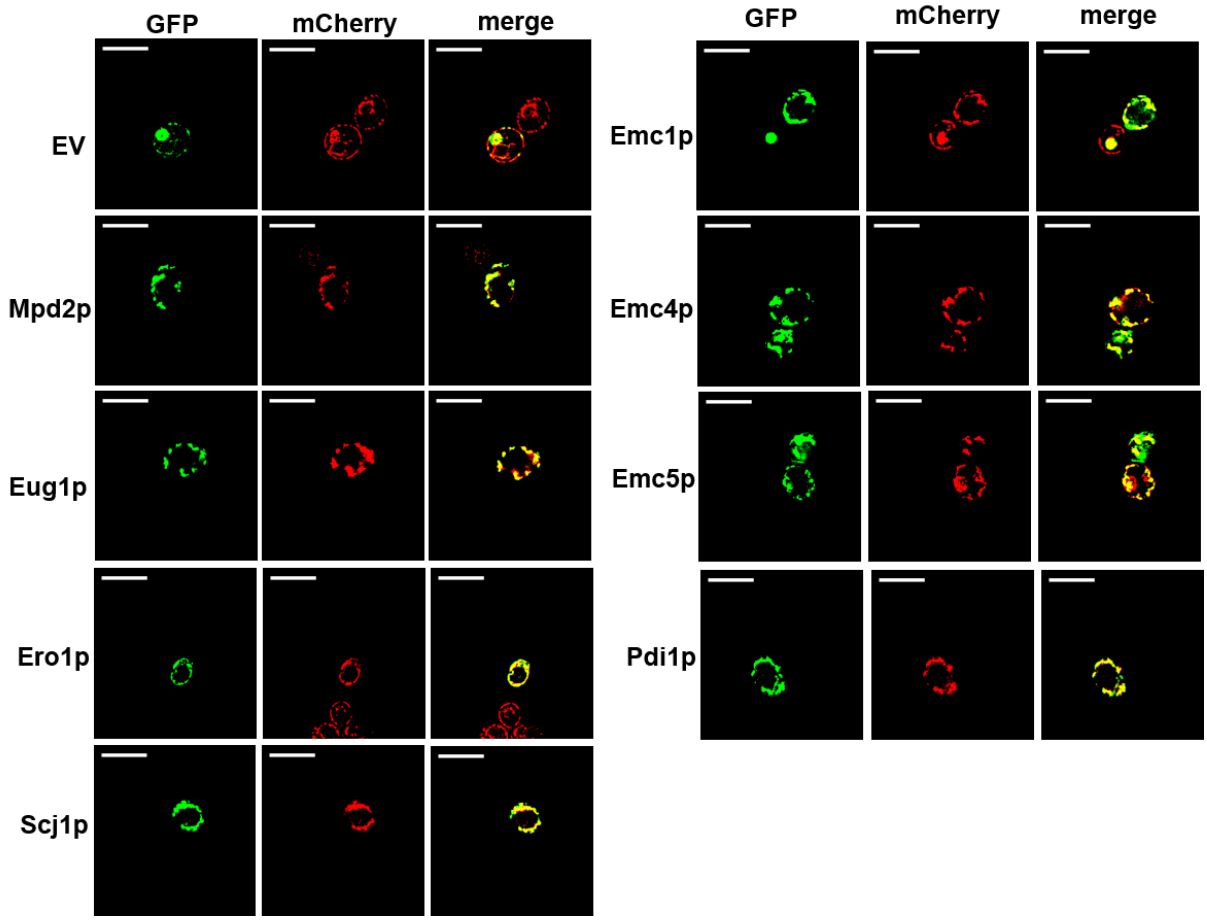

Figure 46: Increased plasma membrane localization of kAE1 after overexpression of ER chaperones. Yeast cells were transformed with the mRFP-tagged PM marker Pma1p (mCherry), the GFP-tagged kAE1 (GFP), and the indicated ER chaperones. The empty vector pBG1805 (EV) served as negative control. Images were generated using SIM. Scale bar: 5 µM.

3.3.7. Other potential possibilities to reduce ER-stress and improve kAE1 secretion

The previous results of this study revealed that overexpression of different ER-luminal chaperones involved in protein folding could decrease ER stress. Next, Hsf1p, Erv29p, and Pah1p, which are involved in the heat shock response (HSR) pathway, as well as the chemical chaperone PBA (4-Phenylbutyric acid), which can reduce ER stress, were tested (Arnaise *et al.*, 2001; Belden & Barlowe, 2001; Malhotra & Wong, 2002; Kolb *et al.*, 2015). As shown in Figure 47, cells simultaneously coexpressing eGFP-kAE1 and Hsf1p, Erv29p, and Pah1p showed a distinct overlap of kAE1 signals (green) with the mCherry-labeled PM marker Pma1p (red) compared to empty vector (pBG1805) control cells. In addition, cells expressing eGFP-kAE1 treated with 10 µg/ml PBA also showed an overlap of GFP with Pma1p. Notably, overexpression of Hsf1p and simultaneous application of PBA led to a dramatic change in the intracellular kAE1 localization based on the SIM images.

Although future EM analyses are required to demonstrate PM localization of kAE1 more clearly, these preliminary data strongly support the hypothesis that misfolded kAE1 accumulates in the ER. However, an improvement in the ER folding capacity is capable to restore the native folding state of the anion transporter. Furthermore, these findings represent a solid starting point to further optimize yeast as model system for studying kAE1 transport to the PM in the future. It should be possible to combine an engineered yeast strain co-expressing individual ER chaperons and GFP-tagged kAE1 with a SIM-based approach to screen or evaluate the role of selected proteins or chemical compounds on kAE1 targeting to the cell surface.

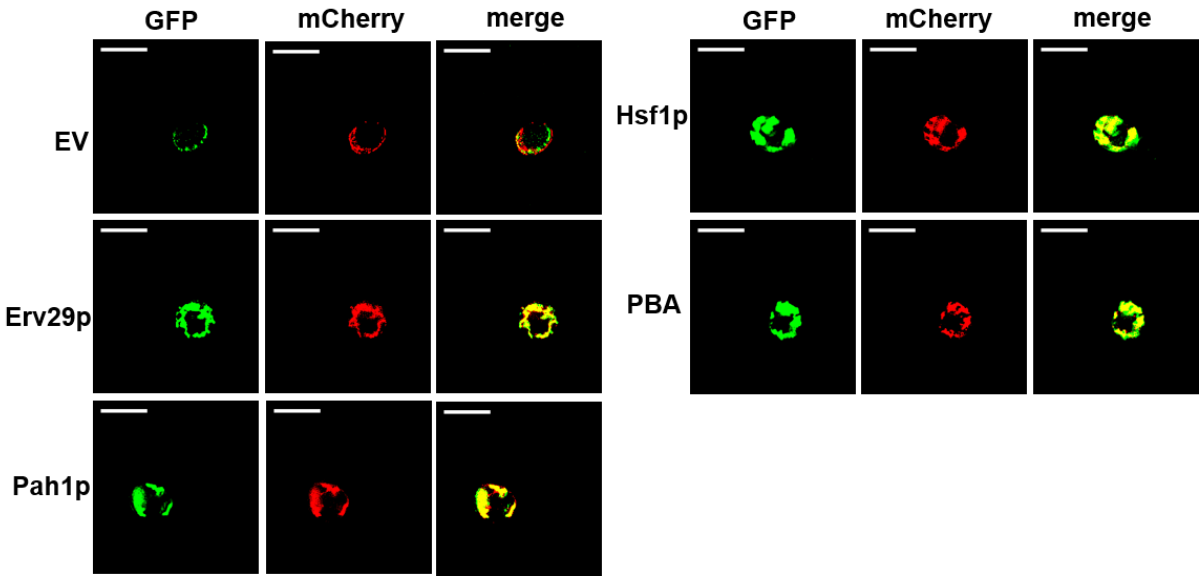

Figure 47: Improvement of kAE1 localization to the yeast cell periphery. Yeast cells were co-transformed with the mCherry-tagged PM marker Pma1p and eGFP-tagged kAE1 as well as Hsf1p, Erv29p, and Pah1p, respectively. Untreated empty vector pBG1805 cells (EV) were used as negative control. Additionally, EV cells were incubated with the chemical chaperone PBA. Fluorescence microscopy was conducted using SIM. Scale bar: 5 µM.

4. Discussion

In mammals, the anion transporter kAE1 localized at the basolateral membrane of α-intercalated cells (α-ICs) in the kidney plays a crucial role in regulating the systemic acid-base homeostasis (Cordat *et al.*, 2006). Mutant variants of kAE1 are associated with the development of a physiological disorder known as distal renal tubular acidosis (dRTA) (Cordat e*t al.*, 2003).

In this study, yeast was used as model system to identify proteins that might affect intracellular kAE1 trafficking to the plasma membrane. It was demonstrated that codon-optimized human kAE1 with HA- and FLAG-tag can be successfully expressed in yeast and results in a partial localization of kAE1 at the plasma membrane as verified by electron microscopy. However, the main fraction of the heterologously expressed anion transporter aggregated in intracellular membrane structures, mainly in ER membranes and COPII vesicles. Further analysis indicated that these aggregations lead to robust activation of the UPR pathway and a significant growth defect in kAE1 expressing yeast cells, which could be substantially compensated by enhancing the folding capacity of the ER. This study demonstrates promising strategies for the redistribution of the ER-accumulated kAE1 proteins, consequently improving the plasma membrane targeting of the transporter in yeast. The findings emphasize the potential of yeast as a model organism in kAE1-related research questions, including the assessment of structural features, as well as the trafficking and degradation of the protein.

Expression of codon-optimized human kAE1 in yeast

S. cerevisiae has been widely utilized to study the expression of mammalian proteins, including human renal proteins (Santos & Nebreda, 1989; Verghese *et al.*, 2012). Former studies already indicated the possibilities to overexpress different AE1 or kAE1 variants in *S. cerevisiae* (Cordat & Reithmeier, 2014; Sarder *et al.*, 2020; Li *et al.*, 2021). Based on these findings, the potential of yeast to express tagged and codon-optimized versions of kAE1 ($kAE1^{HA}$, $kAE1^{V5}$, and $kAE1^{FLAG}$, respectively) was explored. Consistent with previous findings in mammalian cells, successful expression of kAE1 derivatives bearing an HA- or Flag-tag in the third extracellular loop was already demonstrated (Toye *et al.*, 2004; Pittet & Conzelmann, 2007). Furthermore, higher protein levels of $kAE1^{HA}$ and $kAE1^{FLAG}$ could be detected after expression in the genetic background of a yeas *Δend3* deletion mutant. The deletion of *END3* encoding a protein essential for endocytosis might lead to a slower or inhibited recycling of PM-localized kAE1 molecules, thereby decreasing the degradation of the protein (Giardina *et al.*, 2014). $kAE1^{HA}$ and $kAE1^{FLAG}$ were also successfully expressed using an β-estradiol inducible

BY4742-GEV yeast strain allowing a dose-dependent regulation of kAE1 expression. The expression of V5-tagged kAE1 could not be verified regardless of the used expression system.

It has been reported that the use of detergents in the cell lysis buffer can assist with the extraction of intracellular proteins as well as plasma membrane proteins (Koley & Bard, 2010). In correlation with a previous study showing improved separation of membrane proteins from the cell membrane, Triton X-100 (TX100) was used in three different concentrations (0.3%, 1%, and 2%, respectively) as a supplement in the lysis buffer (Silva *et al.*, 2019). As a non-ionic surfactant, TX100 has a hydrophilic polyethylene oxide chain and is frequently applied to isolate, purify, and analyze membrane components. Additionally, the detergent possesses a high solubilization potential and can prevent degradation of proteins or loss of original biological properties (Anacletus *et al.*, 2017). Western analysis of cell lysates of yeast expressing kAE1 variants showed that the amount of kAE1 in the supernatant continuously increased with rising TX100 concentrations. Although most of the heterologous protein remained in the pellet fraction, which is a common phenomenon for many membrane proteins, the addition of TX100 considerably enhanced the solubility of kAE1 (Anacletus *et al.*, 2017).

Localization of full-length kAE1 variants in yeast

Yeast is a popular model for studying the biogenesis, expression, trafficking, and functionality of human proteins, including membrane proteins. However, a prerequisite to successfully examining these types of proteins in yeast is the correct trafficking to the yeast plasma membrane (Bonar & Casey, 2010). Concerning the heterologous expression of the renal membrane protein kAE1 in yeast, proper plasma membrane localization could only be achieved for the N-terminally truncated version of the protein $kAE1^{B3mem}$ (Sekler *et al.*, 1995). This variant consists of the remaining C-terminal membrane domain (360-911 amino acids) of kAE1, which plays a key role in regulating anion exchange (Quilty *et al.*, 2002; Pang *et al.*, 2008).

In this study, the intracellular localization of various full-length yeast codon-optimized kAE1 variants (tagged and untagged) was analyzed using various microscopy techniques. Electron microscopy coupled with immunogold labeling could show that a minor part of the heterologously expressed kAE1 variants was able to reach the yeast plasma membrane. Statistical analysis confirmed that the number of full-length versions of kAE1 trafficked to the yeast PM were similar to the $kAE1^{B3mem}$ variant, contradicting previous theories that the kAE1 N-terminus (from amino acid 182 to 360) prevents the correct targeting (Sekler *et al.*, 1995). Nevertheless, the majority of the transporter accumulated in multivesicular bodies (MVBs), regardless of the analyzed kAE1 derivative. In contrast, control samples containing the empty

vector only showed minimal membrane/vesicle-like structures. These observations correlate with previous findings demonstrating the strong tendency of AE1 to be trapped in intracellular membranes, such as ER structures (Bonar & Casey, 2010). In addition, it has also been shown that heterologously expressed proteins in yeast are usually retained and stacked in ER structures (Umebayashi *et al.*, 1997; Flegelova *et al.*, 2006). The kAE1 aggregations observed after overexpression considerably overlap with the yeast ER, specifically perinuclear ER, rough ER and/or cortical ER structures, indicating disturbances of the proper maturation of the protein and its correct transport through the secretory pathway. The overexpression induced by the strong activity of the used promoters likely leads to these folding problems, subsequently resulting in kAE1 accumulation.

In addition to MVBs, immunogold labeling also showed that kAE1 localized in the vacuole. MVBs are defined by multiple internal vesicles enclosed within an outer, limiting membrane, belonging to a type of late endosomal structure that contains internal vesicles for release into the lysosomal lumen and is involved in the degradation of membrane proteins by fusing to the vacuole/lysosome (Eden *et al.*, 2016; Ye *et al.*, 2018). Therefore, it is likely that the kAE1 fraction found in MVBs is transported to the yeast vacuole for degradation. This hypothesis was supported by the increased amount of kAE1 protein in the vacuole after expression in Δ*pep4* cells, in which the maturation of vacuolar proteinases is defective. Notably, similar results were also observed in the endocytosis-defective yeast BY4742 Δ*end3* cells expressing kAE1 variants suggesting a transport from the Golgi to the vacuole instead of the 'endosomal sorting complex required for transport' (ESCRT)-mediated transport route from the PM to the vacuole (Sarder *et al.*, 2020). Indirect fluorescence microscopy and SIM data confirmed the results of the TEM studies and showed only a minor amount of full-length kAE1 at the PM. In addition, little is known about the influence of kAE1 mutations on ERAD-mediated degradation and their association with the development of dRTA (Hoffman *et al.*, 2019). Based on the described findings, it would also be interesting to explore kAE1 degradation in more detail in the yeast model system.

One limitation of localization studies using yeast is the proximity of the different compartments of the secretory pathway, impeding their clear distinction in microscopy-based approaches of un-labeled target proteins. Therefore, further experiments were conducted to check whether an N-terminal addition of eGFP affects the kAE1 targeting to the yeast cell surface, which. A previous study described that N-terminal modification in mammalian expression systems does not affect kAE1 targeting to the cell surface (Abbas *et al.*, 2018).

Therefore, BY4741 Δ*ist2* cells were transformed with the N-terminally GFP-tagged kAE1 variant and used for SIM imaging. The deletion of *IST2* results in an increased distance between ER and plasma membrane, making it clearer to distinguish cortical ER from plasma membrane structures (Chang *et al.*, 2017; Saheki & De Camilli, 2017; Papouskova *et al.*, 2017). The results showed a partial localization of kAE1 within the yeast PM, indicating that the GFP fusion does not negatively affect PM-targeting of kAE1 in yeast, which is consistent with the scenario in mammalian cells (Bonar & Casey, 2010). To enable an even higher distinction of the secretory pathway compartments, the GFP-tagged kAE1 variant was transformed in *Δist2* mutants co-expressing different mCherry-tagged organelle-specific marker proteins. Co-localization of the kAE1 derivative and the respective marker proteins was analyzed via SIM imaging. The results indicated that kAE1 showed a strong co-localization with the ER marker Sec63p and a partial co-localization with the COPII vesicle marker Sec13p and the cortical ER marker Erg6p, which was consistent with already observed results from a previously conducted EM study (Sarder *et al.*, 2020; Li *et al.*, 2021). Overlap of some kAE1 signals with the COPII vesicle marker Sec13p as well as the Golgi marker Anp1p was visualized, pointing to an anterograde transport of the transporter from the ER to the Golgi (Yuan *et al.*, 2018). Additionally, no co-localization with early and late endosomal compartment markers was visible. However, an evident overlap of kAE1 with the PM marker Pma1p was discovered, clearly indicated kAE1 localization at the yeast PM.

Based on the co-localization of kAE1 with Golgi structures and the PM, but not with endosomal structures, the data hint at an endosome-independent transport of the transporter, directly from the trans-Golgi network (TGN) to the PM; several alternative transport routes (e.g., exomer, AP1 and AP4) are described in yeast allowing the direct transport of a protein cargo from the Golgi to the plasma membrane (Ramirez-Macias *et al.*, 2018). Based on the localization analysis results, a model can be postulated explaining kAE1 transport to the PM by an endosome-independent mechanism (Figure 48). Future experiments could focus on the exit of kAE1 from the yeast TGN and analyze the similarities of the kAE1 PM targeting in yeast compared to mammalian cells (Day *et al.*, 2018; Chen *et al.*, 2019).

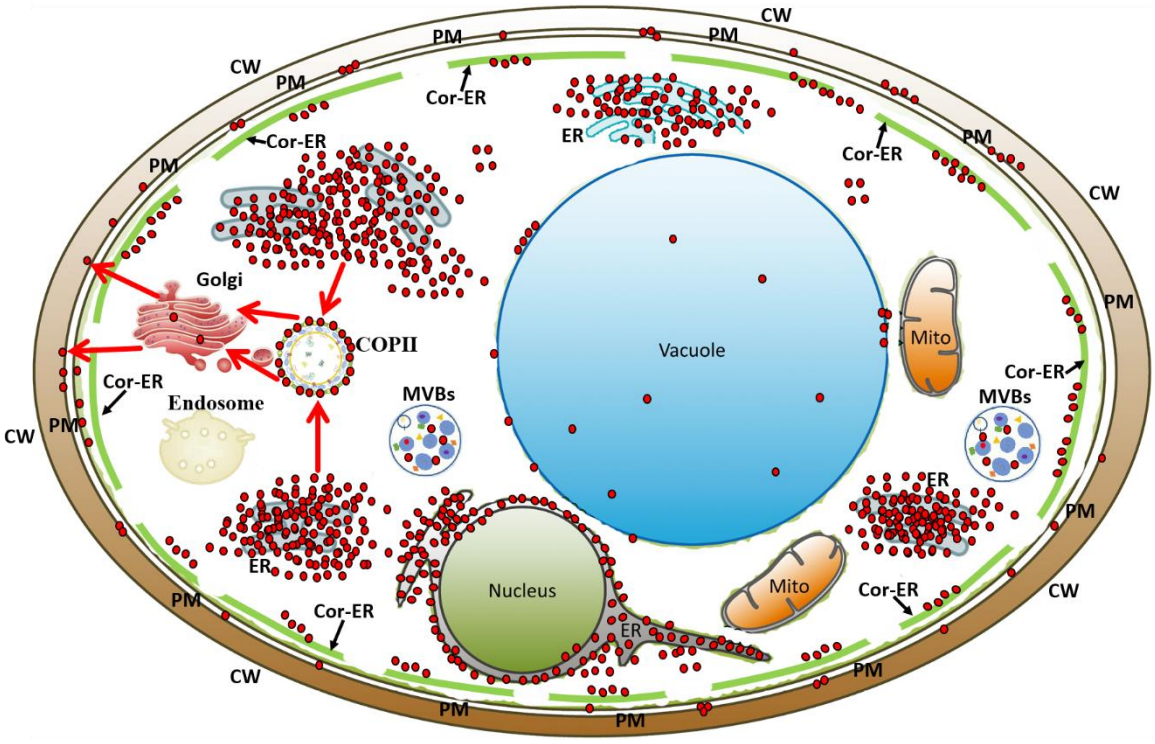

Figure 48: Schematic outline of kAE1 localization in *S. cerevisiae* based on electron and super-resolution microcopy data from the present study. kAE1 is mainly localized in the ER and membrane-like structures originated from the ER. kAE1 is also concentrated in multivesicular bodies (MVBs), the vacuole, and other parts of the secretory pathway. In addition, kAE1 can reach the PM by an endosome-independent transport mechanism, leading directly from the trans-Golgi network (TGN) to the cell surface (Red arrow). Abbreviations: ER: Endoplasmic reticulum; CW: cell wall; PM: plasma membrane; Cor-ER: cortical ER; Golgi: Golgi apparatus; Mito: mitochondrium; MVBs: multivesicular bodies.

kAE1 induces the unfolded protein response (UPR) in yeast

Cellular protein homeostasis is fundamental for all organisms. To maintain normal physiological processes, cellular proteins must be well-regulated from their synthesis to degradation (Walter & Ron, 2011). A crucial regulatory mechanism that can help regulate or overcome ER stress is the unfolded protein response, UPR (Ron & Walter, 2007). As stated before, kAE1 accumulates in the ER and could, thus, provoke several stress responses. Therefore, the induction of ER stress and potential resulting growth defects were further analyzed using different biochemical approaches. First, growth rates of BY4742 cells expressing various kAE1 variants, including unmodified or HA-tagged kAE1, kAE1^{E681Q}, and the truncated kAE1 derivative kAE1^{B3mem}, were measured. Growth rates of all kAE1 expressing cells exhibited a similar pattern as the used positive controls, which were supplemented with strong ER stress inducers (DTT and Tunicamycin). The results clearly indicated that the expression of various kAE1 variants negatively affected yeast cell growth. In yeast cells,

overexpression of either exogenous or endogenous proteins presumably leads to cellular defects due to the accumulation of proteins in the ER impeding their normal physiological functions (Kintaka *et al.*, 2016). Several studies could already show toxic effects of heterologous protein overexpression based on the increased occurrence of protein misfolding triggering ER stress and subsequent UPR induction (Kintaka *et al.*, 2016; Brehme & Voisine, 2016). Therefore, it is likely that the observed growth defects of kAE1 expressing cells are based on high ER stress levels and the activation of cellular UPR. In addition to $kAE1^{B3mem}$, the plasma membrane localization of $kAE1^{E681Q}$ has already been reported in mammalian cells (Toye *et al.*, 2004; Almomani *et al.*, 2016). $kAE1^{E681Q}$ represents a non-functional kAE1 derivative due to the loss of the anion transport activity. However, both kAE1 versions showed the same impaired growth pattern as wild-type kAE1, indicating that the functional domain is not responsible for this distinct phenotype. In the future, it would be interesting to analyze the potential influence of other kAE1 domains on cellular growth after overexpression. Interestingly, overexpression of the yeast HDEL receptor Erd2p showed almost no effect on yeast cell growth. It might be possible that the increased amount of this ER-Golgi shuttle protein accelerates the retrieval of luminal ER proteins, thus, preventing the activation of the UPR in yeast cells (Becker *et al.*, 2016).

Additionally, the Kar2p expression level of yeast expressing various kAE1 derivatives was checked via Western blot. Kar2p is an ATPase that plays an essential role in importing proteins into the ER and their proper folding; additionally, it is involved in the regulation of UPR via its interaction with Ire1p. Because UPR activation leads to an upregulation of the Kar2p-encoding gene, the intracellular level of the chaperone is a direct indicator of ER stress in the cell (Romanos *et al.*, 1992; Ron & Walter, 2007). The results of the Western analysis are consistent with the impaired growth behavior and suggest a substantial upregulation of the chaperone in yeast overexpressing the tested kAE1 constructs ($kAE1^{WT}$, $kAE1^{HA}$, $kAE1^{FLAG}$, and $kAE1^{E681Q}$). Expression of the wild-type kAE1 variant in the β-estradiol inducible yeast strain BY4742-GEV also showed a steady and dose-dependent increase in Kar2p levels in the respective transformants, pointing to an overload of the ER folding capacity based on kAE1 overexpression. The accumulation of unfolded or misfolded proteins in the ER lumen activates the transmembrane ER stress sensor Ire1p, eventually leading to the splicing of the *HAC1* mRNA (Okamura *et al.*, 2000; Ogawa & Mori, 2004). Consequently, the non-conventionally spliced *HAC1* is then translated into the transcription factor Hac1p, activating and regulating UPR-dependent genes (Zhao *et al.*, 2019). In a different approach, kAE1 derivatives were transformed in Δ*hac1* and Δ*ire1* deletion mutants, and the results showed no significant increase

in the Kar2p level highlighting the direct correlation of kAE1 overexpression and the Ire1p-mediated UPR signaling pathway. Additional experiments were designed to study the extent of the UPR induction in kAE1 expressing cells. Therefore, yeast reporter strains were employed in which UPR activation was measurable by either a color change or an increase in GFP fluorescence intensity (Fernandes *et al.*, 2019). The results showed that in both cases, kAE1 expression always induced a strong activation of the UPR, supporting the previous findings of this study.

Based on the experimental data, it can be hypothesized that the significant induction of the UPR pathway by the overexpression of kAE1 can be attributed to the aggregation of the majority of translated kAE1, which is not folded correctly into its native conformation (Figure 49). As a result, the misfolded kAE1 is inefficiently trafficked to the plasma membrane. Similar effects of kAE1 expression and DTT-treatment on cell growth further support this assumption. The correlation of UPR induction and overexpression in yeast is described for many other heterologously expressed proteins (Coudray *et al.*, 2016; Takano *et al.*, 2007). Casagrande et al. (2000) expressed the heavy chain of the murine major histocompatibility complex class I (H-2K^{b}) in yeast and found a robust activation of UPR-mediated pathways. However, they were able to partially compensate for the ER stress by the co-expression of Hac1p (Casagrande *et al.*, 2000).

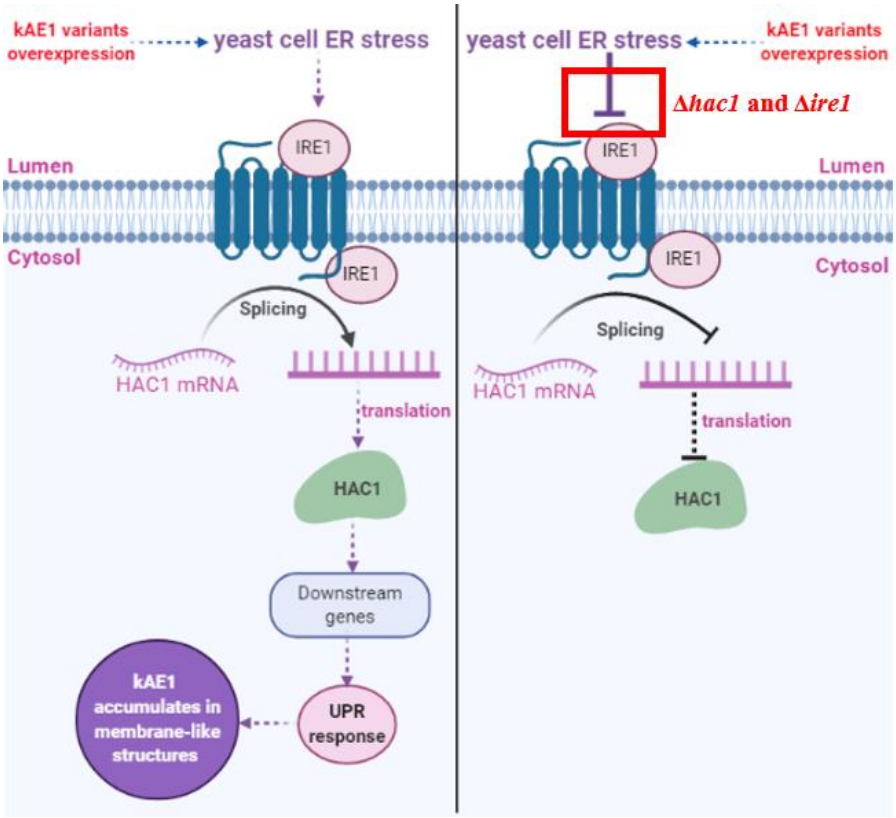

Figure 49: kAE1 induces strong yeast unfolded protein response (UPR). Accumulation of unfolded kAE1 activates the transmembrane ER stress sensor Ire1p. In the cytosol, Ire1p recruits *HAC1* mRNA, mediating its splicing. The spliced mRNA is translated into Hac1p, which activates downstream UPR target genes. Due to the massive ER stress, kAE1 mainly accumulates in membrane-like structures derived from the ER (left side). On the contrary, kAE1 can not trigger Ire1p-mediated UPR processing when expressed in BY4742 Δ*hac1* and Δ*ire1* cells, resulting in no upregulation of Kar2p (right side). Adapted from Zhao *et al.*, 2019.

In this study, both overexpression of an exogenous protein (kAE1) and the endogenous protein Erd2p lead to ER stress in yeast. Besides, it is noteworthy to note that kAE1 induced a much stronger UPR compared to the yeast HDEL receptor Erd2p. As already mentioned, it might be possible that an increased Erd2p level accelerates the retrieval of ER luminal proteins back to the ER (Llewellyn *et al.*, 1997; Capitani *et al.*, 2009); most ER chaperones, including Kar2p and Pdi1p, bear a C-terminal HDEL-retention motif. Therefore, a higher ER folding capacity could be possible, prohibiting the accumulation of misfolded proteins and facilitating the regulation of unfolded proteins (Becker *et al.*, 2016). Surprisingly, the yeast kAE1 homolog Bor1p showed a relatively high UPR activation after its overexpression. Bor1p, belonging to the *SLC4* family, plays important roles in bicarbonate exchange and pH regulation in animals and is responsible for boron transport in yeast as a secondary transporter (Coudray *et al.*, 2016). In *S. cerevisiae*, boron has been shown to stimulate cell growth (Takano *et al.*, 2007). However,

when present in excess, it is toxic for yeast cells (Nozawa *et al.*, 2006). This may somehow explain why the boron transporter Bor1p overexpression in yeast leads to strong UPR activation, which is comparable to the kAE1 scenario.

Different kAE1 domains induce UPR in yeast

The results from this study indicated that the structural kAE1 homolog Bor1p showed a similar effect on ER stress induction as kAE1, albeit the expression level of Bor1p was two times lower. Because the inactive variant $kAE1^{E681Q}$, lacking the bicarbonate exchange activity, and the N-terminal truncated version $kAE1^{B3Mem}$ induced the same amount of ER stress as wild-type kAE1, experiments were designed to analyze the importance of other structural parts and their influence on cellular UPR activation. Therefore, C- and N-terminally truncated variants of the anion exchanger were constructed: $kAE1^{1-666}$ lacks the cytosolic C-terminus as well as transmembrane domains (TMD) 10 to 14 of kAE1, and $kAE1^{1-491}$ misses the N-glycosylation site at position Asn^{577} (correlating to Asn^{642} in AE1) as well as TMD 5 to 14 (Toye *et al.*, 2004; Almomani, 2015). These derivatives, as well as $kAE1^{WT}$, $kAE1^{HA}$, and the already established $kAE1^{B3Mem}$ were expressed in BY4742 cells, and intracellular Kar2p levels were monitored via Western blot. The results showed that cells expressing $kAE1^{1-491}$ and $kAE1^{1-666}$ displayed a significantly reduced Kar2p protein level compared to both $kAE1^{WT}$ and $kAE1^{HA}$ expressing cells. In contrast, no considerable difference in the upregulation of Kar2p was detected between $kAE1^{WT}$ and $kAE1^{B3Mem}$ cells. Taken together, this might indicate that the truncation of the cytosolic N-terminus plays no specific role in UPR activation, whereas the TMD 10-14 and/or the cytosolic C-terminus are crucial for UPR induction in yeast. Because the precise intracellular localization of $kAE1^{1-491}$ and $kAE1^{1-666}$ was not further investigated in this study, a statement of potential improvements of the PM targeting of these truncated kAE1 derivatives is not possible. Additionally, the expression of various kAE1 variants was induced in a dose-dependent manner clearly reducing the amount of kAE1 protein compared to standard induction via galactose supplementation. Therefore, reduced UPR activation in yeast expressing the truncated versions might result from the interplay between the reduced kAE1 load and the missing structural components.

In mammalian cells, the cytosolic C-terminus is the binding site of the majority of the confirmed kAE1 interaction partners (Toye *et al.*, 2004; Yenchitsomanus *et al.*, 2005). It could be possible that the lack of an appropriate interaction partner in yeast hinders the proper folding of the transporter leading to its accumulation in yeast (Sarder *et al.*, 2020). Consequently, co-expression of glycophorin A, a kAE1 interaction partner, significantly improved the PM

targeting of kAE1 in yeast cells and frog oocytes (Overton *et al.*, 2003). It should also be mentioned that several described dRTA-causing mutations are located in the C-terminal region of kAE1. Some of these mutations (e.g., G701D or S779P) are responsible for the improper folding and/or trafficking in mammalian cells (Quilty *et al.*, 2002; Chang *et al.*, 2018). In the future, the construction of additional truncated versions (e.g., kAE1 lacking the cytosolic C-terminal part) is required to potentially correlate the exact region with the induction of the cellular UPR (Figure 50).

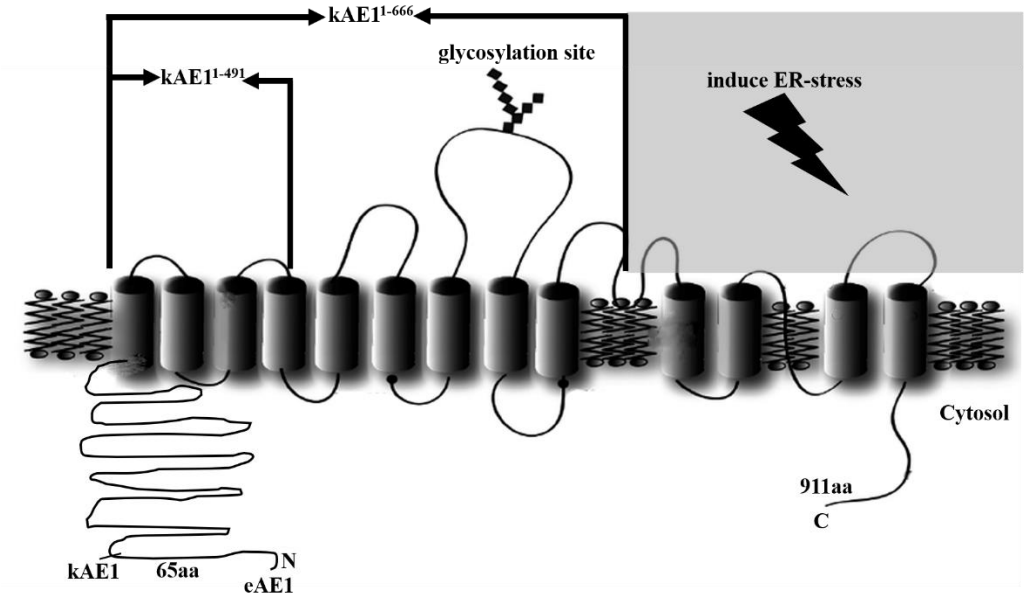

Figure 50: Role of different kAE1 domains in the induction of UPR in yeast. Cells expressing kAE1$^{1-666}$, which lacks transmembrane domains (TMD) 10 to 14, and kAE1$^{1-491}$ missing TMD 5 to 14, displayed a significant reduction of Kar2p levels compared to kAE1^{WT}, indicating that TMD 10-14 are crucial for UPR induction in yeast (shown in grey area).

Reducing ER-stress in kAE1 expressing yeast cells

The ER is the main organelle for synthesis, folding, and processing of secretory and transmembrane proteins and multiple factors play a role in maintaining ER homeostasis (Morishima *et al.*, 2004; Kim *et al.*, 2008). The ER responds to the disturbances by activating mechanisms that increase the capability to eliminate ER stress (Shen *et al.*, 2004). Numerous possibilities had been reported to reduce cellular ER stress in the cell, including overexpression of single ER stress-related genes (Leborgne-Castel *et al.*, 1999; Morishima *et al.*, 2004; Kim *et al.*, 2008). Overexpression of *IRE1*, *HAC1*, or other protein kinase encoding genes can effectively improve protein folding and enhance the capacity of the cellular secretion machinery, thus decreasing the unfolded protein response (Shen *et al.*, 2004; Guerfal *et al.*, 2010). In this

study, selected genes encoding various ER-luminal proteins involved in protein folding were overexpressed and tested for potential effects on UPR activation in kAE1 expressing cells. In a first approach, kAE1 expression was driven from the *GAL1* promoter, and no significant changes in the Kar2p level could be observed after co-expression. However, using the β-estradiol-inducible kAE1 expression system, a significant reduction of the Kar2p amount could be demonstrated after co-expression with the different ER chaperones. These data suggest that improvements in kAE1 folding might prevent kAE1-mediated UPR induction in yeast.

In parallel, kAE1 localization was investigated in yeast co-expressing various ER-lumenal proteins and kAE1. Surprisingly, all cells showed a GFP signal distribution in the form of ring-like structures at the cell periphery, indicating a severe shift in the intracellular localization of kAE1; especially overexpression of Eug1p and Mpd2p led to a significant change in kAE1 localization. The obtained data further strengthen the hypothesis that ER accumulation of the anion transporter represents the major bottleneck in kAE1 trafficking in yeast. Furthermore, the results also demonstrate that UPR activation can only be prevented to a certain extent of kAE1 overexpression. Oslowski *et al.* (2011) pointed out that ER lumenal proteins can play a role in the maintenance of a unique cellular environment by keeping a balance between the ER loading and the necessary capacity to handle the protein load (Oslowski *et al.*, 2011). If overexpression of exogenous proteins induces ER stress over a defined threshold, cells cannot restore ER functions, leading to the induction of apoptotic cell death (Bagnat *et al.*, 2001; Jermy *et al.*, 2006). However, if the induced cellular stress does not exceed a specific limit, the activated signaling pathways and the adaptive cellular response might restore homeostasis (Benedetti *et al.*, 2000; Chakraborty *et al.*, 2016; Fernandes *et al.*, 2019). Taken together, this indicates that a fine-tuned control of the expression parameters is crucial for the proper folding and trafficking of kAE1 in yeast, preventing an excessive induction of ER stress and thereby allowing the cell to cope with the expression of the heterologous protein (Figure 51).

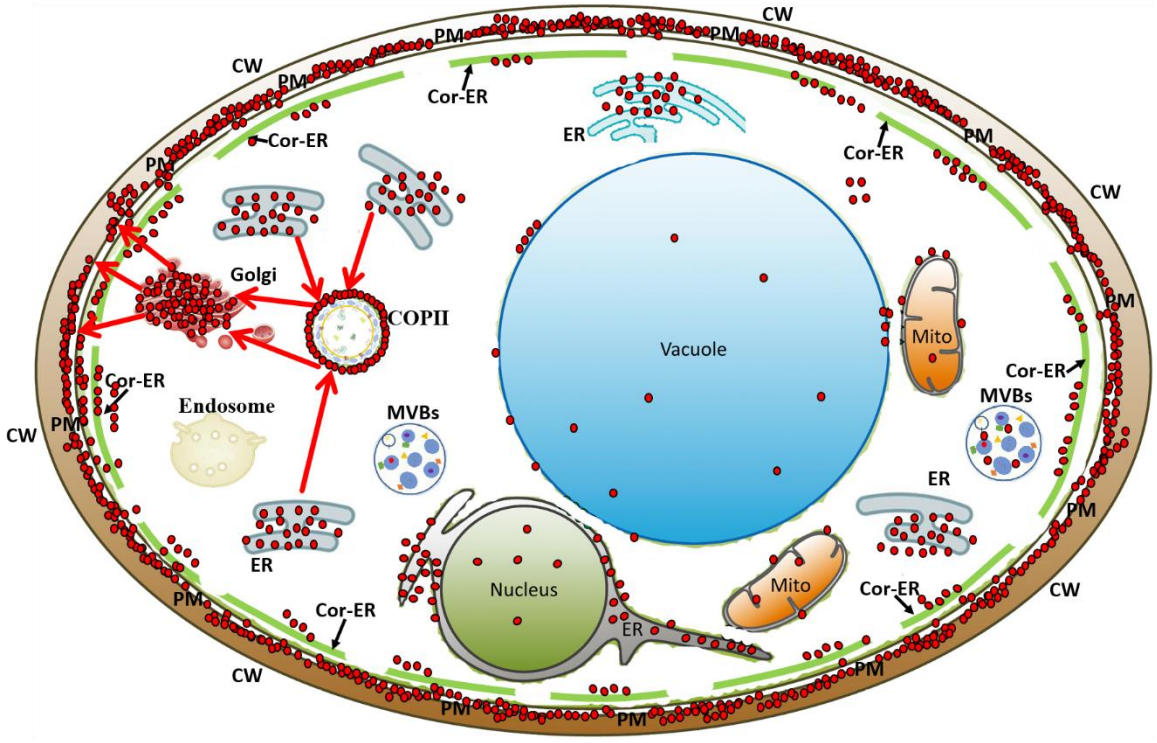

Figure 51: Schematic outline of the improvement of kAE1 transport to the plasma membrane by increasing the protein folding capacity of the ER. Overexpression of ER chaperones together with a reduced kAE1 expression level improve kAE1 localization in the yeast cell periphery. Red dots represent kAE1 localization in the yeast cell. Abbreviations: ER: endoplasmic reticulum; CW: cell wall; PM: plasma membrane; Cor-ER: cortical ER; Golgi: Golgi-Apparatus; Mito: mitochondrium; MVBs: multivesicular bodies.

In addition to the overexpression of ER chaperones, further possibilities were explored to reduce ER stress in kAE1 expressing yeast. In this context, co-expression of *HSF1* whose gene product is involved in the heat shock response (HSR) pathway, led to a significant improvement of PM localization of kAE1. *HSF1* encodes a transcription factor that can activate several genes responsible for a multitude of cellular stress responses, for example, proteotoxic and osmotic stress (Li *et al.*, 2017; Ding *et al.*, 2009). Thus, overexpression of Hsf1p could help to decrease cellular stress and subsequently improve kAE1 trafficking. Additionally, Erv29p and Pah1p were co-expressed with kAE1, and results demonstrated an increase in the trafficking of kAE1 to the PM in both cases. The former is involved in COPII vesicle formation and transport of secretory cargo in *S. cerevisiae*, and previous reports showed that Erv29p is directly involved in packaging glycosylated pro-α-factor into COPII vesicles (Belden & Barlowe, 2001). Hence, facilitation of anterograde transport might assist kAE1 trafficking from the rough ER to the Golgi apparatus, eventually leading to more kAE1 at the yeast PM. Pah1p, in contrast, encodes a phosphatidate phosphatase controlling the expression of *CHO1* (phosphatidylserine synthase),

which is essential for the synthesis of membrane phospholipids (Carman & Han, 2006). As a result, Pah1p overexpression might increase nuclear and ER membranes, leading to an indirect increase of the ER capacity, thereby improving kAE1 folding and trafficking. In addition to the overexpression of auxiliary proteins, kAE1-expressing cells were supplemented with the chemical chaperone 4-Phenylbutyric acid (PBA). Interestingly, kAE1 location was strongly enhanced compared to the control. Previous studies showed that PBA usage in mammalian cells efficiently prevents ER stress and regulates ER stress-induced cell death and autophagy (Uppala *et al.*, 2017). The similar phenotype observed in this study might indicate that PBA has the same effect in yeast cells and can be applied to prevent ER-stress.

The inefficient targeting of kAE1 to the PM poses one of the most significant challenges in using yeast as model to study kAE1 function and transport (Sarder *et al.*, 2020; Li *et al.*, 2021). However, the data of the present study provide a first strategy to overcome this issue and further optimize the yeast *S. cerevisiae* as a model for future trafficking studies. The overexpression of individual ER chaperones and other folding catalysts can efficiently prevent or reduce UPR activation under moderate kAE1 expression levels and, thereby, significantly improve PM targeting of kAE1. In addition to the amount of kAE1 protein in intracellular structures, the selected yeast strain for the heterologous expression plays a crucial factor in the PM targeting. Based on the findings presented in this PhD thesis, the β-estradiol inducible GEV promoter system might be a promising tool for the controlled expression of kAE1. Further, the co-expression of different ER chaperones like Pdi1p or Eug1p significantly increased the PM targeting of the transporter, enabling the study of transport-related questions. However, genomic integration of kAE1 could help to exclude fluctuations in expression level in future experiments. An optimized yeast-based expression system could allow a more detailed analysis of the intracellular kAE1 transport or the impact of dRTA-causing mutations on kAE1 transport and UPR activation.

5. Outlook

In this study, the yeast *Saccharomyces cerevisiae* was implemented as a model system to examine different cellular aspects of kAE1 physiology. It was possible, for the first time, to successfully express a codon-optimized tagged and untagged full-length versions kAE1 in yeast. Additionally, a partial localization of these constructs at the yeast plasma membrane (PM) could be visualized. However, a strong induction of the yeast UPR was observed after overexpression of all analyzed kAE1 derivatives. In the last part of the study, possibilities were explored to reduce cellular ER stress either via overexpression of selected genes encoding luminal ER chaperones or by application of chemical compounds (such as 4-PBA) known for improving the ER folding capacity. Based on the findings presented in this study, the following experiments can be outlined to future research questions in this field:

(1) Although SIM imaging and biochemical assays strongly support the hypothesis that kAE1 folding and PM transport are significantly enhanced after increasing the folding capacity of the ER, EM microscopy studies should be conducted in the future to directly prove this assumption.

(2) Based on the data obtained for yeast cells, it would be interesting to analyze the influence of the appropriate homologs on kAE1 trafficking in mammalian cells to eventually test if they can rescue the dRTA phenotype.

6. References

Abbas, Y. M., Toye, A. M., Rubinstein, J. L., & Reithmeier, R. A. (2018). Band 3 function and dysfunction in a structural context. *Current Opinion in Hematology*, 25 (3), 163-170.

Ahlstrom, D., & Garud, R. (1996). Forgotten paths in medicine: the case of the low protein diet in chronic renal failure. In *Managing Technology in Healthcare* (pp. 155-187). Springer, Boston, MA.

Almomani, E. Y. (2015). Adaptor protein 1 complexes regulate intracellular trafficking of the kidney anion exchanger 1 in epithelial cells. *The American Journal of Physiology: Cell Physiology*, 303: C554–C566.

Almomani, E. Y., Chu, C. Y., & Cordat, E. (2011). Mis-trafficking of bicarbonate transporters: implications to human diseases. *Biochemistry and Cell Biology*, 89 (2), 157-177.

Al-Awqati, Q. (2013). Cell biology of the intercalated cell in the kidney. *FEBS letters*, 587 (13), 1911-1914.

Al-Awqati, Q., & Gao, X. B. (2011). Differentiation of intercalated cells in the kidney. *Physiology*, 26 (4), 266-272.

Almomani, E., Lashhab, R., Alexander, R. T., & Cordat, E. (2016). The carboxyl-terminally truncated kidney anion exchanger 1 R901X dRTA mutant is unstable at the plasma membrane. *American Journal of Physiology-Cell Physiology*, 310 (9), C764-C772.

Almomani, E. Y., Touret, N., & Cordat, E. (2017). Adaptor protein 1 B mu subunit does not contribute to the recycling of kAE1 protein in polarized renal epithelial cells. *Molecular Membrane Biology*, 34 (1-2), 50-64.

Ammerer, G., Hunter, C. P., Rothman, J. H., Saari, G. C., Valls, L. A., & Stevens, T. H. (1986). *PEP4* gene of *Saccharomyces cerevisiae* encodes proteinase A, a vacuolar enzyme required for processing of vacuolar precursors. *Molecular and Cellular Biology*, 6 (7), 2490-2499.

Anacletus, F. C., Nwauche, K. T., & Ighorodje-Monago, C. C. (2017). Effect of Triton X-100 and white rot fungus (*Pleurotus ostratus*) on physico-chemical composition of crude oil impacted soil. *Journal of Applied Life Sciences International*, 12 (3), 1-7.

Bagnat, M., Chang, A., & Simons, K. (2001). Plasma membrane proton ATPase Pma1p requires

raft association for surface delivery in yeast. *Molecular Biology of the Cell*, 12 (12), 4129-4138.

Becker, B., Blum, A., Gießelmann, E., Dausend, J., Rammo, D., Müller, N. C., Tschacksch E, Steimer M., Spindler J., Becherer U., Rettig J., Breinig F., & Schmitt M.J. (2016). H/KDEL receptors mediate host cell intoxication by a viral A/B toxin in yeast. *Scientific Reports*, 6(1), 1-11.

Belden, W. J., & Barlowe, C. (2001). Role of Erv29p in collecting soluble secretory proteins into ER-derived transport vesicles. *Science*, 294 (5546), 1528-1531.

Benedetti, C., Fabbri, M., Sitia, R., & Cabibbo, A. (2000). Aspects of gene regulation during the UPR in human cells. *Biochemical and Biophysical Research Communications*, 278 (3), 530-536.

Berner, N., Reutter, K. R., & Wolf, D. H. (2018). Protein quality control of the endoplasmic reticulum and ubiquitin–proteasome-triggered degradation of aberrant proteins: yeast pioneers the path. *Annual Review of Biochemistry*, 87, 751-782.

Birnboim, H. C., & Doly, J. (1979). A rapid alkaline lysis procedure for screening recombinant plasmid DNA, *Nucleic Acids Research*, 7(6): 1513–1523.

Brehme, M., & Voisine, C. (2016). Model systems of protein-misfolding diseases reveal chaperone modifiers of proteotoxicity. *Disease Models & Mechanisms*, 9 (8), 823-838.

Bogner, A., Jouneau, P. H., Thollet, G., Basset, D., & Gauthier, C. (2007). A history of scanning electron microscopy developments: towards “wet-STEM” imaging. *Micron*, 38 (4), 390-401.

Bonar, P., & Casey, J. R. (2010). Purification of functional human Cl^-/HCO_3^-exchanger, AE1, over-expressed in *Saccharomyces cerevisiae*. *Protein Expression and Purification*, 74 (1), 106-115.

Botstein, D., Chervitz, S. A., & Cherry, M. (1997). Yeast as a model organism. *Science*, 277 (5330), 1259-1260.

Carman, G. M., & Han, G. S. (2006). Roles of phosphatidate phosphatase enzymes in lipid metabolism. *Trends in Biochemical Sciences*, 31 (12), 694-699.

Carpinone, E. M., Li, Z., Mills, M. K., Foltz, C., Brannon, E. R., Carlow, C. K., & Starai, V. J. (2018). Identification of putative effectors of the Type IV secretion system from the

Wolbachia endosymbiont of *Brugia malayi*. *PloS One*, 13 (9): e0204736.

Chakraborty, R., Baek, J. H., Bae, E. Y., Kim, W. Y., Lee, S. Y., & Kim, M. G. (2016). Comparison and contrast of plant, yeast, and mammalian ER stress and UPR. *Applied Biological Chemistry*, 59 (3), 337-347.

Chalfant, M., Barber, K. W., Borah, S., Thaller, D., & Lusk, C. P. (2018). Expression of Torsin A in a heterologous yeast system reveals interactions with conserved lumenal domains of LINC and nuclear pore complexes. *bioRxiv*, 421909.

Chang, W. A., Sheu, C. C., Liu, K. T., Shen, J. H., Yen, M. C., & Kuo, P. L. (2018). Identification of mutations in *SLC4A1*, *GP1BA* and *HFE* in a family with venous thrombosis of unknown cause by next-generation sequencing. *Experimental and Therapeutic Medicine*, 16 (5), 4172-4180.

Chen, Y. T., Wang, I. H., Wang, Y. H., Chiu, W. Y., Hu, J. H., Chen, W. H., & Lee, F. J. S. (2019). Action of Arl1 GTPase and golgin Imh1 in Ypt6-independent retrograde transport from endosomes to the trans-Golgi network. *Molecular Biology of the Cell*, 30 (8), 1008-1019.

Capitani, M., & Sallese, M. (2009). The KDEL receptor: new functions for an old protein. *FEBS letters*, 583 (23), 3863-3871.

Casagrande, R., Stern, P., Diehn, M., Shamu, C., Osario, M., Zúñiga, M., Brwon P., & Ploegh, H. (2000). Degradation of proteins from the ER of *S. cerevisiae* requires an intact unfolded protein response pathway. *Molecular cell*, 5 (4), 729-735.

Cheung, J. C., Li, J., & Reithmeier, R. A. (2005). Topology of transmembrane segments 1- 4 in the human chloride/bicarbonate anion exchanger 1 (AE1) by scanning N-glycosylation mutagenesis. *Biochemical Journal*, 390 (1), 137-144.

Coudray, N., Zhang, Z., Clark, K. M., Ubarretxena, I., Beckstein, O., Dumont, M. E., & Stokes, D. L. (2016). Structure of the Borate Transporter Bor1p by cryo-EM. *Biophysical Journal*, 110 (3), 137a-138a.

Chang, C. L., Chen, Y. J., & Liou, J. (2017). ER-plasma membrane junctions: why and how do we study them? *Biochimica Et Biophysica Acta (BBA)-Molecular Cell Research*, 1864 (9), 1494-1506.

Chen, L., Clark, J. Z., Nelson, J. W., Kaissling, B., Ellison, D. H., & Knepper, M. A. (2019). Renal-tubule epithelial cell nomenclature for single-cell RNA-sequencing studies. *Journal*

of the American Society of Nephrology, 30 (8), 1358-1364.

Cheung, J. C., Li, J., & Reithmeier, R. A. (2005). Topology of transmembrane segments 1-4 in the human chloride/bicarbonate anion exchanger 1 (AE1) by scanning N-glycosylation mutagenesis. *Biochemical Journal*, 390 (1), 137-144.

Cordat, E., Kittanakom, S., Yenchitsomanus, P. T., Li, J., Du, K., Lukacs, G. L., & Reithmeier, R. A. (2006). Dominant and recessive distal renal tubular acidosis mutations of kidney anion exchanger 1 induce distinct trafficking defects in MDCK cells. *Traffic*, 7 (2), 117-128.

Cordat, E., Li, J., & Reithmeier, R. A. (2003). Carboxyl-terminal truncations of human anion exchanger impair its trafficking to the plasma membrane. *Traffic*, 4 (9), 642-651.

Cordat, E., & Reithmeier, R. A. (2014). Structure, function, and trafficking of *SLC4* and *SLC26* anion transporters. *Current Topics in Membranes*, 73, 1-67.

Day, K. J., Casler, J. C., & Glick, B. S. (2018). Budding yeast has a minimal endomembrane system. *Developmental Cell*, 44 (1), 56-72.

Ding, J., Huang, X., Zhang, L., Zhao, N., Yang, D., & Zhang, K. (2009). Tolerance and stress response to ethanol in the yeast *Saccharomyces cerevisiae*. *Applied Microbiology and Biotechnology*, 85 (2), 253.

Eden, E. R., 2016. The formation and function of ER-endosome membrane contact sites. *Biochimica et Biophysica Acta (BBA)-Molecular and Cell Biology of Lipids*, 1861 (8), 874-879.

Fernandes, P., Miotto, B., Saint-Ruf, C., Nahse, V., Ravera, S., Cappelli, E., & Naim, V. (2019). FANCD2 tunes the UPR preventing mitochondrial stress-induced common fragile site instability. *bioRxiv*, 808915.

Flegelova, H., Haguenauer-Tsapis, R., & Sychrova, H. (2006). Heterologous expression of mammalian Na/H antiporters in *Saccharomyces cerevisiae*. *Biochimica et Biophysica Acta (BBA)-General Subjects*, 1760 (3), 504-516.

Flower, T. R., Chesnokova, L. S., Froelich, C. A., Dixon, C., & Witt, S. N. (2005). Heat shock prevents alpha-synuclein-induced apoptosis in a yeast model of Parkinson's disease. *Journal of Molecular Biology*, 351 (5), 1081-1100.

Geiler-Samerotte, K. A., Dion, M. F., Budnik, B. A., Wang, S. M., Hartl, D. L., & Drummond,

D. A. (2011). Misfolded proteins impose a dosage-dependent fitness cost and trigger a cytosolic unfolded protein response in yeast. *Proceedings of the National Academy of Sciences*, 108 (2), 680-685.

Genetet, S., Desrames, A., Chouali, Y., Ripoche, P., Lopez, C., & Mouro-Chanteloup, I. (2017). Stomatin modulates the activity of the Anion Exchanger 1 (AE1, *SLC4A1*). *Scientific Reports*, 7, 46170.

Gershon, H., & Gershon, D. (2000). The budding yeast, *Saccharomyces cerevisiae*, as a model for aging research: a critical review. *Mechanisms of Ageing and Development*, 120 (1-3), 1-22.

Giardina, B. J., Stein, K., & Chiang, H. L. (2014). The endocytosis gene *END3* is essential for the glucose-induced rapid decline of small vesicles in the extracellular fraction in *Saccharomyces cerevisiae*. *Journal of Extracellular Vesicles*, 3, 23497.

Graham, J. B., Canniff, N. P., & Hebert, D. N. (2019). TPR-containing proteins control protein organization and homeostasis for the endoplasmic reticulum. *Critical Reviews in Biochemistry and Molecular Biology*, 54 (2), 103-118.

Groves, J. D., Falson, P., Le Maire, M., & Tanner, M. J. (1996). Functional cell surface expression of the anion transport domain of human red cell band 3 (AE1) in the yeast *Saccharomyces cerevisiae*. *Proceedings of the National Academy of Sciences*, 93 (22), 12245-12250.

Groves, J. D., Parker, M. D., Askin, D., Falson, P., le Maire, M., & Tanner, M. J. (1999). Heterologous expression of the red-cell anion exchanger (band 3; AEI). *Biochemical Society Transactions*, 27 (6), 917-923.

Guerfal, M., Ryckaert, S., Jacobs, P. P., Ameloot, P., Van Craenenbroeck, K., Derycke, R., & Callewaert, N. (2010). The *HAC1* gene from *Pichia pastoris*: characterization and effect of its overexpression on the production of secreted, surface displayed and membrane proteins. *Microbial Cell Factories*, 9 (1), 49.

Guzel, E., Arlier, S., Guzeloglu-Kayisli, O., Tabak, M., Ekiz, T., Semerci, N., Larsen K., Schatz F., Lockwood C.J., & Kayisli, U. (2017). Endoplasmic reticulum stress and homeostasis in reproductive physiology and pathology. *International Journal of Molecular Sciences*, 18 (4), 792.

Hauser, M., Narita, V., Donhardt, A. M., Naider, F., & Becker, J. M. (2001). Multiplicity and regulation of genes encoding peptide transporters in *Saccharomyces cerevisiae*. *Molecular Membrane Biology*, 18 (1), 105-112.

Hoffman, H. K., Fernandez, M. V., Groves, N. S., Freed, E. O., & van Engelenburg, S. B. (2019). Genomic tagging of endogenous human ESCRT-I complex preserves ESCRT-mediated membrane-remodeling functions. *Journal of Biological Chemistry*, 294 (44), 16266-16281.

Hollien, J. (2013). Evolution of the unfolded protein response. *Biochimica et Biophysica Acta (BBA)-Molecular Cell Research*, 1833 (11), 2458-2463.

Hopkins, T. R. (1991). Physical and chemical cell disruption for the recovery of intracellular proteins. *Bioprocess Technol*, 12, 57-83.

Howie, A. J. (2019). Properties of intermediate parietal epithelial cells of Bowman's capsule. *Kidney International*, 96 (5), 1240-1241.

Hsu, W. T., Pang, C. N. I., Sheetal, J., & Wilkins, M. R. (2007). Protein–protein interactions and disease: Use of *S. cerevisiae* as a model system. *Biochimica et Biophysica Acta (BBA)-Proteins and Proteomics*, 1774 (7), 838-847.

Ishikawa, T., Taniguchi, Y., Okada, T., Takeda, S., & Mori, K. (2011). Vertebrate unfolded protein response: mammalian signaling pathways are conserved in medaka fish. *Cell Structure and Function*, 36(2), 247-59.

Iwata, Y., & Koizumi, N. (2012). Plant transducers of the endoplasmic reticulum unfolded protein response. *Trends in Plant Science*, 17(12), 720-727.

Jain, G., Kalra, S., & Joshi, D. (2019). Distal renal tubular acidosis with hemolytic anemia and myotonia: Unusual phenotype of a known mutation. *Asian Journal of Pediatric Nephrology*, 2 (2), 91-93.

Jamshidian, M., Coombs, R. J., Ratnam, S., & Malhotra, D. (2018). Medullary sponge kidney with distal renal tubular acidosis: A case report and review of the literature. *Scholarena Journal of Case Reports*, 5: 204.

Jermy, A. J., Willer, M., Davis, E., Wilkinson, B. M., & Stirling, C. J. (2006). The Brl domain in *Sec63p* is required for assembly of functional endoplasmic reticulum translocons. *Journal of Biological Chemistry*, 281 (12), 7899-7906.

Jiang, H., Zhang, X., Chen, X., Aramsangtienchai, P., Tong, Z., & Lin, H. (2018). Protein lipidation: occurrence, mechanisms, biological functions, and enabling technologies. *Chemical Reviews*, 118 (3), 919-988.

Juretzek, T., Wang, H. J., Nicaud, J. M., Mauersberger, S., & Barth, G. (2000). Comparison of promoters suitable for regulated overexpression of β-galactosidase in the alkane-utilizing yeast *Yarrowia lipolytica*. *Biotechnology and Bioprocess Engineering*, 5 (5), 320-326.

Kalli, A. C., & Reithmeier, R. A. (2018). Molecular dynamics simulations reveal specific interactions of the band 3 anion exchanger with lipids and glycophorin A. *Biophysical Journal*, 114 (3), 330a.

Kaksonen, M., & Roux, A. (2018). Mechanisms of clathrin-mediated endocytosis. *Nature Reviews Molecular Cell Biology*, 19 (5), 313-326.

Karet, F. E. (2004). A novel missense mutation in AE1 causing autosomal dominant distal renal tubular acidosis retains normal transport function but is mistargeted in polarized epithelial cells. *Journal of Biological Chemistry*, 279 (14), 13833-13838.

Katzmann, D. J., Sarkar, S., Chu, T., Audhya, A., & Emr, S. D. (2004). Multivesicular body sorting: ubiquitin ligase Rsp5 is required for the modification and sorting of carboxypeptidase S. *Molecular Biology of the Cell*, 15 (2), 468-480.

Kawai, S., Hashimoto, W. and Murata, K., 2010. Transformation of *Saccharomyces cerevisiae* and other fungi: methods and possible underlying mechanism. *Bioengineered Bugs*, 1(6), pp.395-403.

Kaya, A., Karakaya, H. C., Fomenko, D. E., Gladyshev, V. N., & Koc, A. (2009). Identification of a novel system for boron transport: *Atr1* is a main boron exporter in yeast. *Molecular and Cellular Biology*, 29 (13), 3665-3674.

Kaur, J., & Bachhawat, A. K. (2007). Yct1p, a novel, high-affinity, cysteine-specific transporter from the yeast *Saccharomyces cerevisiae*. *Genetics*, 176 (2), 877-890.

Kim, I., Xu, W., & Reed, J. C. (2008). Cell death and endoplasmic reticulum stress: disease relevance and therapeutic opportunities. *Nature Reviews Drug discovery*, 7 (12), 1013-1030.

Kimata, Y., & Kohno, K. (2011). Endoplasmic reticulum stress-sensing mechanisms in yeast and mammalian cells. *Current Opinion in Cell Biology*, 23 (2), 135-142.

Kimata, Y., Ishiwata-Kimata, Y., Yamada, S., & Kohno, K. (2006). Yeast unfolded protein response pathway regulates expression of genes for anti-oxidative stress and for cell surface proteins. *Genes to Cells*, 11 (1), 59-69.

Kintaka, R., Makanae, K., & Moriya, H. (2016). Cellular growth defects triggered by an overload of protein localization processes. *Scientific Reports*, 6 (1), 1-11.

Kittanakom, S., Cordat, E., Akkarapatumwong, V., Yenchitsomanus, P. T., & Reithmeier, R. A. (2004). Trafficking defects of a novel autosomal recessive distal renal tubular acidosis mutant (S773P) of the human kidney anion exchanger (kAE1). *Journal of Biological Chemistry*, 279 (39), 40960-40971.

Kolb, A. R., Buck, T. M., & Brodsky, J. L. (2011). *Saccharomyces cerivisiae* as a model system for kidney disease: what can yeast tell us about renal function? *American Journal of Physiology-Renal Physiology*, 301 (1), F1-F11.

Kolb, P. S., Ayaub, E. A., Zhou, W., Yum, V., Dickhout, J. G., & Ask, K. (2015). The therapeutic effects of 4-phenylbutyric acid in maintaining proteostasis. *The International Journal of Biochemistry & Cell Biology*, *61*, 45-52.

Koley, D., & Bard, A. J. (2010). Triton X-100 concentration effects on membrane permeability of a single HeLa cell by scanning electrochemical microscopy (SECM). *Proceedings of the National Academy of Sciences*, 107 (39), 16783-16787.

Lajoie, P., Moir, R. D., Willis, I. M., & Snapp, E. L. (2012). Kar2p availability defines distinct forms of endoplasmic reticulum stress in living cells. *Molecular Biology of the Cell*, 23 (5), 955-964.

Lashhab, R., Ullah, A. S., & Cordat, E. (2019). Renal collecting duct physiology and pathophysiology. *Biochemistry and Cell Biology*, 97 (3), 234-242.

Lashhab, R., Rumley, A. C., Arutyunov, D., Rizvi, M., You, C., Dimke, H., Touret, N., Zimmermann, R., Jung, M., Chen, X. Z., Alexander, T., and Cordat, E. (2019). The kidney anion exchanger 1 affects tight junction properties via claudin-4. *Scientific Reports*, 9 (1), 1-16.

Leborgne-Castel, N., Jelitto-Van Dooren, E. P., Crofts, A. J., & Denecke, J. (1999). Overexpression of *BiP* in tobacco alleviates endoplasmic reticulum stress. *The Plant Cell*, 11 (3), 459-469.

Lee, K., Tirasophon, W., Shen, X., Michalak, M., Prywes, R., Okada, T., Mori, K., & Kaufman, R. J. (2002). IRE1-mediated unconventional mRNA splicing and S2P-mediated ATF6 cleavage merge to regulate XBP1 in signaling the unfolded protein response. *Genes & Development*, 16 (4), 452-466.

Lee, K. P., Dey, M., Neculai, D., Cao, C., Dever, T. E., & Sicheri, F. (2008). Structure of the dual enzyme Ire1 reveals the basis for catalysis and regulation in nonconventional RNA splicing. *Cell*, 132 (1), 89-100.

Lee, J., & Ozcan, U. (2014). Unfolded protein response signaling and metabolic diseases. *Journal of Biological Chemistry*, 289 (3), 1203-1211.

Li, J., Labbadia, J., & Morimoto, R. I. (2017). Rethinking HSF1 in stress, development, and organismal health. *Trends in Cell Biology*, 27 (12), 895-905.

Lippincott-Schwartz, J., Freed, E. O., & Van Engelenburg, S. B. (2017). A consensus view of ESCRT-mediated human immunodeficiency virus type 1 abscission. *Annual Review of Virology*, 4, 309-325.

Li, X., Cordat, E., Schmitt, M. J., & Becker, B. (2021). Boosting ER folding capacity reduces UPR activation and intracellular accumulation of human kidney anion exchanger 1 in *S. cerevisiae*. *Yeast*, 1-14.

Lewis, M. J., & Pelham, H. R. (1996). SNARE-mediated retrograde traffic from the Golgi complex to the endoplasmic reticulum. *Cell*, 85 (2), 205-215.

Li, W., Mo, W., Shen, D., Sun, L., Wang, J., Lu, S., Gitschier J.M., & Zhou, B. (2005). Yeast model uncovers dual roles of mitochondria in the action of artemisinin. *PLoS Genetics*, 1 (3), e36.

Lindholm, D., Korhonen, L., Eriksson, O., & Kõks, S. (2017). Recent insights into the role of unfolded protein response in ER stress in health and disease. *Frontiers in Cell and Developmental Biology*, 5, 48.

Linster, E., & Wirtz, M. (2018). N-terminal acetylation: an essential protein modification emerges as an important regulator of stress responses. *Journal of Experimental Botany*, 69 (19), 4555-4568.

Li, H., Korennykh, A. V., Behrman, S. L., & Walter, P. (2010). Mammalian endoplasmic reticulum stress sensor IRE1 signals by dynamic clustering. *Proceedings of the National*

Academy of Sciences, 107 (37), 16113-16118.

Llewellyn, D. H., Roderick, H. L., & Rose, S. (1997). KDEL receptor expression is not coordinatedly up-regulated with ER stress-induced reticuloplasmin expression in HeLa cells. *Biochemical and Biophysical Research Communications*, 240 (1), 36-40.

Malhotra, V., & Wong, H. R. (2002). Interactions between the heat shock response and the nuclear factor-κB signaling pathway. *Critical Care Medicine*, 30 (1), S89-S95.

McIsaac, R. S., Silverman, S. J., McClean, M. N., Gibney, P. A., Macinskas, J., Hickman, M. J., Petti A, Botstein D, Boone C & Botstein, D. (2011). Fast-acting and nearly gratuitous induction of gene expression and protein depletion in *Saccharomyces cerevisiae*. *Molecular Biology of the Cell*, 22 (22), 4447-4459.

Mesquita, F. S., van der Goot, F. G., & Sergeeva, O. A. (2020). Mammalian membrane trafficking as seen through the lens of bacterial toxins. *Cellular Microbiology*, 22 (4): e13167.

Miao, Y., & Abraham, S. N. (2014). Kidney α-intercalated cells and lipocalin 2: defending the urinary tract. *The Journal of Clinical Investigation*, 124 (7), 2844-2846.

Momcilovic, M., Hong, S. P., & Carlson, M. (2006). Mammalian TAK1 activates Snf1 protein kinase in yeast and phosphorylates AMP-activated protein kinase in vitro. *Journal of Biological Chemistry*, 281 (35), 25336-25343.

Moraes, I., Evans, G., Sanchez-Weatherby, J., Newstead, S., & Stewart, P. D. S. (2014). Membrane protein structure determination-the next generation. *Biochimica et Biophysica Acta (BBA)-Biomembranes*, 1838 (1), 78-87.

Mori, K. (2009). Signaling pathways in the unfolded protein response: development from yeast to mammals. *Journal of Biochemistry*, 146 (6), 743-750.

Morishima, N., Nakanishi, K., Tsuchiya, K., Shibata, T., & Seiwa, E. (2004). Translocation of Bim to the endoplasmic reticulum (ER) mediates ER stress signaling for activation of caspase-12 during ER stress-induced apoptosis. *Journal of Biological Chemistry*, 279 (48), 50375-50381.

Mori, K. (2015). The unfolded protein response: the dawn of a new field. *Proceedings of the Japan Academy, Series B*, 91 (9), 469-480.

Momcilovic, M., Hong, S. P., & Carlson, M. (2006). Mammalian TAK1 activates Snf1 protein

kinase in yeast and phosphorylates AMP-activated protein kinase in vitro. *Journal of Biological Chemistry*, 281 (35), 25336-25343.

Morishima, N., Nakanishi, K., Tsuchiya, K., Shibata, T., & Seiwa, E. (2004). Translocation of Bim to the endoplasmic reticulum (ER) mediates ER stress signaling for activation of caspase-12 during ER stress-induced apoptosis. *Journal of Biological Chemistry*, 279 (48), 50375-50381.

Münch, C. (2018). The different axes of the mammalian mitochondrial unfolded protein response. *BMC biology*, 16 (1), 81.

Natochin, Y. V. (2019). Principles of Evolution of the Excretory Organs and the System of Homeostasis. *Journal of Evolutionary Biochemistry and Physiology*, 55 (5), 398-410.

Nozawa, A., Takano, J., Kobayashi, M., Von Wirén, N., & Fujiwara, T. (2006). Roles of *BOR1*, *DUR3*, and *FPS1* in boron transport and tolerance in *Saccharomyces cerevisiae*. *FEMS microbiology letters*, 262 (2), 216-222.

Okamura, K., Kimata, Y., Higashio, H., Tsuru, A., & Kohno, K. (2000). Dissociation of Kar2p/BiP from an ER sensory molecule, Ire1p, triggers the unfolded protein response in yeast. *Biochemical and Biophysical Research Communications*, 279 (2), 445-450.

Ogawa, M., Itakura, M., & Sakamoto, H. (2017). Interrelationship between ClC-5-containing vesicle trafficking and sorting of the vacuolar H^+-ATPase and NHE3 in response to NH_4Cl-induced acidosis in the mouse kidney. *Kitasato Medical Journal*, 47, 62-70.

Opekarová, M., Robl, I., & Tanner, W. (2002). Phosphatidyl ethanolamine is essential for targeting the arginine transporter Can1p to the plasma membrane of yeast. *Biochimica et Biophysica Acta (BBA)-Biomembranes*, 1564 (1), 9-13.

Oslowski, C. M., & Urano, F. (2011). Measuring ER stress and the unfolded protein response using mammalian tissue culture system. *Methods in Enzymology*, 490:71-92

Ogawa, N., & Mori, K. (2004). Autoregulation of the *HAC1* gene is required for sustained activation of the yeast unfolded protein response. *Genes Cells*, 9 (2), 95-104.

Quilty, J. A., Li, J., & Reithmeier, R. A. (2002). Impaired trafficking of distal renal tubular acidosis mutants of the human kidney anion exchanger kAE1. *American Journal of Physiology-Renal Physiology*, 282 (5), F810-F820.

Overton, M. C., Chinault, S. L., & Blumer, K. J. (2003). Oligomerization, biogenesis, and

signaling is promoted by a glycophorin A-like dimerization motif in transmembrane domain 1 of a yeast G protein-coupled receptor. *Journal of Biological Chemistry*, 278 (49), 49369-49377.

Pang, A. J., Bustos, S. P., & Reithmeier, R. A. (2008). Structural characterization of the cytosolic domain of kidney chloride/bicarbonate anion exchanger 1 (kAE1). *Biochemistry*, 47 (15), 4510-4517.

Papouskova, K., Andrsova, M., & Sychrova, H. (2017). Lack of cortical endoplasmic reticulum protein *Ist2* alters sodium accumulation in *Saccharomyces cerevisiae* cells. *FEMS yeast research*, 17 (2), fox011.

Parker, M. D., & Boron, W. F. (2013). The divergence, actions, roles, and relatives of sodium-coupled bicarbonate transporters. *Physiological Reviews*, 93 (2), 803-959.

Patil, C., & Walter, P. (2001). Intracellular signaling from the endoplasmic reticulum to the nucleus: the unfolded protein response in yeast and mammals. *Current Opinion in Cell Biology*, 13 (3), 349-355.

Piña, F. J., Fleming, T., Pogliano, K., & Niwa, M. (2016). Reticulons regulate the ER inheritance block during ER stress. *Developmental Cell*, 37 (3), 279-288.

Pittet, M., & Conzelmann, A. (2007). Biosynthesis and function of GPI proteins in the yeast *Saccharomyces cerevisiae*. *Biochimica et Biophysica Acta (BBA)-Molecular and Cell Biology of Lipids*, 1771 (3), 405-420.

Petschnigg, J., Moe, O. W., & Stagljar, I. (2011). Using yeast as a model to study membrane proteins. *Current Opinion in Nephrology and Hypertension*, 20 (4), 425-432.

Pyle, E., Guo, C., Hofmann, T., Schmidt, C., Ribiero, O., Politis, A., & Byrne, B. (2019). Protein-Lipid interactions stabilize the oligomeric state of BOR1p from *Saccharomyces cerevisiae*. *Analytical Chemistry*, 91 (20), 13071-13079.

Rabouille, C. (2017). Pathways of unconventional protein secretion. *Trends in Cell Biology*, 27 (3), 230-240.

Ramirez-Macias, I., Barlow, L. D., Anton, C., Spang, A., Roncero, C., & Dacks, J. B. (2018). Evolutionary cell biology traces the rise of the exomer complex in Fungi from an ancient eukaryotic component. *Scientific Reports*, 8 (1), 1-12.

Reithmeier, R. A., Casey, J. R., Kalli, A. C., Sansom, M. S., Alguel, Y., & Iwata, S. (2016).

Band 3, the human red cell chloride/bicarbonate anion exchanger (AE1, *SLC4A1*), in a structural context. *Biochimica et Biophysica Acta (BBA)-Biomembranes*, 1858 (7), 1507-1532.

Rivera-Santiago, R., Harper, S. L., Sriswasdi, S., Hembach, P., & Speicher, D. W. (2017). Full-length anion exchanger 1 structure and interactions with ankyrin-1 determined by zero length crosslinking of erythrocyte membranes. *Structure*, 25 (1), 132-145.

Romanos, M. A., Scorer, C. A., & Clare, J. J. (1992). Foreign gene expression in yeast: a review. *Yeast*, 8(6), 423-488.

Ron, D., & Walter, P. (2007). Signal integration in the endoplasmic reticulum unfolded protein response. *Nature reviews Molecular Cell Biology*, 8 (7), 519-529.

Roy, A., Al-bataineh, M. M., & Pastor-Soler, N. M. (2015). Collecting duct intercalated cell function and regulation. *Clinical Journal of the American Society of Nephrology*, 10 (2), 305-324.

Saheki, Y., & De Camilli, P. (2017). Endoplasmic reticulum-plasma membrane contact sites. *Annual Review of Biochemistry*, 86, 659-684.

Sanders, S.L., Whitfield, K.M., Vogel, J.P., Rose, M.D. and Schekman, R.W., 1992. Sec61p and BiP directly facilitate polypeptide translocation into the ER. *Cell*, 69(2), pp.353-365.

Sarder, H. A., Li, X., Funaya, C., Cordat, E., Schmitt, M. J., & Becker, B. (2020). *Saccharomyces cerevisiae*: First steps to a suitable model system to study the function and intracellular transport of human kidney anion exchanger 1. *mSphere*, *5*(1), e00802-19.

Schröder, M. (2008). Endoplasmic reticulum stress responses. *Cellular and Molecular Life Sciences*, 65 (6), 862-894.

Sekler, I., Kopito, R., & Casey, J. R. (1995). High level expression, partial purification, and functional reconstitution of the human AE1 anion exchanger in *Saccharomyces cerevisiae*. *Journal of Biological Chemistry*, 270 (36), 21028-21034.

Shamu, C. E., Cox, J. S., & Walter, P. (1994). The unfolded-protein-response pathway in yeast. *Trends in Cell Biology*, 4 (2), 56-60.

Santos, E., & Nebreda, A. R. (1989). Structural and functional properties of ras proteins. *The FASEB Journal*, 3 (10), 2151-2163.

Shen, H., Huang, H., Luo, K., Yi, Y., & Shi, X. (2019). Two different pathogenic gene mutations coexisted in the same hereditary spherocytosis family manifested with heterogeneous phenotypes. *BMC Medical Genetics*, 20 (1), 90.

Shen, X., Zhang, K., & Kaufman, R. J. (2004). The unfolded protein response-a stress signaling pathway of the endoplasmic reticulum. *Journal of Chemical Neuroanatomy*, 28 (1-2), 79-92.

Shpilka, T., & Haynes, C. M. (2018). The mitochondrial UPR: mechanisms, physiological functions, and implications in ageing. *Nature Reviews Molecular Cell Biology*, 19 (2), 109.

Silva, S. J. B. E., Ferreira, G. M. D., de Lemos, L. R., Rodrigues, G. D., & Mageste, A. B. (2019). Liquid–Liquid equilibrium of aqueous two-phase systems composed of nonionic surfactant (Triton X-100, Triton X-165, or Triton X-305) and choline chloride. *Journal of Chemical & Engineering Data*, 64 (4), 1632-1639.

Sorrell, S. L., Golder, Z. J., Johnstone, D. B., & Frankl, F. E. K. (2016). Renal peroxiredoxin 6 interacts with anion exchanger 1 and plays a novel role in pH homeostasis. *Kidney International*, 89 (1), 105-112.

Su, Y., Al-Lamki, R. S., Blake-Palmer, K. G., Best, A., Golder, Z. J., Zhou, A., & Frankl, F. E. K. (2015). Physical and functional links between anion exchanger-1 and sodium pump. *Journal of the American Society of Nephrology*, 26 (2), 400-409.

Sun, S., Zhang, D., Sun, G., Song, Y., Cai, J., Fan, Z., & Wang, H. (2019). Solute carrier family 4 member 1 might participate in the pathogenesis of Meniere's disease in a murine endolymphatic hydrop model. *Acta Oto-laryngologica*, 139 (11), 966-976.

Suzuki, K., & Ohsumi, Y. (2007). Molecular machinery of autophagosome formation in yeast, *Saccharomyces cerevisiae*. *FEBS Letters*, 581 (11), 2156-2161.

Takano, J., Miwa, K., Yuan, L., von Wirén, N., & Fujiwara, T. (2005). Endocytosis and degradation of BOR1, a boron transporter of *Arabidopsis thaliana*, regulated by boron availability. *Proceedings of the National Academy of Sciences*, 102 (34), 12276-12281.

Takano, J., Kobayashi, M., Noda, Y., & Fujiwara, T. (2007). *Saccharomyces cerevisiae* Bor1p is a boron exporter and a key determinant of boron tolerance. *FEMS Microbiology Letters*, 267(2), 230-235.

Takeuchi, T., & Hattori-Kato, M. (2017). Introduction of single nucleotide variations into the promoter region of the mouse kidney anion exchanger 1 gene downstream of a TATA box changes its transcriptional activity. *bioRxiv*, 198457.

Takano, J., Kobayashi, M., Noda, Y., & Fujiwara, T. (2007). *Saccharomyces cerevisiae* Bor1p is a boron exporter and a key determinant of boron tolerance. *FEMS Microbiology Letters*, 267 (2), 230-235.

Takeuchi, T., Hattori-Kato, M., Okuno, Y., Kanatani, A., Zaitsu, M., & Mikami, K. (2016). A single nucleotide polymorphism in kidney anion exchanger 1 gene is associated with incomplete type 1 renal tubular acidosis. *Scientific Reports*, 6, 35841.

Thurtle-Schmidt, B. H., & Stroud, R. M. (2016). Structure of Bor1 supports an elevator transport mechanism for *SLC4* anion exchangers. *Proceedings of the National Academy of Sciences*, 113 (38), 10542-10546.

Toye, A. M., Banting, G., & Tanner, M. J. (2004). Regions of human kidney anion exchanger 1 (kAE1) required for basolateral targeting of kAE1 in polarised kidney cells: mis-targeting explains dominant renal tubular acidosis (dRTA). *Journal of Cell Science*, 117 (8), 1399-1410.

Umebayashi, K., Hirata, A., Fukuda, R., Horiuchi, H., Ohta, A., & Takagi, M. (1997). Accumulation of misfolded protein aggregates leads to the formation of russell body-like dilated endoplasmic reticulum in yeast. *Yeast*, 13 (11), 1009-1020.

Uppala, J. K., Gani, A. R., & Ramaiah, K. V. (2017). Chemical chaperone, TUDCA unlike PBA, mitigates protein aggregation efficiently and resists ER and non-ER stress induced HepG2 cell death. *Scientific Reports*, 7:3831.

Verghese, J., Abrams, J., Wang, Y., & Morano, K. A. (2012). Biology of the heat shock response and protein chaperones: budding yeast (*Saccharomyces cerevisiae*) as a model system. *Microbiology and Molecular Biology Reviews*, 76 (2), 115-158.

Vichot, A. A., Zsengellér, Z. K., Shmukler, B. E., Adams, N. D., Dahl, N. K., & Alper, S. L. (2016). Loss of kAE1 expression in collecting ducts of end-stage kidneys from a family with *SLC4A1* G609R-associated distal renal tubular acidosis. *Clinical Kidney Journal*, 10 (1), 135-140.

Wang, S., & Kaufman, R. J. (2012). The impact of the unfolded protein response on human

disease. *Journal of Cell Biology*, 197 (7), 857-867.

Walter, P., & Ron, D. (2011). The unfolded protein response: from stress pathway to homeostatic regulation. *Science*, 334 (6059), 1081-1086.

Wu, H., Ng, B.S. and Thibault, G., 2014. Endoplasmic reticulum stress response in yeast and humans. *Bioscience Reports*, *34*(4): :e00118.

Yadav, A., & Sinha, H. (2018). Gene-gene and gene-environment interactions in complex traits in yeast. *Yeast*, 35 (6), 403-416.

Ye, M., Lehigh, K. M., & Ginty, D. D. (2018). Multivesicular bodies mediate long-range retrograde NGF-TrkA signaling. *Elife*, 7, e33012.

Yenchitsomanus, P. T., Kittanakom, S., Rungroj, N., Cordat, E., & Reithmeier, R. A. (2005). Molecular mechanisms of autosomal dominant and recessive distal renal tubular acidosis caused by *SLC4A1* (AE1) mutations. *Journal of Molecular and Genetic Medicine*, 1 (2), 49-62.

Young, C.L., Raden, D.L. and Robinson, A.S., 2013. Analysis of ER resident proteins in *Saccharomyces cerevisiae*: implementation of H/KDEL retrieval sequences. *Traffic*, 14(4), pp.365-381.

Yoshida, H., Matsui, T., Hosokawa, N., Kaufman, R. J., Nagata, K., & Mori, K. (2003). A time-dependent phase shift in the mammalian unfolded protein response. *Developmental Cell*, 4 (2), 265-271.

You, S., Zhang, J., Yin, Q., Qi, W., Su, R., & He, Z. (2017). Development of a novel integrated process for co-production of β-galactosidase and ethanol using lactose as substrate. *Bioresource Technology*, 230, 15-23.

Yuan, L., Kenny, S. J., Hemmati, J., Xu, K., & Schekman, R. (2018). TANGO1 and SEC12 are copackaged with procollagen I to facilitate the generation of large COPII carriers. *Proceedings of the National Academy of Sciences*, 115 (52), E12255-E12264.

Zimmerman, K. A., Gonzalez, N. M., Chumley, P., Chacana, T., Harrington, L. E., Yoder, B. K., & Mrug, M. (2019). Urinary T cells correlate with rate of renal function loss in autosomal dominant polycystic kidney disease. *Physiological Reports*, 7 (1), e13951.

Zhao, R., & Reithmeier, R. A. (2001). Expression and characterization of the anion transporter homologue YNL275w in *Saccharomyces cerevisiae*. *American Journal of Physiology-*

Cell Physiology, 281 (1), C33-C45.

Zhao, W., Cui, H. J., Qiu, K. P., Zhou, T., Hong, X. S., & Liu, X. G. (2019). Yeast molecular chaperone gene *SSB2* is involved in the endoplasmic reticulum stress response. *Antonie van Leeuwenhoek*, 112 (4), 589-598.

7. Appendix

kAE1 sequences are listed below: (**a**) yeast codon-optimized kAE1 sequence, (**b**) yeast codon-optimized kAE1 sequence with an integrated FLAG-tag in the third extracellular loop between amino acid 557 and 578 (according to AE1 sequence), **(c)** yeast codon-optimized kAE1 sequence with an integrated HA-tag in the third extracellular loop between amino acid 557 and 578 (according to AE1 sequence), **(d)** the sequence of a N-terminal HA-tagged, truncated kAE1 version (aa 361 to 911), **(e)** truncated yeast codon-optimized kAE1 sequence containing amino acid 1 to 491 of kAE1, (**f**) truncated yeast codon-optimized kAE1 sequence containing amino acid 1 to 666 of kAE1. Small letters indicate the restriction site; bold letters indicate the corresponding epitope-tag.

(a) kAE1^{WT}

ctcgaggaattcATGGACGAAAAGAATCAAGAATTGAGATGGATGGAAGCTGCTAGATGGGTTCA
ATTGGAAGAAAATTTGGGTGAAAATGGTGCTTGGGGTAGACCACATTTGTCTCATTTGACT
TTTTGGTCCTTGTTGGAATTGAGAAGAGTTTTCACTAAGGGTACTGTCTTGTTGGACTTGC
AAGAAACTTCTTTGGCTGGTGTTGCCAATCAATTATTGGACAGATTCATTTTCGAAGATCAA
ATCAGACCACAAGATAGAGAAGAATTATTGAGAGCCTTGTTGTTGAAGCACTCTCATGCTG
GTGAATTGGAAGCTTTAGGTGGTGTTAAGCCAGCTGTTTTGACTAGATCTGGTGATCCATC
ACAACCATTATTGCCACAACATTCTTCATTGGAAACCCAATTATTCTGCGAACAAGGTGATG
GTGGTACTGAAGGTCATTCTCCATCTGGTATTTTGGAAAAGATTCCACCAGATTCTGAAGCC
ACTTTGGTTTTGGTTGGTAGAGCTGATTTTTTGGAACAACCAGTTTTGGGTTTCGTTAGATT
GCAAGAAGCTGCTGAATTAGAAGCAGTTGAATTGCCAGTTCCAATCAGATTCTTGTTCGTT
TTGTTGGGTCCAGAAGCTCCACATATTGATTATACTCAATTGGGTAGAGCCGCTGCTACTTT
GATGTCTGAAAGAGTTTTTAGAATCGACGCTTACATGGCTCAATCCAGAGGTGAATTATTGC
ATTCTTTGGAAGGTTTCTTGGACTGCTCTTTAGTTTTGCCACCAACTGATGCTCCATCTGAA
CAAGCTTTGTTGTCTTTGGTTCCAGTTCAAAGAGAATTATTGAGAAGAAGATACCAATCCT
CTCCAGCTAAACCAGACTCTTCATTTTACAAGGGTTTGGATTTGAATGGTGGTCCAGATGAT
CCATTGCAACAAACTGGTCAATTATTCGGTGGTTTGGTTAGAGACATCAGAAGAAGATATC
CTTACTACTTGTCCGATATCACCGATGCTTTTTCACCACAAGTTTTGGCTGCTGTTATCTTCA
TCTATTTCGCTGCTTTGTCACCAGCTATTACTTTTGGTGGTTTATTAGGTGAAAAGACCAGA
AATCAAATGGGTGTTTCCGAATTATTGATCTCCACTGCTGTTCAAGGTATTTTGTTTGCTTTG
TTAGGTGCCCAACCTTTGTTGGTTGTTGGTTTTTCTGGTCCATTATTGGTCTTTGAAGAAGC
TTTCTTCTCCTTCTGTGAAACTAACGGTTTGGAATATATCGTCGGTAGAGTTTGGATTGGTTT
CTGGTTAATTTTGTTGGTCGTTTTGGTCGTCGCTTTCGAAGGTTCATTTTTGGTAAGATTCAT
CTCCAGATACACCCAAGAAATCTTTTCTTTCTTGATCTCCTTGATTTTCATCTACGAAACCTT
CTCCAAGTTGATCAAGATCTTCCAAGATCACCCATTGCAAAAGACCTACAACTACAACGTT
TTGATGGTTCCAAAACCACAAGGTCCATTGCCAAATACTGCTTTATTATCCTTGGTTTTAATG
GCCGGTACTTTCTTCTTTGCCATGATGTTGAGAAAGTTCAAGAACTCCTCTTACTTCCCAGG
TAAGTTGAGAAGAGTCATTGGTGATTTTGGTGTCCCAATCTCCATTTTGATTATGGTCTTGG
TTGACTTCTTCATCCAAGATACTTACACCCAAAAGTTGTCTGTTCCAGATGGTTTCAAGGTC

AGTAATTCTTCAGCTAGAGGTTGGGTTATTCATCCATTGGGTTTGAGATCCGAATTTCCAAT
TTGGATGATGTTCGCTTCTGCTTTGCCAGCTTTATTGGTTTTTATCTTGATATTCTTGGAATCC
CAAATCACCACCTTGATCGTTTCTAAACCTGAAAGAAAGATGGTCAAGGGTTCTGGTTTTC
ACTTGGATTTGTTGTTAGTTGTCGGTATGGGTGGTGTTGCAGCTTTGTTTGGTATGCCATGG
TTGTCTGCTACTACTGTTAGATCTGTTACTCATGCTAACGCTTTGACTGTTATGGGTAAAGCT
TCTACTCCAGGTGCTGCTGCTCAAATTCAAGAAGTAAAAGAACAAAGAATTTCCGGTTTGT
TGGTAGCCGTTTTAGTTGGTTTGTCAATCTTGATGGAACCTATCTTGTCTAGAATCCCATTGG
CTGTTTTGTTCGGTATTTTCTTGTACATGGGTGTCACATCCTTGTCCGGTATCCAATTATTTG
ATAGAATCTTGTTGTTATTCAAGCCACCAAAGTACCATCCAGATGTTCCTTATGTTAAGAGA
GTCAAGACTTGGAGAATGCATTTGTTCACCGGTATTCAAATTATCTGCTTGGCAGTTTTGTG
GGTTGTTAAGTCAACTCCAGCTTCTTTAGCATTGCCATTCGTTTTGATTTTGACCGTCCCATT
AAGAAGAGTCTTGTTGCCATTGATATTCAGAAACGTCGAATTGCAATGTTTGGATGCTGAT
GATGCTAAGGCTACTTTTGACGAAGAAGAAGGTAGAGACGAATACGATGAAGTTGCTATGC
CAGTTAAggatccgtcgac

(b) kAE1^{FLAG}

CTCGAGATGGACGAAAAGAATCAAGAATTGAGATGGATGGAAGCTGCTAGATGGGTTCAA
TTGGAAGAAAATTTGGGTGAAAATGGTGCTTGGGGTAGACCACATTTGTCTCATTTGACTT
TTTGGTCCTTGTTGGAATTGAGAAGAGTTTTCACTAAGGGTACTGTCTTGTTGGACTTGCA
AGAAACTTCTTTGGCTGGTGTTGCCAATCAATTATTGGACAGATTCATTTTCGAAGATCAAA
TCAGACCACAAGATAGAGAAGAATTATTGAGAGCCTTGTTGTTGAAGCACTCTCATGCTGG
TGAATTGGAAGCTTTAGGTGGTGTTAAGCCAGCTGTTTTGACTAGATCTGGTGATCCATCAC
AACCATTATTGCCACAACATTCTTCATTGGAAACCCAATTATTCTGCGAACAAGGTGATGGT
GGTACTGAAGGTCATTCTCCATCTGGTATTTTGGAAAAGATTCCACCAGATTCTGAAGCCA
CTTTGGTTTTGGTTGGTAGAGCTGATTTTTTGGAACAACCAGTTTTGGGTTTCGTTAGATTG
CAAGAAGCTGCTGAATTAGAAGCAGTTGAATTGCCAGTTCCAATCAGATTCTTGTTCGTTT
TGTTGGGTCCAGAAGCTCCACATATTGATTATACTCAATTGGGTAGAGCCGCTGCTACTTTG
ATGTCTGAAAGAGTTTTTAGAATCGACGCTTACATGGCTCAATCCAGAGGTGAATTATTGCA
TTCTTTGGAAGGTTTCTTGGACTGCTCTTTAGTTTTGCCACCAACTGATGCTCCATCTGAAC
AAGCTTTGTTGTCTTTGGTTCCAGTTCAAAGAGAATTATTGAGAAGAAGATACCAATCCTC
TCCAGCTAAACCAGACTCTTCATTTTACAAGGGTTTGGATTTGAATGGTGGTCCAGATGATC
CATTGCAACAAACTGGTCAATTATTCGGTGGTTTGGTTAGAGACATCAGAAGAAGATATCC
TTACTACTTGTCCGATATCACCGATGCTTTTTCACCACAAGTTTTGGCTGCTGTTATCTTCAT
CTATTTCGCTGCTTTGTCACCAGCTATTACTTTTGGTGGTTTATTAGGTGAAAAGACCAGAA
ATCAAATGGGTGTTTCCGAATTATTGATCTCCACTGCTGTTCAAGGTATTTTGTTTGCTTTGT
TAGGTGCCCAACCTTTGTTGGTTGTTGGTTTTTCTGGTCCATTATTGGTCTTTGAAGAAGCT
TTCTTCTCCTTCTGTGAAACTAACGGTTTGGAATATATCGTCGGTAGAGTTTGGATTGGTTT
CTGGTTAATTTTGTTGGTCGTTTTGGTCGTCGCTTTCGAAGGTTCATTTTTGGTAAGATTCAT
CTCCAGATACACCCAAGAAATCTTTTCTTTCTTGATCTCCTTGATTTTCATCTACGAAACCTT
CTCCAAGTTGATCAAGATCTTCCAAGATCACCCATTGCAAAAGACCTACAACTACAA**CGAC**
TACAAGGATGACGACGATAAGGTTTTGATGGTTCCAAAACCACAAGGTCCATTGCCAAAT
ACTGCTTTATTATCCTTGGTTTTAATGGCCGGTACTTTCTTCTTTGCCATGATGTTGAGAAAG
TTCAAGAACTCCTCTTACTTCCCAGGTAAGTTGAGAAGAGTCATTGGTGATTTTGGTGTCC
CAATCTCCATTTTGATTATGGTCTTGGTTGACTTCTTCATCCAAGATACTTACACCCAAAAGT
TGTCTGTTCCAGATGGTTTCAAGGTCAGTAATTCTTCAGCTAGAGGTTGGGTTATTCATCCA

TTGGGTTTGAGATCCGAATTTCCAATTTGGATGATGTTCGCTTCTGCTTTGCCAGCTTTATTG
GTTTTTATCTTGATATTCTTGGAATCCCAAATCACCACCTTGATCGTTTCTAAACCTGAAAG
AAAGATGGTCAAGGGTTCTGGTTTTCACTTGGATTTGTTGTTAGTTGTCGGTATGGGTGGTG
TTGCAGCTTTGTTTGGTATGCCATGGTTGTCTGCTACTACTGTTAGATCTGTTACTCATGCTA
ACGCTTTGACTGTTATGGGTAAAGCTTCTACTCCAGGTGCTGCTGCTCAAATTCAAGAAGT
AAAAGAACAAAGAATTTCCGGTTTGTTGGTAGCCGTTTTAGTTGGTTTGTCAATCTTGATG
GAACCTATCTTGTCTAGAATCCCATTGGCTGTTTTGTTCGGTATTTTCTTGTACATGGGTGTC
ACATCCTTGTCCGGTATCCAATTATTTGATAGAATCTTGTTGTTATTCAAGCCACCAAAGTAC
CATCCAGATGTTCCTTATGTTAAGAGAGTCAAGACTTGGAGAATGCATTTGTTCACCGGTAT
TCAAATTATCTGCTTGGCAGTTTTGTGGGTTGTTAAGTCAACTCCAGCTTCTTTAGCATTGC
CATTCGTTTTGATTTTGACCGTCCCATTAAGAAGAGTCTTGTTGCCATTGATATTCAGAAAC
GTCGAATTGCAATGTTTGGATGCTGATGATGCTAAGGCTACTTTTGACGAAGAAGAAGGTA
GAGACGAATACGATGAAGTTGCTATGCCAGTTTAAGGATCC

(c) kAE1^{HA}

ctcgagATGGACGAAAAGAATCAAGAATTGAGATGGATGGAAGCTGCTAGATGGGTTCAATTG
GAAGAAAATTTGGGTGAAAATGGTGCTTGGGGTAGACCACATTTGTCTCATTTGACTTTTT
GGTCCTTGTTGGAATTGAGAAGAGTTTTCACTAAGGGTACTGTCTTGTTGGACTTGCAAGA
AACTTCTTTGGCTGGTGTTGCCAATCAATTATTGGACAGATTCATTTTCGAAGATCAAATCA
GACCACAAGATAGAGAAGAATTATTGAGAGCCTTGTTGTTGAAGCACTCTCATGCTGGTGA
ATTGGAAGCTTTAGGTGGTGTTAAGCCAGCTGTTTTGACTAGATCTGGTGATCCATCACAA
CCATTATTGCCACAACATTCTTCATTGGAAACCCAATTATTCTGCGAACAAGGTGATGGTGG
TACTGAAGGTCATTCTCCATCTGGTATTTTGGAAAAGATTCCACCAGATTCTGAAGCCACTT
TGGTTTTGGTTGGTAGAGCTGATTTTTTGGAACAACCAGTTTTGGGTTTCGTTAGATTGCAA
GAAGCTGCTGAATTAGAAGCAGTTGAATTGCCAGTTCCAATCAGATTCTTGTTCGTTTTGTT
GGGTCCAGAAGCTCCACATATTGATTATACTCAATTGGGTAGAGCCGCTGCTACTTTGATGT
CTGAAAGAGTTTTTAGAATCGACGCTTACATGGCTCAATCCAGAGGTGAATTATTGCATTCT
TTGGAAGGTTTCTTGGACTGCTCTTTAGTTTTGCCACCAACTGATGCTCCATCTGAACAAG
CTTTGTTGTCTTTGGTTCCAGTTCAAAGAGAATTATTGAGAAGAAGATACCAATCCTCTCCA
GCTAAACCAGACTCTTCATTTTACAAGGGTTTGGATTTGAATGGTGGTCCAGATGATCCATT
GCAACAAACTGGTCAATTATTCGGTGGTTTGGTTAGAGACATCAGAAGAAGATATCCTTAC
TACTTGTCCGATATCACCGATGCTTTTTCACCACAAGTTTTGGCTGCTGTTATCTTCATCTAT
TTCGCTGCTTTGTCACCAGCTATTACTTTTGGTGGTTTATTAGGTGAAAAGACCAGAAATCA
AATGGGTGTTTCCGAATTATTGATCTCCACTGCTGTTCAAGGTATTTTGTTTGCTTTGTTAGG
TGCCCAACCTTTGTTGGTTGTTGGTTTTTCTGGTCCATTATTGGTCTTTGAAGAAGCTTTCT
TCTCCTTCTGTGAAACTAACGGTTTGGAATATATCGTCGGTAGAGTTTGGATTGGTTTCTGG
TTAATTTTGTTGGTCGTTTTGGTCGTCGCTTTCGAAGGTTCATTTTTGGTAAGATTCATCTCC
AGATACACCCAAGAAATCTTTTCTTTCTTGATCTCCTTGATTTTCATCTACGAAACCTTCTCC
AAGTTGATCAAGATCTTCCAAGATCACCCATTGCAAAAGACCTACAACTACAAC**TACCCAT**
ACGATGTTCCAGATTACGCTGTTTTGATGGTTCCAAAACCACAAGGTCCATTGCCAAATA
CTGCTTTATTATCCTTGGTTTTAATGGCCGGTACTTTCTTCTTTGCCATGATGTTGAGAAAGT
TCAAGAACTCCTCTTACTTCCCAGGTAAGTTGAGAAGAGTCATTGGTGATTTTGGTGTCCC
AATCTCCATTTTGATTATGGTCTTGGTTGACTTCTTCATCCAAGATACTTACACCCAAAAGTT
GTCTGTTCCAGATGGTTTCAAGGTCAGTAATTCTTCAGCTAGAGGTTGGGTTATTCATCCAT
TGGGTTTGAGATCCGAATTTCCAATTTGGATGATGTTCGCTTCTGCTTTGCCAGCTTTATTG

GTTTTTATCTTGATATTCTTGGAATCCCAAATCACCACCTTGATCGTTTCTAAACCTGAAAG
AAAGATGGTCAAGGGTTCTGGTTTTCACTTGGATTTGTTGTTAGTTGTCGGTATGGGTGGTG
TTGCAGCTTTGTTTGGTATGCCATGGTTGTCTGCTACTACTGTTAGATCTGTTACTCATGCTA
ACGCTTTGACTGTTATGGGTAAAGCTTCTACTCCAGGTGCTGCTGCTCAAATTCAAGAAGT
AAAAGAACAAAGAATTTCCGGTTTGTTGGTAGCCGTTTTAGTTGGTTTGTCAATCTTGATG
GAACCTATCTTGTCTAGAATCCCATTGGCTGTTTTGTTCGGTATTTTCTTGTACATGGGTGTC
ACATCCTTGTCCGGTATCCAATTATTTGATAGAATCTTGTTGTTATTCAAGCCACCAAAGTAC
CATCCAGATGTTCCTTATGTTAAGAGAGTCAAGACTTGGAGAATGCATTTGTTCACCGGTAT
TCAAATTATCTGCTTGGCAGTTTTGTGGGTTGTTAAGTCAACTCCAGCTTCTTTAGCATTGC
CATTCGTTTTGATTTTGACCGTCCCATTAAGAAGAGTCTTGTTGCCATTGATATTCAGAAAC
GTCGAATTGCAATGTTTGGATGCTGATGATGCTAAGGCTACTTTTGACGAAGAAGAAGGTA
GAGACGAATACGATGAAGTTGCTATGCCAGTTTAAggatcc

(d) kAE1^{B3mem} (aa 361 to 911)

gtcgacggattcctcgagATG**TACCCATACGATGTTCCAGATTACGCT**ggtggtggtggtagtGGTTTGGAT
TTGAATGGTGGTCCAGATGATCCATTGCAACAAACTGGTCAATTATTCGGTGGTTTGGTTAG
AGACATCAGAAGAAGATATCCTTACTACTTGTCCGATATCACCGATGCTTTTTCACCACAAG
TTTTGGCTGCTGTTATCTTCATCTATTTCGCTGCTTTGTCACCAGCTATTACTTTTGGTGGTTT
ATTAGGTGAAAAGACCAGAAATCAAATGGGTGTTTCCGAATTATTGATCTCCACTGCTGTTC
AAGGTATTTTGTTTGCTTTGTTAGGTGCCCAACCTTTGTTGGTTGTTGGTTTTTCTGGTCCAT
TATTGGTCTTTGAAGAAGCTTTCTTCTCCTTCTGTGAAACTAACGGTTTGGAATATATCGTC
GGTAGAGTTTGGATTGGTTTCTGGTTAATTTTGTTGGTCGTTTTGGTCGTCGCTTTCGAAGG
TTCATTTTTGGTAAGATTCATCTCCAGATACACCCAAGAAATCTTTTCTTTCTTGATCTCCTT
GATTTTCATCTACGAAACCTTCTCCAAGTTGATCAAGATCTTCCAAGATCACCCATTGCAAA
AGACCTACAACTACAACGTTTTGATGGTTCCAAAACCACAAGGTCCATTGCCAAATACTGC
TTTATTATCCTTGGTTTTAATGGCCGGTACTTTCTTCTTTGCCATGATGTTGAGAAAGTTCAA
GAACTCCTCTTACTTCCCAGGTAAGTTGAGAAGAGTCATTGGTGATTTTGGTGTCCCAATCT
CCATTTTGATTATGGTCTTGGTTGACTTCTTCATCCAAGATACTTACACCCAAAAGTTGTCT
GTTCCAGATGGTTTCAAGGTCAGTAATTCTTCAGCTAGAGGTTGGGTTATTCATCCATTGGG
TTTGAGATCCGAATTTCCAATTTGGATGATGTTCGCTTCTGCTTTGCCAGCTTTATTGGTTTT
TATCTTGATATTCTTGGAATCCCAAATCACCACCTTGATCGTTTCTAAACCTGAAAGAAAGA
TGGTCAAGGGTTCTGGTTTTCACTTGGATTTGTTGTTAGTTGTCGGTATGGGTGGTGTTGCA
GCTTTGTTTGGTATGCCATGGTTGTCTGCTACTACTGTTAGATCTGTTACTCATGCTAACGCT
TTGACTGTTATGGGTAAAGCTTCTACTCCAGGTGCTGCTGCTCAAATTCAAGAAGTAAAAG
AACAAAGAATTTCCGGTTTGTTGGTAGCCGTTTTAGTTGGTTTGTCAATCTTGATGGAACCT
ATCTTGTCTAGAATCCCATTGGCTGTTTTGTTCGGTATTTTCTTGTACATGGGTGTCACATCC
TTGTCCGGTATCCAATTATTTGATAGAATCTTGTTGTTATTCAAGCCACCAAAGTACCATCCA
GATGTTCCTTATGTTAAGAGAGTCAAGACTTGGAGAATGCATTTGTTCACCGGTATTCAAAT
TATCTGCTTGGCAGTTTTGTGGGTTGTTAAGTCAACTCCAGCTTCTTTAGCATTGCCATTCG
TTTTGATTTTGACCGTCCCATTAAGAAGAGTCTTGTTGCCATTGATATTCAGAAACGTCGAA
TTGCAATGTTTGGATGCTGATGATGCTAAGGCTACTTTTGACGAAGAAGAAGGTAGAGACG
AATACGATGAAGTTGCTATGCCAGTTTAAggatccgagctc

(e) kAE1$^{1-491}$

CTCGAGGAATTCATGGACGAAAAGAATCAAGAATTGAGATGGATGGAAGCTGCTAGATGG

GTTCAATTGGAAGAAAATTTGGGTGAAAATGGTGCTTGGGGTAGACCACATTTGTCTCATT
TGACTTTTTGGTCCTTGTTGGAATTGAGAAGAGTTTTCACTAAGGGTACTGTCTTGTTGGA
CTTGCAAGAAACTTCTTTGGCTGGTGTTGCCAATCAATTATTGGACAGATTCATTTTCGAAG
ATCAAATCAGACCACAAGATAGAGAAGAATTATTGAGAGCCTTGTTGTTGAAGCACTCTCA
TGCTGGTGAATTGGAAGCTTTAGGTGGTGTTAAGCCAGCTGTTTTGACTAGATCTGGTGAT
CCATCACAACCATTATTGCCACAACATTCTTCATTGGAAACCCAATTATTCTGCGAACAAGG
TGATGGTGGTACTGAAGGTCATTCTCCATCTGGTATTTTGGAAAAGATTCCACCAGATTCTG
AAGCCACTTTGGTTTTGGTTGGTAGAGCTGATTTTTTGGAACAACCAGTTTTGGGTTTCGT
TAGATTGCAAGAAGCTGCTGAATTAGAAGCAGTTGAATTGCCAGTTCCAATCAGATTCTTG
TTCGTTTTGTTGGGTCCAGAAGCTCCACATATTGATTATACTCAATTGGGTAGAGCCGCTGC
TACTTTGATGTCTGAAAGAGTTTTTAGAATCGACGCTTACATGGCTCAATCCAGAGGTGAAT
TATTGCATTCTTTGGAAGGTTTCTTGGACTGCTCTTTAGTTTTGCCACCAACTGATGCTCCAT
CTGAACAAGCTTTGTTGTCTTTGGTTCCAGTTCAAAGAGAATTATTGAGAAGAAGATACCA
ATCCTCTCCAGCTAAACCAGACTCTTCATTTTACAAGGGTTTGGATTTGAATGGTGGTCCAG
ATGATCCATTGCAACAAACTGGTCAATTATTCGGTGGTTTGGTTAGAGACATCAGAAGAAG
ATATCCTTACTACTTGTCCGATATCACCGATGCTTTTTCACCACAAGTTTTGGCTGCTGTTAT
CTTCATCTATTTCGCTGCTTTGTCACCAGCTATTACTTTTGGTGGTTTATTAGGTGAAAAGAC
CAGAAATCAAATGGGTGTTTCCGAATTATTGATCTCCACTGCTGTTCAAGGTATTTTGTTTG
CTTTGTTAGGTGCCCAACCTTTGTTGGTTGTTGGTTTTTCTGGTCCATTATTGGTCTTTGAAG
AAGCTTTCTTCTCCTTCTGTGAAACTAACGGTTTGGAATATATCGTCGGTAGAGTTTGGATT
GGTTTCTGGTTAATTTTGTTGGTCGTTTTGGTCGTCGCTTTCGAAGGTTCATTTTTGGTAAG
ATTCATCTCCAGATACACCCAAGAAATCTTTTCTTTCTTGATCTCCTTGATTTTCATCTACGA
AACCTTCTCCAAGTTGATCAAGATCTTCCAAGATCACCCATTGCAAAAGACCTACAACTAC
AACTAAGGATCCGTCGAC

(f) kAE1$^{1-666}$

CTCGAGGAATTCATGGACGAAAAGAATCAAGAATTGAGATGGATGGAAGCTGCTAGATGG
GTTCAATTGGAAGAAAATTTGGGTGAAAATGGTGCTTGGGGTAGACCACATTTGTCTCATT
TGACTTTTTGGTCCTTGTTGGAATTGAGAAGAGTTTTCACTAAGGGTACTGTCTTGTTGGA
CTTGCAAGAAACTTCTTTGGCTGGTGTTGCCAATCAATTATTGGACAGATTCATTTTCGAAG
ATCAAATCAGACCACAAGATAGAGAAGAATTATTGAGAGCCTTGTTGTTGAAGCACTCTCA
TGCTGGTGAATTGGAAGCTTTAGGTGGTGTTAAGCCAGCTGTTTTGACTAGATCTGGTGAT
CCATCACAACCATTATTGCCACAACATTCTTCATTGGAAACCCAATTATTCTGCGAACAAGG
TGATGGTGGTACTGAAGGTCATTCTCCATCTGGTATTTTGGAAAAGATTCCACCAGATTCTG
AAGCCACTTTGGTTTTGGTTGGTAGAGCTGATTTTTTGGAACAACCAGTTTTGGGTTTCGT
TAGATTGCAAGAAGCTGCTGAATTAGAAGCAGTTGAATTGCCAGTTCCAATCAGATTCTTG
TTCGTTTTGTTGGGTCCAGAAGCTCCACATATTGATTATACTCAATTGGGTAGAGCCGCTGC
TACTTTGATGTCTGAAAGAGTTTTTAGAATCGACGCTTACATGGCTCAATCCAGAGGTGAAT
TATTGCATTCTTTGGAAGGTTTCTTGGACTGCTCTTTAGTTTTGCCACCAACTGATGCTCCAT
CTGAACAAGCTTTGTTGTCTTTGGTTCCAGTTCAAAGAGAATTATTGAGAAGAAGATACCA
ATCCTCTCCAGCTAAACCAGACTCTTCATTTTACAAGGGTTTGGATTTGAATGGTGGTCCAG
ATGATCCATTGCAACAAACTGGTCAATTATTCGGTGGTTTGGTTAGAGACATCAGAAGAAG
ATATCCTTACTACTTGTCCGATATCACCGATGCTTTTTCACCACAAGTTTTGGCTGCTGTTAT
CTTCATCTATTTCGCTGCTTTGTCACCAGCTATTACTTTTGGTGGTTTATTAGGTGAAAAGAC
CAGAAATCAAATGGGTGTTTCCGAATTATTGATCTCCACTGCTGTTCAAGGTATTTTGTTTG

CTTTGTTAGGTGCCCAACCTTTGTTGGTTGTTGGTTTTTCTGGTCCATTATTGGTCTTTGAAG
AAGCTTTCTTCTCCTTCTGTGAAACTAACGGTTTGGAATATATCGTCGGTAGAGTTTGGATT
GGTTTCTGGTTAATTTTGTTGGTCGTTTTGGTCGTCGCTTTCGAAGGTTCATTTTTGGTAAG
ATTCATCTCCAGATACACCCAAGAAATCTTTTCTTTCTTGATCTCCTTGATTTTCATCTACGA
AACCTTCTCCAAGTTGATCAAGATCTTCCAAGATCACCCATTGCAAAAGACCTACAACTAC
AACGTTTTGATGGTTCCAAAACCACAAGGTCCATTGCCAAATACTGCTTTATTATCCTTGGT
TTTAATGGCCGGTACTTTCTTCTTTGCCATGATGTTGAGAAAGTTCAAGAACTCCTCTTACT
TCCCAGGTAAGTTGAGAAGAGTCATTGGTGATTTTGGTGTCCCAATCTCCATTTTGATTATG
GTCTTGGTTGACTTCTTCATCCAAGATACTTACACCCAAAAGTTGTCTGTTCCAGATGGTTT
CAAGGTCAGTAATTCTTCAGCTAGAGGTTGGGTTATTCATCCATTGGGTTTGAGATCCGAAT
TTCCAATTTGGATGATGTTCGCTTCTGCTTTGCCAGCTTTATTGGTTTTTATCTTGATATTCTT
GGAATCCCAAATCACCACCTTGATCGTTTCTAAACCTGAAAGAAAGATGGTCAAGGGTTCT
GGTTTTCACTTGGATTTGTTGTTAGTTGTCGGTATGGGTGGTGTTGCAGCTTTGTTTGGTAT
GCCATGGTTGTCTGCTACTACTGTTAGATCT TAAGGATCCGTCGAC

Acknowledgments

How time flies! 5 years' Ph.D. study time felt just like a dream to me. In this long and interesting scientific journey, I did not only learn about science itself, but also had the possibility to encounter many friendly people, and I am very grateful for numerous help- or cheerful words and conversations.

First and foremost, I want to thank my primary supervisor Prof. Dr. Manfred Schmitt for all the given opportunities and great help during my Ph.D. study period. I am deeply grateful to Prof. Schmitt for the opportunity to have him as my Ph.D. supervisor, and it was a great experience to be a member of his inspiring and supporting working group. Warm thanks should also go to my co-supervisor Prof. Dr. Bruce Morgan from Saarland University, and Prof. Dr. Emmanuelle Cordat from the University of Alberta, for their creative suggestions and nice comments regarding my project. Thanks should also go to my good friend and amazing guy Dr. Björn Becker, because he did not spare any effort to help and supervise me during the 4 years. It was really a good, unforgettable, and honorable experience. It has been a truly adventurous time and an honor to study at Saarland University and to be able to take part in the groundbreaking research in the field of molecular and cellular biology. It has surely been an unforgettable experience for me, that I will remember all my life!

Secondly, I want to thank our IRTG 1830 trainee's great "mother" Dr. Gabriele Amoroso, who took care of countless organizational issues during my time in IRTG. It was indeed my great honor to become a member of IRTG 1830. This wonderful platform provided me a flourishing environment to communicate with scientists from other labs, which will benefit me a lot in my future career. In the same breath, I also want to thank our lab's excellent secretary Nicole Jundel for her outstanding organizational support in the past 4 years concerning my research or my daily life!

Thirdly, I would also like to thank Dr. Jennifer Kirwan from the Berlin Institute of Health Metabolomics Platform and Max Delbrück Center for Molecular Medicine for her great help in

my thesis correction and her creative suggestions. It was my great honor to meet you 4 years ago in Berlin, you helped and taught me a lot about science or life attitude *etc*.

Finally, thanks should also go to my former/current lab members for their great help and support. Thanks to PD Dr. Frank Breinig for his daily kind help. Besides, I really enjoyed talking with our excellent technicians Andrea and Sabine during my time in the lab, and it is always given me a good feeling to get along with Matthias every day in the office. Special thanks to Stefanie and Achim for their helpful comments on my thesis. Thanks should also go to every member of the lab, all of you provided me with new perspectives and I learned a lot from you!

Concerning my private life, I am also thankful for the infinite support of my family, and especially for the constant faith of my parents and my wife. Thanks to my mother, in particular, for flying from China to Germany to take care of our child, creating a carefree environment for us to concentrate on our research, *etc*.

Life is a process of running; I am expecting the next journey and am ready to face the next challenge……

Eidesstattliche Versicherung

Hiermit versichere ich an Eides statt, dass ich die vorliegende Arbeit selbstständig und ohne Benutzung anderer als der angegebenen Hilfsmittel angefertigt habe. Die aus anderen Quellen oder indirekt übernommenen Daten und Konzepte sind unter Angabe der Quelle gekennzeichnet. Die Arbeit wurde bisher weder im In- noch im Ausland in gleicher oder ähnlicher Form in einem Verfahren zur Erlangung eines akademischen Grades vorgelegt.

Saarbrücken, 2021

(Xiaobing Li)